

Combined Turbo Coding and Interference Rejection for DS-CDMA.

by

Emmanuel Oluremi Bejide

School of Electrical, Electronic and Computer Engineering,
University of KwaZulu-Natal



Submitted in fulfillment of the academic requirements for the degree of Doctor of
Philosophy in Electronic Engineering.

2004.

Preface.

The research work in this thesis was performed by Emmanuel Oluremi Bejide under the supervision of Professor Fambirai Takawira in the School of Electrical, Electronic and Computer Engineering of the University of KwaZulu-Natal, Durban, South Africa. This work was partly supported by Alcatel SA and Telkom SA under the Centre of Excellence Programme.

The whole thesis, unless specifically indicated to the contrary in the text, is the authors work, and has not been submitted in part, or in whole to any other university.

Dedication.

This work is dedicated to

The “very present help” in times of need.

Abstract.

Combined Turbo Coding and Interference Rejection for DS-CDMA

By

Emmanuel Oluremi Bejide

Doctor of Philosophy in Electronic Engineering

University of KwaZulu-Natal, Durban, South Africa, 2004

Supervisor: Professor Fambirai Takawira.

This dissertation presents interference cancellation techniques for both the Forward Error Correction (FEC) coded and the uncoded Direct Sequence Code Division Multiple Access (DS-CDMA) systems. Analytical models are also developed for the adaptive and the non-adaptive Parallel Interference Cancellation (PIC) receivers. Results that are obtained from the computer simulations of the PIC receiver types confirm the accuracy of the analytical models that are developed. Results show that the Least Mean Square (LMS) algorithm based adaptive PIC receivers have bit error rate performances that are better than those of the non-adaptive PIC receivers.

In the second part of this dissertation, a novel iterative multiuser detector for the Turbo coded DS-CDMA system is developed. The performance of the proposed receiver in the multirate CDMA system is also investigated. The developed receiver is found to have an error rate performance that is very close to the single user limit after a few numbers of iterations. The receiver is also resilient against the near-far effect. A methodology is also presented on the use of the Gaussian approximation method in the convergence analysis of iterative interference cancellation receivers for turbo coded DS-CDMA systems.

Table of Contents.

1. INTRODUCTION.....	1.1
1.1 MULTIUSER DETECTION IN UNCODED CDMA SYSTEMS.....	1.2
1.2 MULTIUSER DETECTION FOR CODED CDMA SYSTEMS.....	1.4
1.3 GOALS AND CONTRIBUTIONS OF THE DISSERTATION.....	1.6
1.4 LIST OF PUBLICATIONS.....	1.7
2. PERFORMANCE ANALYSIS OF PARALLEL INTERFERENCE CANCELLATION TECHNIQUES FOR DS-CDMA IN MULTIPATH FADING CHANNELS.....	2.1
2.1 INTRODUCTION.....	2.1
2.2 SYSTEM MODEL.....	2.4
2.3 COMPARISON OF THE SOFT TENTATIVE DECISION-BASED AND THE HARD TENTATIVE DECISION-BASED PIC RECEIVERS.....	2.11
2.4 PERFORMANCE ANALYSIS.....	2.19
2.5 OPTIMAL WEIGHTS DETERMINATION FOR THE WEIGHTED PIC RECEIVER.....	2.23
2.6 DISCUSSION OF NUMERICAL RESULTS.....	2.25
3. ADAPTIVE PARALLEL INTERFERENCE CANCELLATION RECEIVERS FOR DS-CDMA.....	3.1
3.2 LMS IMPLEMENTATION OF ADAPTIVE PIC RECEIVER.....	3.2
3.3 ERROR RATE PERFORMANCE OF THE ADAPTIVE PIC RECEIVER.....	3.4
3.4 CONCLUSION.....	3.9
4. CONVERGENCE ANALYSIS OF ITERATIVE INTERFERENCE CANCELLATION RECEIVERS FOR TURBO-CODED DS-CDMA SYSTEMS.....	4.1
4.1 INTRODUCTION.....	4.1
4.2 GAUSSIAN APPROXIMATION METHOD FOR THE ANALYSIS OF TURBO DECODERS. ...	4.4
4.3 ERROR RATE PERFORMANCES OF ITERATIVE INTERFERENCE CANCELLATION RECEIVERS.....	4.10
4.4 CONVERGENCE ANALYSIS.....	4.12
4.5 CONCLUSIONS.....	4.19
5. AN ITERATIVE MULTIUSER DETECTOR FOR TURBO CODED DS-CDMA SYSTEMS.....	5.1
5.1 INTRODUCTION.....	5.1
5.2 SYSTEM MODEL.....	5.2
5.3 THE ITERATIVE MULTIUSER DETECTOR.....	5.5
5.4 IMPLEMENTING THE ITERATIVE DETECTOR.....	5.13
5.5 PERFORMANCE DISCUSSION.....	5.14
5.6 CONCLUSION.....	5.21
6. PERFORMANCE OF THE ITERATIVE MULTIUSER DETECTION IN MULTIRATE DS-CDMA SYSTEMS.....	6.1
6.1 INTRODUCTION.....	6.1

6.2 MULTIRATE CDMA SYSTEM MODEL.....	6.3
6.3 SIMULATION MODEL OF MULTIRATE CDMA.....	6.6
6.4 DISCUSSION OF RESULTS.....	6.6
6.5 CONCLUSION.....	6.9
7. CONCLUSION.....	7.1
REFERENCES.....	R.1
APPENDIX A. DERIVATION OF EQUATION 2.2.1.....	A.1
APPENDIX B: VARIANCES OF THE RESIDUAL MULTIPLE ACCESS INTERFERENCE FOR THE TOTAL AND THE WEIGHTED PARALLEL INTERFERENCE CANCELLATION RECEIVERS.....	A.2

List of Figures.

Figure 2.1: The time delay impulse multipath model.	2-7
Figure 2.2: The MRC diversity-based RAKE receiver.	2-7
Figure 2.3: Functional Block Diagram of the Total Parallel Interference Cancellation Receiver.	2-11
Figure 2.4: Functional Block Diagram of the Weighted Parallel Interference Cancellation Receiver.	2-12
Figure 2.5: Functional Block Diagram of the Partial Parallel Interference Cancellation Receiver.	2-12
Figure 2.6: Illustration of the multistage implementation of the PIC receiver.	2-13
Figure 2.7: BER Performance of the PIC Schemes with increasing SNR at the variance of the channel gain estimation error of 0.06.	2-16
Figure 2.8: BER performance of HD-PIC and SD-PIC with channel gain estimation error.	2-16
Figure 2.9: BER Performances of the HD-PIC and the SD-PIC with Channel Phase Estimation Errors.	2-17
Figure 2.10: BER performance of HD-PIC and SD-PIC with channel Gain and phase estimation errors.	2-17
Figure 2.11: BER performance of PIC schemes with channel gain estimation error and increasing stages.	2-18
Figure 2.12: BER performance of PIC schemes with channel phase estimation error and increasing stages.	2-18
Figure 2.13: BER results to show the accuracy of the proposed analytical model for the RAKE receiver.	2-26
Figure 2.14: BER vs SNR for RAKE receiver and the total PIC receiver. $L=3, M=3, m=1, \delta=0.2, k=10, N=15$.	2-26
Figure 2.15: BER vs SNR for RAKE receiver and the total PIC receiver. $L=5, M=5, m=1, \delta=0.2, k=10, N=15$.	2-27
Figure 2.16: BER vs SNR for RAKE receiver and the first stage of weighted PIC receiver. $L=3, M=3, m=1, \delta=0.2, k=10, N=15$. Cancellation weight = 0.7.	2-27

Figure 2.17: BER vs SNR for RAKE receiver and the two stages of weighted PIC receiver. $L=3, M=3, m=1, \delta=0.2, k=10, N=15$. Cancellation weight = 0.7.	2-28
Figure 2.18: BER vs SNR for three stages of weighted PIC receiver. $L=3, M=3, m=0.75, \delta=0.2, k=10, N=15$.	2-29
Figure 3.1: BER vs SNR results for the single stage adaptive PIC receiver.	3-8
Figure 3.2: BER vs SNR results for the two stage adaptive PIC receiver.	3-8
Figure 4.1: Iterative Multiuser Detector for Turbo Coded Systems.	4-4
Figure 4.2: The nonlinear dynamic model of the turbo decoder.	4-7
Figure 4.3: Functional block diagram of the iterative interference cancellation receiver.	4-11
Figure 4.4: Error rate performances of the iterative interference cancellation receiver. Framelength=200.	4-12
Figure 4.5: Iteration Schedule for the iterative interference cancellation receiver.	4-15
Figure 4.6: Error rate performance of the iterative interference cancellation receiver after one iteration.	4-16
Figure 4.7: Error rate performance of the iterative interference cancellation receiver after two iterations.	4-16
Figure 4.8: Error rate performance of the iterative interference cancellation receiver after three iterations. Dashed line for simulation results. Solid line for analytical results.	4-17
Figure 4.9(a): The noise figure of the turbo decoder over $\left(\frac{PT}{N_o}\right)_{dB}$ of 0dB to 4dB.	4-17
Figure 4.9(b): The noise figure of the turbo decoder over $\left(\frac{PT}{N_o}\right)_{dB}$ of 2.5dB to 3dB.	4-18
Figure 4.10: Convergence Analysis of the Iterative Interference Cancellation Receiver.	4-18
Figure 5.1: A Turbo Coded CDMA transmission System.	5-3
Figure 5.2: The Proposed Iterative Multiuser Detector.	5-7

Figure 5.3: Forward and reverse state probability recursions.	5-10
Figure 5.4: Functional diagram of the proposed iterative multiuser detector.	5-14
Figure 5.5: Comparison of the performance of the “Turbo IC” and the Conventional Iterative Interference Canceller. Cross-Correlation = 0.25, K=10, Framelength=200.	5-16
Figure 5.6: Comparison of the performance of the “Turbo IC” and the Conventional Iterative Interference Canceller. Cross-Correlation = 0.3, K=10, Framelength=200.	5-17
Figure 5.7: Performance of the “Turbo IC” with various cross-correlation values. K=10, Framelength=200.	5-17
Figure 5.8: Performance of the “Turbo IC” with various numbers of users. Cross correlation=0.3, Framelength=200.	5-18
Figure 5.9: Performance of the “Turbo IC” in near-far scenarios. Cross-correlation=0.3, Framelength=200.	5-19
Figure 5.10: Performance of the “Turbo IC” in the asynchronous DS-CDMA system.	5-21
Figure 6.1(a): Illustration of the bit interaction of interfering bits in a dual multirate CDMA system when the user of interest has the higher processing gain.	6-5
Figure 6.1(b): Illustration of the bit interaction of interfering bits in a dual multirate CDMA system when the user of interest has the lower processing gain.	6-5
Figure 6.2: BER performance of the multiuser detector in the multirate CDMA system with variations in the number of detection iterations.	6-7
Figure 6.3: BER performance of the multiuser detector in the multirate CDMA system with variations in the size of the framelength.	6-8
Figure 6.4: Comparison of the BER performance of the multiuser detector and the Turbo decoder in the multirate CDMA system. Number of iteration is one. Frame Length = 200.	6-8
Figure B.1: BER vs SNR the first stage of Total PIC receiver. L=3, M=3, m=1, $\delta=0.2$, k=10, N=15.	A-7
Figure B.2: BER vs SNR the first stage of weighted PIC receiver. L=3, M=3, m=1, $\delta=0.2$, k=10, N=15. Cancellation weight = 0.7.	A-8

List of Acronyms.

AWGN	Additive White Gaussian Noise.
BER	Bit Error Rate.
BPSK	Binary Phase Shift Keying.
CDMA	Code Division Multiple Access.
DA	Data Aided.
DD	Decision Directed.
DFE	Decision Feedback Equaliser.
DS-CDMA	Direct Sequence Code Division Multiple Access.
FEC	Forward Error Correcting.
GA	Gaussian Approximation.
HD-PIC	Hard Tentative Decision Parallel Interference Cancellation.
LDPC	Low Density Parity Check.
LMS	Least Mean Square.
MAI	Multiple Access Interference.
MAP	Maximum a-Posteriori..
MIMO	Multiple Input Multiple Output.
MIP	Multipath Intensity Profile.
ML	Maximum Likelihood.
MLSE	Maximum Likelihood Sequence Estimation.
MMSE	Minimum Mean Square Error.
MRC	Maximum Ratio Combining.
MUD	Multiuser Detector.
PDF	Probability Density Function.
PIC	Parallel Interference Cancellation.
PSD	Power Spectral Density.
RSC	Recursive Systematic Convolutional.
SD-PIC	Soft Tentative Decision Parallel Interference Cancellation.
SI	Side Information.

SIC	Serial Interference Cancellation.
SNR	Signal-to-Noise Ratio.
UMTS	Universal Mobile Telecommunication System.
WCDMA	Wideband Code Division Multiple Access

Acknowledgements.

I would like to thank my PhD dissertation supervisor, Professor Fambirai Takawira, for his guidance and valuable suggestions throughout the course of this work.

The support received from Telkom SA and Alcatel SA under the Center of Excellence programme is gratefully acknowledged.

Support, suggestions and comments received from my colleagues at the Centre for Radio Access Technologies of the University of KwaZulu-Natal are gratefully acknowledged. Particularly, appreciation is due to Tom Walingo for his steadfast support during the very trying days of this work and to Bruce Harrison, the network administrator, for making the network available for running simulations for this work.

I would like to thank the very many people who have been sources of encouragement to me at critical junctions in my journey through the pursuit of academic excellence. First of all is my mother, Cecilia Olabisi Bejide, without whose efforts I will definitely not have the opportunity of a University education nor have the privilege of presenting this dissertation, and my father J. D. Bejide for his many encouragements. My gratitude goes also to Dr. S. Adeniran, of the Obafemi Awolowo University, Nigeria, who is a great influence on my academic career and my perception of issues. I would also want to thank Prof. G. O. Ajayi, also of the Obafemi Awolowo University, Nigeria, for creating an enabling environment for me to dream and to pursue my dreams.

At this juncture I would like to remember the late Caroline Olusola Odeyemi a sister and a worthy role model.

Last but definitely not the least I would like to thank my wife, Olanike, and my daughter, Oluwatosin, for their patience and understanding.

I give thanks unto the LORD; for he is good: for his mercy endures for ever.

Chapter 1

Introduction

A strong candidate for the actualisation of the goal of “communication anywhere” is wireless communication. With wireless communication technology, there is no physical restriction on where information can be exchanged. Because many users will be accessing the common communication channel in wireless communication, there is therefore the need to devise means of sharing the communication channel. This is to prevent interference arising from the effects of the signals of other users that access the channel simultaneously. Some techniques have been developed to allow simultaneous access of a communication channel by many users. These techniques are referred to as multiple access techniques.

Code Division Multiple Access (CDMA) is an enabling multiple access technology for the purpose of providing wideband services in wireless communication. CDMA is the access technology specified for the second generation cellular system IS-95 [Gar97] and for various third generation cellular communication systems like the Universal Mobile Telecommunication System (UMTS) [Chi92], and Wideband CDMA (WCDMA) [Pra98]. CDMA is also the access technology for wireless local area network systems like the IEEE 802.11 standard [Gar97]. Numerous satellite communication systems also use CDMA as their radio access technology [Mag94]. In general CDMA has received a wide acceptance in the communication industry.

The interest in CDMA can be attributed to some of its advantages over the narrowband systems. Some of the advantages are [Mag94][Sch77][Vit79]:

- Low probability of Interception,
- Multipath mitigation capability,
- Anti-jam capability,
- Interference rejection capability,
- Multiple access and
- Accurate ranging.

However, the performance of the CDMA systems degrades when they are used in a multiple access environment. In such a situation the capacity of the system decreases and the probability of error of the system increases as the number of co-located systems on the channel increases. The interference on the signal of the user of interest from other co-located CDMA systems is referred to as the Multiple Access Interference (MAI).

Multiuser detection techniques are developed in order to counteract the effects of the multiple access interference. The objective of designing multiuser detectors is to increase the fidelity of the signal of the user of interest to the level it would have been if other CDMA systems are not accessing the channel.

1.1. Multiuser Detection in Uncoded CDMA Systems

Multiuser Detectors (MUD) are designed by using some characteristics of all the received signals in the multiple access channel to reduce the effects of the multiple access interference, mutually on all the users. Multiuser information theory is a discipline that is many decades old. With respect to CDMA however, the pioneering work in designing a MUD for CDMA is the work of Verdu [Ver86a] that was published in 1986. The detector of [Ver86a] is often referred to as the optimum multiuser detector because its performance is exactly the single user performance.

In the optimum MUD, the Maximum Likelihood Sequence Estimation (MLSE) of the signal of the user of interest is performed given the signals of the other users in the multiple access channel [Mos96][Ver86a][And02]. Although the MLSE receiver has an optimum performance, its shortcoming is its prohibitively high computational complexity. The computational complexity of the optimum MUD increases exponentially with the number of users (K), that is $O(2^K)$.

Because of the high complexity of the optimum multiuser detector, several sub-optimal multiuser detectors have been developed. These types of receivers have computational complexities that are very low when compared with that of the optimum multiuser detector. The low complexity is, however, at the expense of performance. Sub-optimal MUD can be classified into two categories:

1. Linear Multiuser Detectors,
2. Non-Linear Multiuser Detectors.

In linear MUD, linear filters are used to extract the signal of the user of interest from the received signal and to suppress the MAI at the same time. Examples of linear MUD's includes the decorrelating MUD (which multiplies the received signal sequence by the inverse of the correlation matrix of all the active users on the channel), the interference whitening filter (in which the filter coefficients are dependent on the spreading code of the user of interest), the Minimum Mean Square Error (MMSE) receiver (in which the MMSE criterion is invoked in detecting the signal of the user of interest) [Ver86a][Ver86b][Ver89][Lup89][Mos96][Hon95].

Nonlinear MUD includes the Decision Feedback Equaliser (DFE) receiver and interference cancellation receivers. Interference cancellation receivers can be classified as Serial Interference Cancellers (SIC) and Parallel Interference Cancellers (PIC) [Var90][Div95][Puz99][Yoo93][Hui98][Div98][Vit90].

The SIC and the PIC have received a considerable amount of attention in the literature because of their ease of practical implementation. In the SIC, the interferences of all the users are estimated. For the user of interest, the estimated interference due to all other users are subtracted, one user at a time (starting with the user that has the highest power), from the received signal. An improved received signal, from the point of view of the user of interest, is obtained as the estimate of the interference of each user is sequentially subtracted [Vit90][Mos96].

In PIC, the MAI on the user of interest is estimated at once from the signal of all other co-located users. The estimated MAI is then subtracted from the received signal (from the point of view of the user of interest). This procedure is carried-out for all the users simultaneously (in parallel).

An advantage of the PIC over the SIC is that the delay experienced in SIC is much more than the delay experienced in PIC. This has made the PIC much more accepted in practical system designs than the SIC [Mos96]. A more detailed description of the PIC scheme is made in Chapter 2.

1.2 Multiuser Detection for Coded CDMA Systems

Error correcting codes are often used to improve the performance of CDMA systems. Realizing that error correction alone cannot remove the effects of the multiple access interference effectively, a lot of emphasis is now being placed on designing multiuser detectors for channel coded CDMA systems. Pioneering work in this respect is the work of Giallorenzi and Wilson [Gia96a] where the optimum detector of [Ver86a] is combined with convolutional decoding. The complexity of the receiver of [Gia96a] increases exponentially with the product of the number of users and the constraint length of the convolutional encoder. Some sub-optimal implementations of the receiver of [Gia96a] were proposed in [Gia96b]. Another suboptimum type of the optimum MUD with

channel coding is found in [Wei97] where the low complexity breadth-first algorithm of [Sim90] was used in the MLSE of [Gia96a] for convolutionally coded CDMA systems.

The advent of Turbo codes [Ber93] and the generalization of the “Turbo principle” in many aspects of digital communication [Hag97] have inspired the development of many “iterative” multiuser detectors. In [Ale99], the “super trellis” of the joint convolutionally coded and the time varying CDMA coded system was transverse, based on the Maximum a-Posteriori (MAP) criterion. This is in contrast to the work of [Gia96a] where the Viterbi algorithm was used. The work of [Ale99] has the same prohibitive complexity as the receiver designed in [Gia96a].

Work done on reducing the complexity of iterative detectors to levels that can be practically implemented has mainly focused on combining various sub-optimal multiuser detectors with iterative channel decoding in an integrated manner. The decorrelating decision feedback MUD was studied in [Hsu01] for a Turbo coded DS-CDMA system. The MMSE filter was iteratively combined with channel decoding for the convolutionally coded CDMA system in [Gam00]. Several other attempts to combine sub-optimal multiuser detectors with channel decoding in an iterative manner can be found in the following references: [Mar01a][Mar01b][Wan99][Qin01].

On the combination of interference cancellation and iterative decoding, an iterative interference canceller was proposed for convolutionally coded CDMA in [Ale98]. This scheme integrates the subtraction of the estimated multiple access interference and channel decoding. The iterative interference canceller was also studied in [Ker99] and [Moh99]. The iterative receiver of [Ker99] tries to improve on the ones proposed in [Ale98] and [Moh99] by subtracting a weighted estimate of the multiple access interference from the received signal. The partial interference canceller of [Div98] was combined with Turbo decoding in [Wu01]. In a nutshell, iterative interference cancellation (and some of its variants) has received wide acceptance. This could possibly be due to its low level of complexity. Iterative interference cancellers for turbo coded CDMA are discussed in greater details in Chapters 4 and 5.

A major problem with iterative interference cancellers is that the direct subtraction of the estimated MAI from the received signal could lead to erroneous detection when the MAI estimation is not very reliable [Shi01]. This is more likely when the cross-correlation between the signals of the co-located users is high. In that case, the error variance of the iterative interference canceller becomes very large [Bej03][Ker99]. It is, therefore, necessary to find a novel way of using the MAI estimate in Turbo coded CDMA systems to mitigate the effects of the MAI effectively.

1.3 Goals and Contributions of the Dissertation

Much of the work done on the development of MUD for channel coded CDMA systems have focused on convolutionally coded CDMA. Little work has been done on investigating the combination of MUD and Turbo coding. Also, the concept of iterative detection [Hag97] opens a lot of opportunities on how channel decoding and other detection processes like the MUD could be combined. The statements in the two sentences above motivated this work. This dissertation investigates performances of existing iterative interference cancellation techniques for uncoded and turbo coded CDMA systems and proposes a novel way of implementing the MUD-channel decoding integration (with emphasis on improved error rate performance and increased capacity).

In the process of achieving the goals set for this work, the following original contributions were made to the field of MUD for CDMA:

1. In Chapter 2, analytical models for various types of PIC are presented. These models are shown to be in good agreement with simulation results. The models are useful in the Bit Error Rate (BER) analysis of PIC receivers for DS-CDMA. Also, an expression for the optimal cancellation weights for the weighted PIC receiver is presented.

2. In Chapter 3, adaptive PIC receivers that are based on the Least Mean Square (LMS) algorithm are presented. An analytical model for the adaptive PIC receivers is also presented.
3. The density evolution approach is used in the analysis of iterative interference cancellers for Turbo coded CDMA systems in Chapter 4. A methodology for the convergence analysis of the receiver is presented by using the density evolution based Gaussian approximation method.
4. A novel iterative interference canceller is developed in Chapter 5. The detector is developed by using the estimate of the MAI as additional information in the iterative decoder. A direct subtraction of the estimate of the MAI is avoided in order to prevent the effects of the estimation error variance. The developed receiver has a better error rate performance than that of the existing iterative interference canceller. The improvement in performance is much more obvious at higher values of cross correlation between users.

1.4 List of Publications.

The following publications have resulted from this work

- E O Bejide and F Takawira, "Performance of Parallel Interference Cancellation Receivers for DS-CDMA in Frequency-Selective Fading Channels". *In: SATCAM 2000 Proceedings of the Communications and Signal Processing Chapter of the SA Section of the IEEE*, pp. 48-53, Somerset West. (CD-Rom. ISBN: 0-620-26497-7)
- E O Bejide and F Takawira, "Error Probabilities of Parallel Interference Cancellers for CDMA in Nakagami Multipath Fading Channel with an Imperfect Channel Estimation" *South Africa Telecommunication and Networking Conference (SATNAC)*, 2-5 September 2001, pp. 147-151 (CD-Rom. ISBN: 0-620-27769-6).

- E. Oluremi Bejide and F. Takawira, "An Iterative Multiuser Detector for DS-CDMA.". South Africa Telecommunication and Networking Conference (SATNAC), 7-10 September 2003.
- Emmanuel Oluremi Bejide and F. Takawira, "An Iterative Multiuser Detector for DS-CDMA Systems in Multipath Fading Channels". IEEE Wireless Communication and Networking Conference, March 2004.
- Emmanuel Oluremi Bejide and F. Takawira, "Performance of MRC diversity RAKE Receivers for DS-CDMA systems in Nakagami Multipath Fading Channels". Submitted to IEEE Communication Letters.
- Emmanuel Oluremi Bejide and F. Takawira, "Iterative Multiuser Detector for Cellular CDMA Systems". Submitted to IEEE Transactions on Vehicular Technology.
- Emmanuel Oluremi Bejide and F. Takawira, "Analytical Models for the Error Rate Performance of Parallel Interference Cancellation Receivers". To be submitted to IEE Proceedings Communications.

Chapter 2

Performance Analysis of Parallel Interference Cancellation Techniques for DS-CDMA in Multipath Fading Channels.

2.1 Introduction.

Parallel Interference Cancellation (PIC) is a widely accepted technique in the wireless communication community [Mos96]. This technique has been the subject of many research activities in the last decade. The wide acceptance of the PIC technique is due to its low complexity of implementation while still providing substantial reductions in the effect of the multiple access interference.

Parallel interference cancellation was first proposed in [Var90]. It was derived through the Maximum Likelihood (ML) estimation of the desired user's transmitted bit, given the received signal. For illustration purpose, let the transmitted bit at some particular time instance for user j ($1 \leq j \leq K$) in a multiple access environment having K number of users that are transmitting simultaneously be b_j . Let the signal at the output of a matched filter that is matched to the signature sequence of user j be Y . The parallel interference cancellation technique determines $P(b_j|Y)$. The ML estimation, as computed in [Var90], produces a receiver structure in which the improved received signal for the user of interest is obtained by the subtraction of the estimate of the multiple access interference from the received signal. The improved received signal that results is then matched filtered to determine the transmitted bit of the user of interest.

Parallel interference cancellation can be (and is often) implemented in a multistage manner. Each additional PIC stage in a multistage system improves on the performance obtainable from the previous stage.

With improvement in the fidelity of signals at subsequent cancellation stages of the multistage PIC receiver, the reliability of the estimate of the multiple access interference that is obtained by using these statistics increases. This prompted the development of a variant of the PIC receiver that is referred to as the weighted PIC receiver. In this receiver type fractional value of the estimated multiple access interference is subtracted from the received signal. The amount of the fraction that is subtracted is increased as the processing moves from a lower stage to higher stages of interference cancellation. This is done because estimates of the multiple access interference in higher stages of interference cancellation are more reliable than at lower stages of interference cancellation.

In [Div98] another type of PIC technique was derived based on the ML estimation of the message bit of the user of interest, given the received signal and the estimated message bit at the immediately previous cancellation stage. That is $P(b_j | Y, \hat{b}_j^{(f-1)})$. This is the detection metric used at the f^{th} cancellation stage. This resulted in a PIC receiver in which fractions of the estimated MAI and the soft information on the transmitted bit of the user of interest in the $(f-1)^{th}$ cancellation stage are subtracted from some fraction of the received signal. This type of PIC receiver is referred to as the partial PIC receiver. PIC receivers that have no form of fractional cancellation are referred to as total PIC receivers.

In estimating the MAI, the tentative decision that is taken on the soft “information” of all other co-located users could be any of the many decision techniques that are available. The soft, the hard, the threshold and the tanh () decision techniques have been suggested in the literature [Div98][Hui98][Div95]. It has also been noted, as also presented briefly

in Section 2.3 of this Chapter, that the use of the soft tentative decision leads to PIC receivers that have error rate performances that are very poor when compared with those of PIC receivers that are based on the hard tentative decision[Bue99][Cor99]. This behaviour was explained in [Bue99] to be due to the fact that the decision statistic is biased when the soft tentative decision is used. In this dissertation therefore, our focus shall be on PIC receivers that are based on the hard tentative decision.

Error rate performance analyses of the total PIC have been presented in [Yoo93] and [Hui98] for the Rayleigh multipath fading channel. To the best of our knowledge, no work has been presented in the literature on the error rate performance analysis of the weighted PIC receivers in the literature. Also, error rate performance analyses of the PIC receivers in the Nakagami multipath fading channel have not been presented in the literature. It is important to have analytical models for these receivers in the Nakagami multipath fading channel for the following reasons

[Alh85][Lom99][Woj86][Eft97][Eng95]:

1. The Nakagami distribution fits experimental data that are obtained from urban radio multipath channels accurately.
2. The Nakagami distribution is a generalized distribution which can model different environments and could be approximated to different distributions. For instance, the Rayleigh, the Rician and the one-sided Gaussian distributions are special cases of the Nakagami distribution.
3. The Nakagami distribution can account for shadowing and other large-scale effects.
4. Amplitude fading that is due to ionospheric scintillation follows the Nakagami distribution.

In this Chapter therefore, the error rate analyses of the total and the weighted PIC are presented for the Nakagami multipath fading channel. The Gaussian approximation approach is used in the analyses. The Gaussian approximation method has been found to be accurate for the error rate performance analyses of DS-CDMA systems in the

multipath fading environment [Jul02]. The following contributions are made in this chapter:

1. A simple expression for the average BER of DS-CDMA systems in the Nakagami multipath fading channel with Maximum Ratio Combining (MRC) is proposed. The expression that is obtained is computationally simpler than the result that was reported in [Eng95].
2. A procedure for determining the average BER of the total and the weighted PIC receivers in the Nakagami multipath fading channel is presented. The approach that is used in this Chapter for the estimation of the variance of the residual MAI is different from and more accurate than methods that have been reported in the literature so far.
3. The expression for the optimal cancellation weights for the weighted PIC receiver is presented.

The rest of the Chapter is outlined as follows. The system model for the asynchronous DS-CDMA system is presented in Section 2.2. In Section 2.3 a comparison between the PIC receiver that employs the hard tentative decision and the PIC receiver that employs the soft tentative decision is made. Analytical models for the error rate performance of the PIC receivers are presented in Section 2.4. Optimal cancellation weights for the weighted PIC receiver are derived in Section 2.5. Numerical results are presented in Section 2.6. Section 2.7 concludes this Chapter.

2.2 System Model

2.2.1 Received Signal Model

The signal that is transmitted by a single user k ($1 \leq k \leq K$) in a multiple access scenario that comprises of K active users can be represented as

$$s_k(t) = \sqrt{2P_k} a_k(t) b_k(t) \cos(\omega_c t) \quad (2.1)$$

Notation P_k represents the power of the signal of user k , $a_k(t)$ represents the antipodal waveform of the random spreading code of user k , ω_c is the carrier frequency and $b_k(t)$ represents the antipodal waveform of the message sequence of user k . Notation T_c represents the bit duration of the spreading code. The summation of the signals that are transmitted by all users in the multiple access environment can be represented as

$$S(t) = \sum_{k=1}^K \sqrt{2P_k} a_k(t) b_k(t) \cos(\omega_c t + \phi_k) \quad (2.2)$$

ϕ_k is the modulation angle of user k .

The multipath fading channel as seen by the receiver of user k is modeled as a time-delay impulse channel model [Eng95][Pro01] as illustrated in Figure 2.1. The response of the channel can be represented as

$$h_k(t) = \sum_{l=1}^L \beta_{lk} \delta(t - \tau_{lk}) e^{i\theta_{lk}} \quad (2.3)$$

where β_{lk} , τ_{lk} and θ_{lk} are the l^{th} path's channel gain, delay and phase shift respectively for the k^{th} user's signal. We assume that $\tau_{lk} \in [0, T]$ and is independent of the channel gain coefficient. Notation T is the message bit duration. Also, let the processing gain of the system be represented as N . The received signal can therefore be represented as

$$r(t) = \sum_{k=1}^K \sqrt{2P_k} \sum_{l=1}^L \beta_{lk} a_k(t - \tau_{lk}) b_k(t - \tau_{lk}) \cos(\omega_c t + \psi_{lk}) + n(t) \quad (2.4)$$

$\psi_{lk} = \theta_{lk} + \phi_k + \omega_c \tau_{lk}$ and $\psi_{lk} \in [0, 2\pi]$. Each user's signals are taken to be propagated through L different paths.

The Maximum Ratio Combining (MRC) based RAKE receiver is used for diversity combining. Figure 2.2 shows a rake receiver that employs the MRC diversity scheme.

The output of the RAKE receiver that has M fingers can be expressed as [Eft97]

$$\begin{aligned}
 X_j &= \sum_{\zeta=1}^M \left\{ \int_{\tau_{\zeta,j}}^{\tau_{\zeta,j}+T} \beta_{\zeta,j} r(t) a_j(t-\tau_{\zeta,j}) \cos(\omega_c t + \psi_{\zeta,j}) dt \right\} \\
 &= \sum_{\zeta=1}^M \{ U_{\zeta,j} + V_{\zeta,j} + W_{\zeta,j} + \eta_{\zeta} \}
 \end{aligned} \tag{2.5}$$

where

$$U_{j\zeta} = \sqrt{\frac{P_j}{2}} b_{o,j} T (\beta_{\zeta,j})^2 \tag{2.6}$$

$$V_{j\zeta} = \sum_{\substack{k=1 \\ k \neq j}}^K \sqrt{\frac{P_k}{2}} \sum_{l=1}^L \beta_{\zeta,j} \beta_{lk} \{ b_{-1,k} R_{kj}(\tau_{lk} - \tau_{\zeta,j}) + b_{o,k} \hat{R}_{kj}(\tau_{lk} - \tau_{\zeta,j}) \} \cos(\psi_{lk} - \psi_{\zeta,j}) \tag{2.7}$$

$$W_{j\zeta} = \sqrt{\frac{P_j}{2}} \sum_{\substack{l=1 \\ l \neq \zeta}}^L \beta_{\zeta,j} \beta_{lj} \{ b_{-1,j} R_{jj}(\tau_{lj} - \tau_{\zeta,j}) + b_{o,j} \hat{R}_{jj}(\tau_{lj} - \tau_{\zeta,j}) \} \cos(\psi_{lj} - \psi_{\zeta,j}) \tag{2.8}$$

$$\eta_{\zeta} = \int_{\zeta T_c}^{T+\zeta T_c} n(t) \beta_{\zeta,j} a_j(t-\tau_{\zeta,j}) \cos(\omega_c t + \psi_{\zeta,j}) dt \tag{2.9}$$

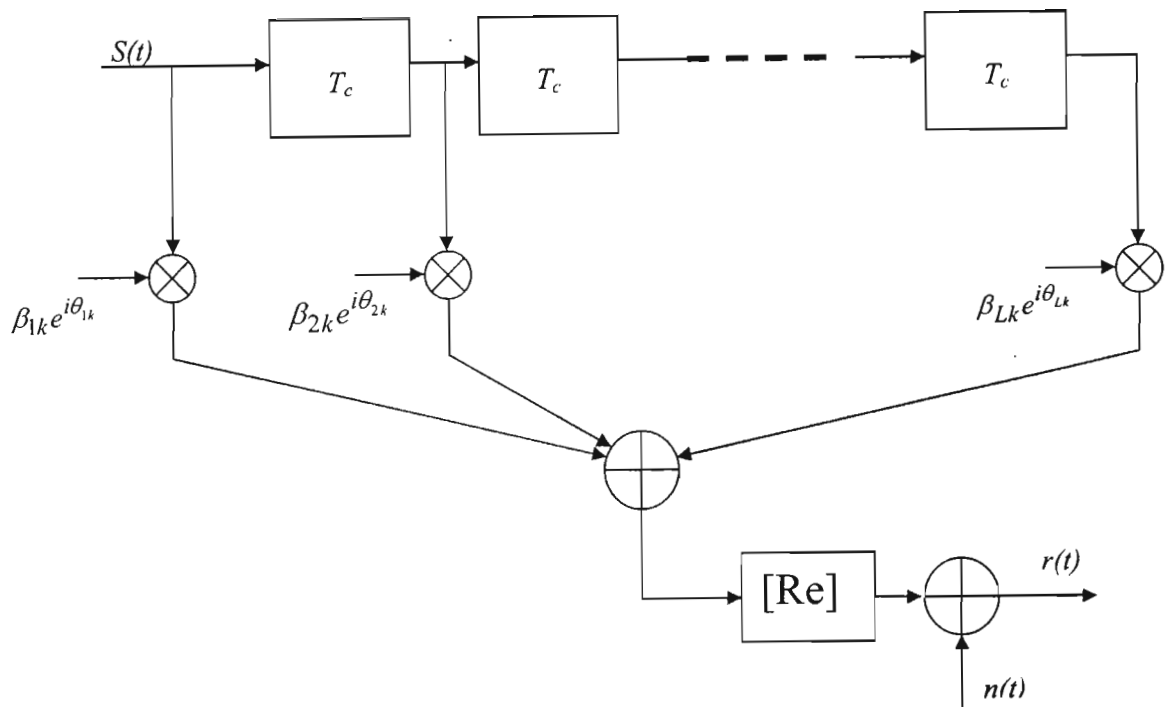


Figure 2.1: The time delay impulse multipath model.

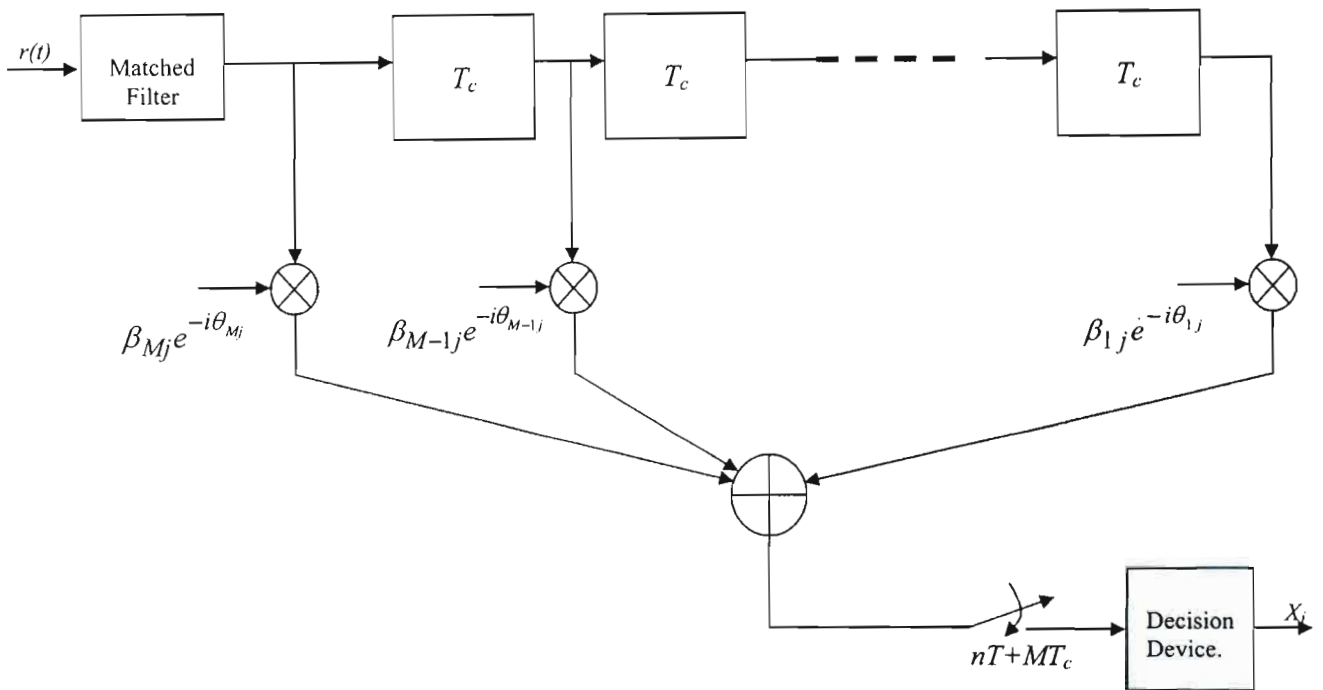


Figure 2.2: The MRC diversity-based RAKE receiver.

Notations $U_{\zeta j}, V_{\zeta j}, W_{\zeta j}$ and η_{ζ} represent the desired user's signal, the MAI component, the Side Interference (SI) component and the AWGN component respectively. Also, $R_{kj}(\tau) = \int_0^{\tau} a_k(t-\tau)a_j(t)dt$ and $\hat{R}_{kj}(\tau) = \int_{\tau}^T a_k(t-\tau)a_j(t)dt$. Notations $b_{o,k}$ and $b_{-1,k}$ represent the message bit to be detected and the preceding bit respectively.

The relationship between the power of the direct signal and other reflected signals in the multipath fading channel has been modeled in a variety of ways. This relationship is referred to as the Multipath Intensity Profile (MIP) which is defined as the average power at the output of the channel as a function of path delay [Eft97]. The uniform, the exponential and the Gaussian MIP has been discussed in the literature [Eng95] [Eft97]. A measure of the average power of a given path is the second moment of the fading gain coefficient for that path. In a multipath channel that has the uniform MIP, all signals on all the propagation paths have the same second moment, that is

$E(\beta_{1k}^2) = E(\beta_{2k}^2) = \dots = E(\beta_{Lk}^2)$ for a multipath channel that has L paths. In the multipath channel that has the exponential MIP the second moment of the first incoming path is related to the second moment of other paths through the relationship $E(\beta_{lk}^2) = E(\beta_{1k}^2)e^{-\delta l}$ with δ being the decay factor ($\delta \geq 0$).

Experimental measurements made by Turin [Tur72] have shown that the MIP in urban environment is exponential. Based on this understanding, the exponential MIP will be used throughout this dissertation.

The channel gain coefficients used in this Chapter are modeled as Nakagami m -distribution variates having the Probability Density Function (PDF) given as

$$P(\beta) = \frac{2m^m \beta^{2m-1}}{\Gamma(m)\Omega^m} e^{-(m/\Omega)\beta^2} \tag{2.10}$$

where $\Omega = E[\beta^2]$ and $m = \frac{\Omega^2}{\text{var}[(\beta)^2]} = \frac{\Omega^2}{E[(\beta^2 - \Omega)^2]}$. The variable Ω defines the second moment of β . In particular $\Omega_{nk} = E[(\beta_{nk})^2]$. With our selection of the exponential multipath intensity profile (MIP), Ω_{nk} is related to the signal strength of the first path by $\Omega_{nk} = \Omega_{1k}e^{-n\delta}$. In this dissertation, the second moments of the initial path's fading statistics of all users are modeled to be the same. Therefore we can simply write $\Omega_{nk} = \Omega_1e^{-n\delta}$. Changing the values of m in equation (2.10) can enable us to change the channel model from a very good channel (with no fading) when $m = \infty$ and to the worst fading case when $m = 0.5$, the case when $m = 1$ corresponds to the Rayleigh fading distribution. Other fading models can be approximated by an appropriate selection of the parameter m .

2.2.2 Parallel Interference Cancellation Models.

Mathematical representations of the parallel interference cancellation are presented in this Section. For the total PIC receiver, tentative hard decisions are taken on the decision statistics of the users' signals in the system. For a given user of interest, tentative decisions from all other co-located users are used in the estimation of the MAI. The estimate of the MAI after the f^{th} stage in the multipath fading environment that was discussed in Section 2.2.1 of this dissertation can be expressed as

$$\hat{V}_{\zeta j}^{(f)} = \sum_{\substack{k=1 \\ k \neq j}}^K \sqrt{\frac{P_k}{2}} \sum_{l=1}^L \beta_{\zeta j} \beta_{lk} \left\{ \hat{b}_{-1,k}^{(f-1)} R_{kj}(\tau_{lk} - \tau_{\zeta j}) + \hat{b}_{0,k}^{(f-1)} \hat{R}_{kj}(\tau_{lk} - \tau_{\zeta j}) \right\} \cos(\psi_{lk} - \psi_{\zeta j}) \quad (2.11)$$

where $\hat{b}_{0,k}^{(f-1)}$ and $\hat{b}_{-1,k}^{(f-1)}$ represent the tentative bit of user k that correspond to the present and the immediately past instances respectively.

For the total PIC process, the output of the receiver at the end of the f^{th} cancellation stage can be expressed as

$$\hat{X}_j^{(f)} = X_j - \sum_{\zeta=1}^M \left\{ \hat{v}_{\zeta j}^{(f)} \right\} \quad (2.12)$$

For the weighted PIC receiver, the output of the receiver at the end of the f^{th} cancellation stage can be expressed as

$$\hat{X}_j^{(f)} = X_j - \lambda^{(f)} \sum_{\zeta=1}^M \left\{ \hat{v}_{\zeta j}^{(f)} \right\} \quad (2.13)$$

where $\lambda^{(f)}$ is the cancellation weight for the f^{th} cancellation stage.

Finally, the decision statistics at the end of the f^{th} cancellation stage for the partial PIC receiver can be expressed as

$$\hat{X}_j^{(f)} = \lambda^{(f)} \left(X_j - \sum_{\zeta=1}^M \left\{ \hat{v}_{\zeta j}^{(f)} \right\} \right) + (1 - \lambda^{(f)}) \hat{X}_j^{(f-1)} \quad (2.14)$$

Figures 2.3 to 2.5 show the functional block diagrams of the PIC techniques that are discussed in this chapter. The multistage implementation of the PIC scheme is presented in Figure 2.6. In these Figures, $R_k^f(t)$ represents the improved received signal at the end of the f^{th} cancellation stage for the k^{th} user.

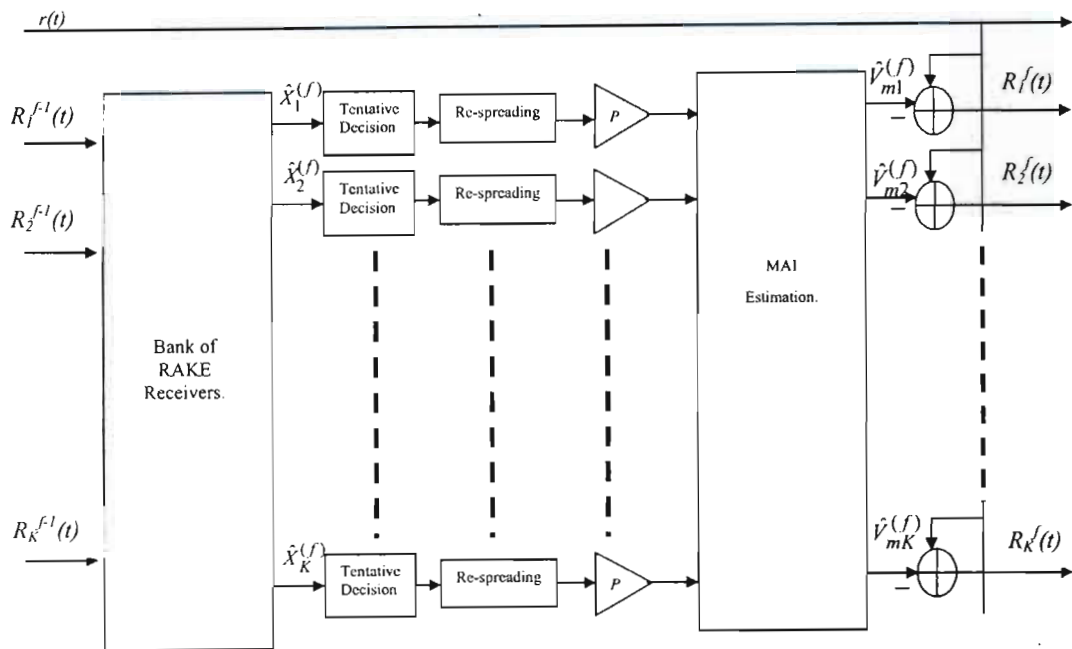


Figure 2.3: Functional Block Diagram of the Total Parallel Interference Cancellation Receiver.

2.3 Comparison of the Soft Tentative Decision-Based and the Hard Tentative Decision-Based PIC Receivers.

The objective of this Section is to compare the performances of the PIC receiver that is based on the hard tentative decision (HD-PIC) with those of the PIC receiver that is based on the soft tentative decision (SD-PIC). The comparison is carried-out through computer simulations. The studies are carried-out in the multipath Nakagami fading channel. For the purpose of the comparison, the bit rate of the system is taken to be 64Kbps. Performances with varying Signal to Noise Ratio (SNR) and with changing number of

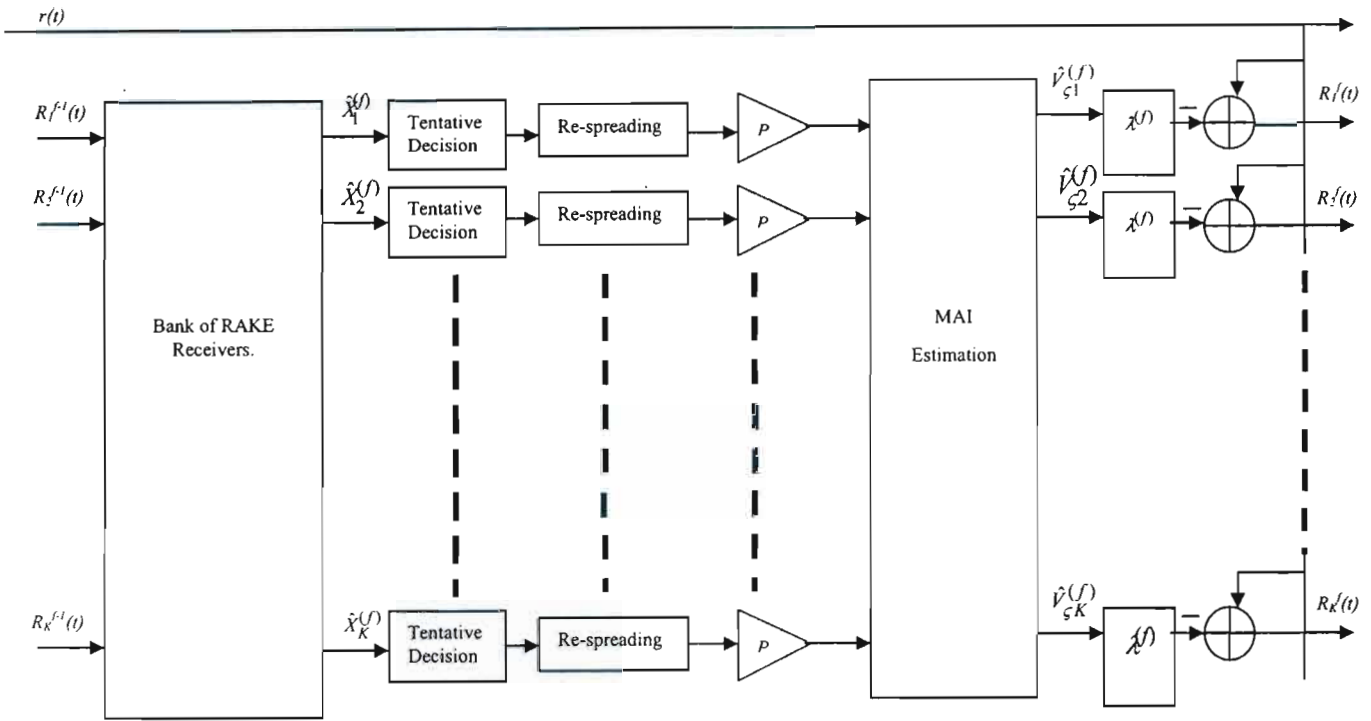


Figure 2.4: Functional Block Diagram of the Weighted Parallel Interference Cancellation Receiver.

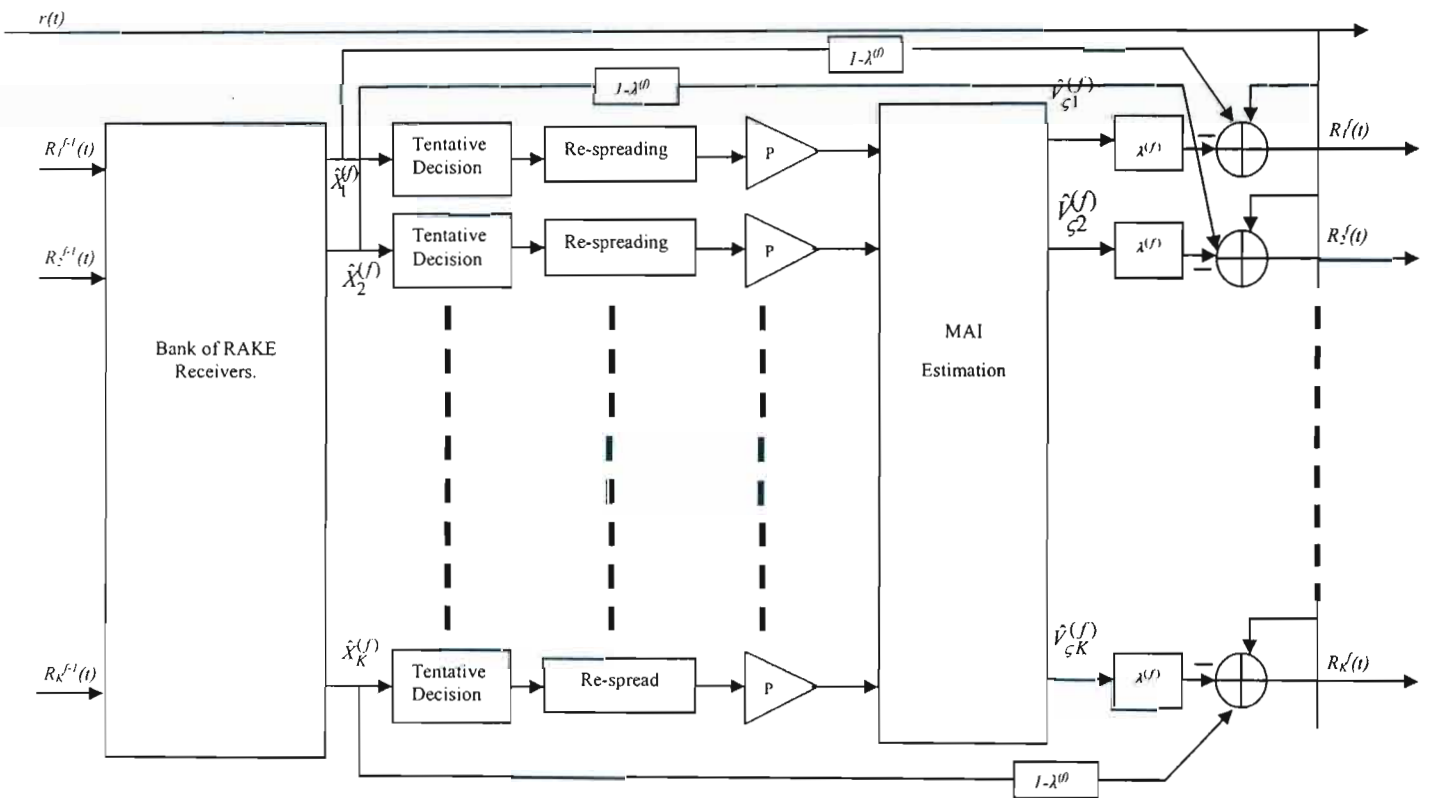


Figure 2.5: Functional Block Diagram of the Partial Parallel Interference Cancellation Receiver.

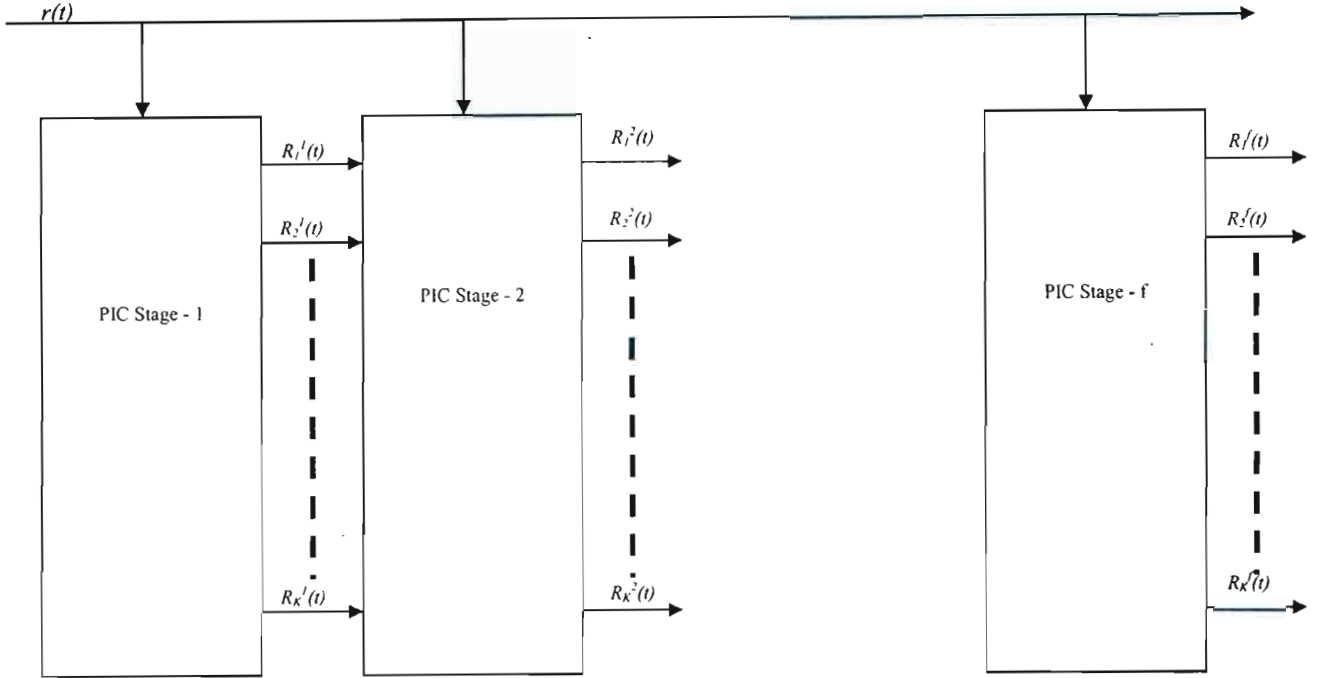


Figure 2.6: Illustration of the multistage implementation of the PIC receiver.

users are studied. The Signal-to-Noise (SNR) is defined as $\frac{PT\Omega_1}{N_0}$. Symbol P represents the transmitted power and this is taken to have the same value for all users. The unit energy constraint is assumed. Furthermore, simulation results are also presented for the situation where the channel fading gain and phase shift are erroneously estimated at the receiver.

Channel estimation techniques could either be Decision Directed (DD), where estimation is made based on the decision that is made on the received data, or Data Aided (DA), where a pilot signal is transmitted along with the data to aid the estimation process [Jun98]. In either case there are still some estimation errors that are made. Therefore, the estimated channel parameters are sums of the actual parameter and the estimation noise. That is

$$\hat{\beta}_{lk} = \beta_{lk} + \Delta\beta_{lk} \quad (2.15)$$

$$\hat{\phi}_{lk} = \phi_{lk} + \Delta\phi_{lk} \quad (2.16)$$

where $\Delta\beta_{lk}$ and $\Delta\phi_{lk}$ are errors made in estimating the channel gain and phase respectively. In this work, we modeled $\Delta\beta_{lk}$ and $\Delta\phi_{lk}$ as zero mean Gaussian random variables having variance of $\sigma_{\beta_{lk}}^2$ and $\sigma_{\phi_{lk}}^2$ respectively. This model has been reported to be valid for both the DA and the DD channel estimation techniques [Fre99][Eng97].

The performance of both the SD-PIC and the HD-PIC were studied through a computer simulation. A multiuser DS-CDMA system using Gold codes of length 63 was simulated for various channel parameter estimation errors with 5 active users. The value of the parameter m in the Nakagami fading channel model is selected as one. This corresponds to the Rayleigh fading channel model. The transmitting frequency of the active users was taken to be 2GHz and the mobiles were modeled to be traveling at a velocity of 80Km/h. Therefore, the maximum Doppler's spread, f_m , of the fading channel is 148.13Hz. The channel is modeled to be correlated. A MRC Rake receiver using 3 fingers was used both between cancellation stages and at the front-end of the receiver. The number of cancellation stages for both the HD-PIC and the SD-PIC detection was 3. We optimized the estimated MAI by using weighted sum of the estimate for each user for cancellation.

$$\text{That is } \hat{X}_j^{(f)} = X_j - \lambda_f \sum_{\zeta=1}^M \left\{ \hat{Y}_{\zeta j}^{(f)} \right\}.$$

In this comparison, we estimate the optimal cancellation weights through computer searches and we take the cancellation weights to be constant for all users on all paths at a given cancellation stage. For the HD-PIC, our optimal cancellation weights are 0.4, 0.7, and 1 for the first, second and the third stage of cancellation respectively. For the SD-PIC, our optimal cancellation weights are 0.0003, 0.0006, and 0.0009 for the first, second and the third stage of cancellation respectively. The very small fraction of the estimated MAI that is subtracted from the received signal in the case of the SD-PIC is due to the over-estimation of the MAI when the soft tentative decision is employed. It was even

found in [Div98] that the SD-PIC receiver performs worse than the RAKE receiver in some situations.

The simulation results are presented in Figures 2.7 to 2.12. We use notation like SD-PIC3 to represent the third stage of SD-PIC cancellation and so on. Figure 2.7 compares the BER performance of the HD-PIC and the SD-PIC with variation in SNR in a frequency selective fading channel when the variance of the channel gain estimation error is 0.06. The HD-PIC is observed to have a better performance than the SD-PIC. Our remaining simulation results are presented at 21dB SNR with variation in the variance of the channel estimation errors. From Figures 2.8 and 2.9, it is observed that although the HD-PIC has a better BER performance than the SD-PIC, (as also earlier noted for the additive white Gaussian noise channel in [Bue99]), the HD-PIC is more sensitive to both the channel gain and phase estimation error than the SD-PIC. However, there is more to be gained in using the HD-PIC receiver as long as accurate estimations of the channel gain and phase responses are obtained.

Figure 2.10 illustrates that the two PIC schemes are more sensitive to gain estimation errors than to phase estimation errors. From Figures 2.11 and 2.12 we observe that the sensitivity of the PIC schemes to channel estimation errors increases with increasing stages of cancellation as will be expected since the decision statistics at a cancellation stage are dependent on those of the previous stages. This way the unreliability of the decision made at previous stages is propagated to subsequent stages. With channel gain estimation error, the performance of the third stage of HD-PIC fell below that of its second stage when the variance of the estimation error was about 0.09. The same observation was made in the case of the SD-PIC at the variance of 0.14

The performance of PIC schemes in a fading channel was evaluated. The performance of the HD-PIC was observed to be better than that of the SD-PIC even with channel parameter estimation errors. The PIC schemes are more sensitive to channel gain estimation error than they are to channel phase estimation error.

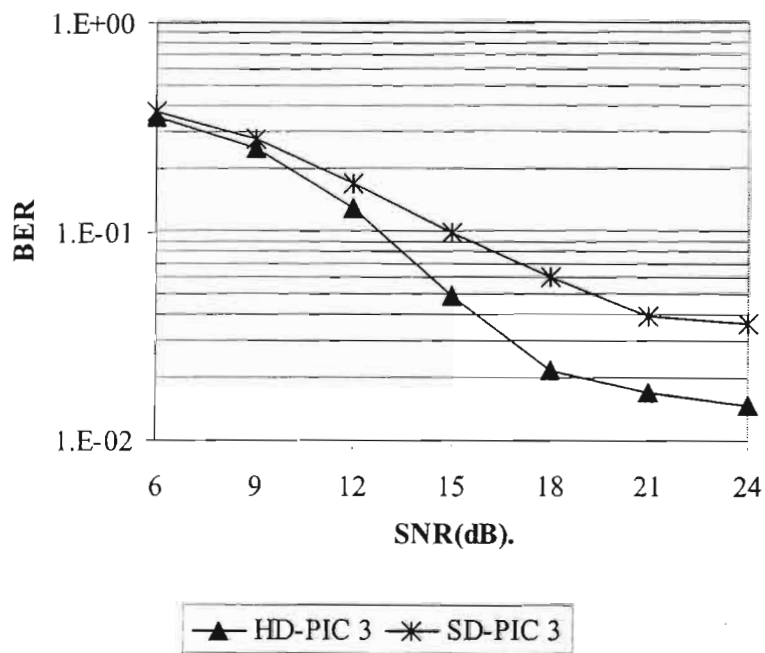


Figure 2.7: BER Performance of the PIC Schemes with increasing SNR at the variance of the channel gain estimation error of 0.06.

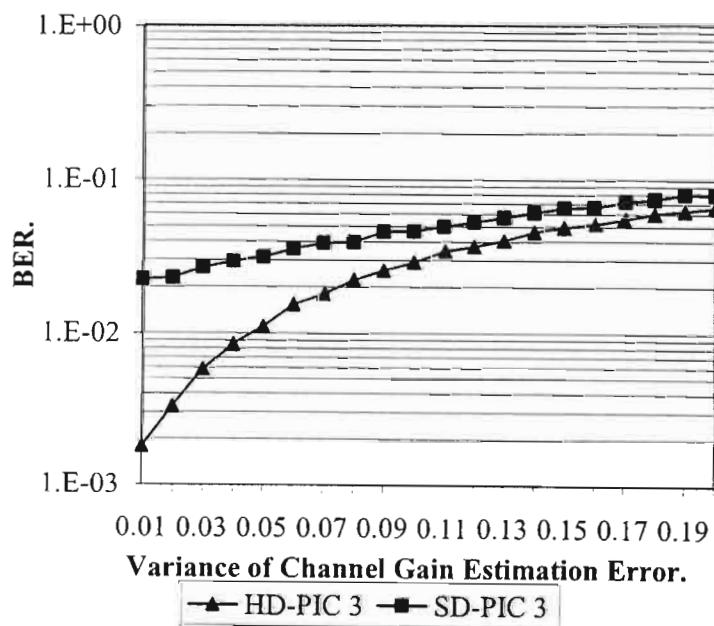


Figure 2.8: BER performance of HD-PIC and SD-PIC with channel gain estimation error.

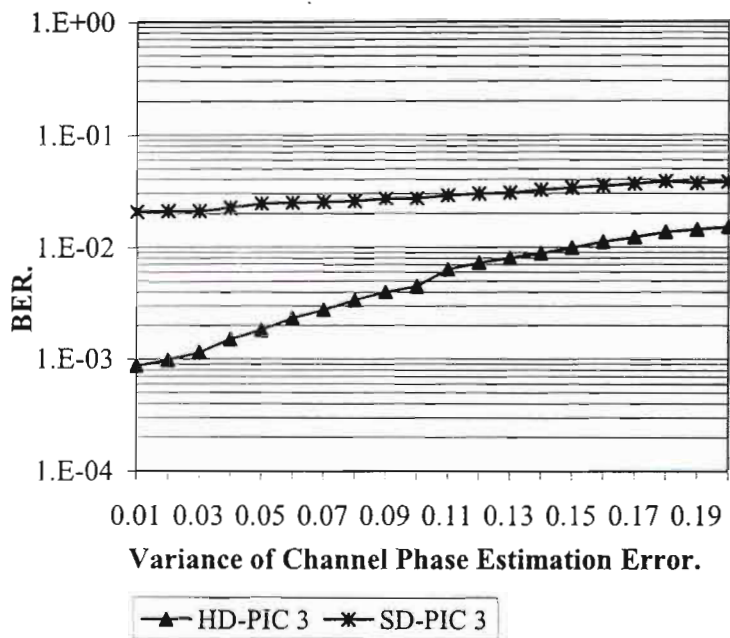


Figure 2.9: BER Performances of the HD-PIC and the SD-PIC with Channel Phase Estimation Errors.

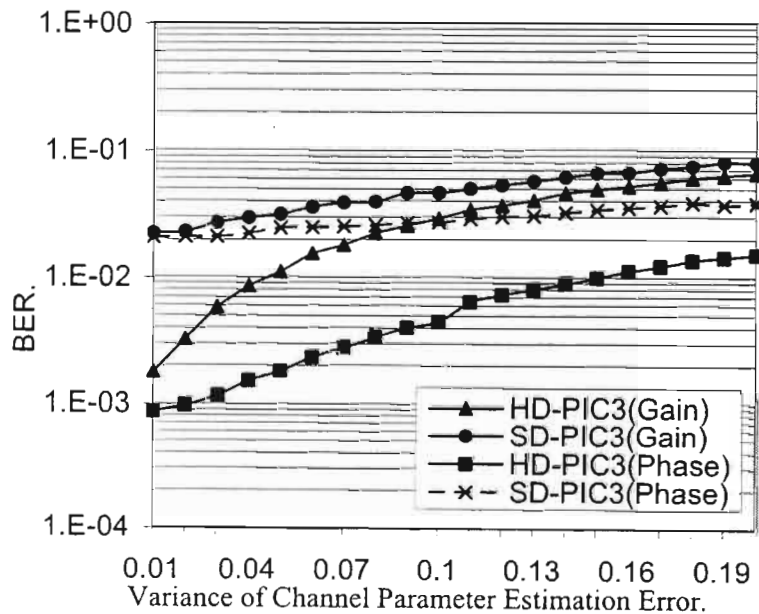


Figure 2.10: BER performance of HD-PIC and SD-PIC with channel Gain and phase estimation errors.

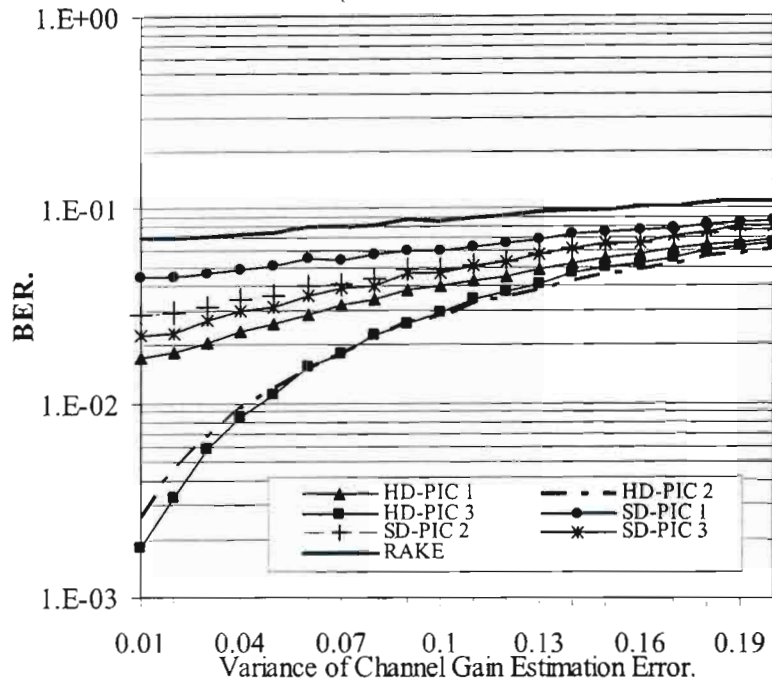


Figure 2.11: BER performance of PIC schemes with channel gain estimation error and increasing stages.

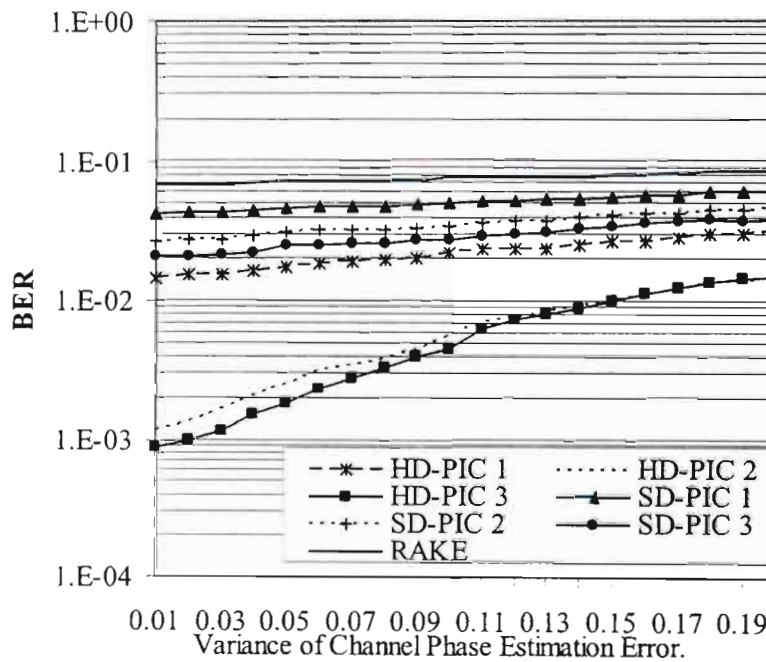


Figure 2.12: BER performance of PIC schemes with channel phase estimation error and increasing stages.

2.4 Performance Analysis.

We will use the Gaussian Approximation (GA) method in this section to analyse the performances of the total and weighted PIC receivers in a multipath fading channel. It is assumed that all users are transmitting at the same power. Random spreading codes are used by all the users. The scenario that is considered in this section corresponds to the single cell situation in a cellular communication system. The single cell scenario is considered because the PIC receiver assumes knowledge of the spreading code of the interfering users. Therefore, it is not possible for the PIC receiver to estimate the out-of-cell interference.

2.4.1 Initial Stage.

By initial stage we refer to the output of the RAKE receiver before any form of interference cancellation. The BER performance at this stage can be analysed by the usual GA method where the conditional BER (conditioned on the channel gain coefficient of the desired user) is given as:

$$P^{(j)} = Q \left[\sqrt{\frac{\sum_{\zeta=1}^M U_{j\zeta}^2}{2\sigma_T^2}} \right] \quad (2.17)$$

where $\sigma_T^2 = \sum_{\zeta=1}^M \{ \text{var}[V_{j\zeta}] + \text{var}[W_{j\zeta}] + \text{var}[\eta_{\zeta}] \}$. $Q[x]$ is the Q-function of x defined as

$$Q[x] = \frac{1}{\pi} \int_0^{\pi/2} e^{-x^2 / (2 \sin^2 \theta)} d\theta \quad \text{for } x > 0. \text{ The notation } \text{var}[Y] \text{ stands for the variance of}$$

the random variable Y . Expressions for $\text{var}[V_{j\zeta}]$, $\text{var}[W_{j\zeta}]$ and $\text{var}[\eta_{\zeta}]$ were derived in [Eng95] and [Eft97]. For systems with random spreading sequences we have:

$$\text{var}[V_{j\zeta}] = \frac{T^2(\beta_{\zeta j})^2}{6N} \sum_{\substack{k=1 \\ k \neq j}}^K P_k q(L, \delta) \Omega_1 \quad (2.18)$$

$$\text{var}[W_{j\zeta}] = \frac{T^2(\beta_{\zeta j})^2 \Omega_1}{4N} P_j [q(L, \delta) - 1] \quad (2.19)$$

and

$$\text{var}[\eta_{\zeta}] = \frac{TN_o(\beta_{\zeta j})^2}{4} \quad (2.20)$$

$$\text{where } q(L, \delta) = \sum_{l=1}^L e^{-l\delta} = \frac{1 - e^{-L\delta}}{1 - e^{-\delta}}$$

For simplicity from hereon, we assume an equal transmitted power for all the users, that is $P_k = P$ for all $1 \leq k \leq K$. Therefore,

$$\frac{\sum_{\zeta=1}^M U_{j\zeta}^2}{2\sigma_T^2} = \frac{\sum_{\zeta=1}^M (\beta_{\zeta j})^2}{\Omega_1} \left[\frac{2(K-1)q(L, \delta)}{3N} + \frac{[q(L, \delta) - 1]}{N} + \frac{N_o}{\Omega_1 PT} \right]^{-1} \quad (2.21)$$

Let us define a parameter S as $S = \frac{1}{\Omega_1} \sum_{\zeta=1}^M (\beta_{\zeta j})^2$ then,

$$\begin{aligned} \frac{\sum_{\zeta=1}^M U_{j\zeta}^2}{2\sigma_T^2} &= S \left[\frac{2(K-1)q(L, \delta)}{3N} + \frac{[q(L, \delta) - 1]}{N} + \frac{N_o}{\Omega_1 PT} \right]^{-1} \\ &= S \gamma^{(j)} \end{aligned} \quad (2.22)$$

and the conditional bit error probability can be expressed as $P^{(j)} = Q\left[\sqrt{S \gamma^{(j)}}\right]$. The average error probability of the initial stage, $\rho^{(j)}$, for user j is then obtained by taking the expectation of $Q\left[\sqrt{S \gamma^{(j)}}\right]$ with respect to the PDF of S . The average BER is

$\rho^{(j)} = \int_0^{\infty} P^{(j)} P(S) dS$ where $P(S)$ for equal $\frac{C}{\Omega}$ on all the combining fingers is

$$P(S) = \left(\frac{m_T}{\Omega_T}\right)^{m_T} \frac{S^{m_T-1}}{\Gamma(m_T)} e^{-\left(\frac{m_T S}{\Omega_T}\right)}, \quad (2.23)$$

where $m_T = \sum_{i=1}^M m_i = m \frac{q(M, \delta)^2}{q(M, 2\delta)}$, $\Omega_T = \sum_{i=1}^M \Omega_i = q(M, \delta)$.

Consequently, it is straightforward to show that (see Appendix A)

$$\rho^{(j)} = \frac{1}{\pi} \int_0^{\frac{\pi}{2}} \frac{\sin^{2m_T} \theta d\theta}{(\sin^2 \theta + \gamma')^{m_T}} \quad (2.24)$$

where $\gamma' = \frac{\gamma \Omega_T}{2m_T}$.

2.4.2 Total PIC.

The decision statistics at the end of the f^{th} stage of a total PIC receiver can be expressed as

$$X_j = \sum_{\zeta=1}^M \left\{ U_{j\zeta} + V_{j\zeta}^{\text{Total}}[f] + W_{j\zeta} + N_{\zeta} \right\} \quad (2.25)$$

where $V_{j\zeta}^{Total}[f] = V_{j\zeta} - \hat{V}_{j\zeta}[f]$. Also, the variance of the residual MAI component of the f^{th} stage can be shown to be $\text{var}[V_{j\zeta}^{Total}[f]] = \left(4Q[\sqrt{\gamma[f-1]q(\delta, M)}]\right) \text{var}[V_{j\zeta}]$. (See Appendix B). This new expression for the residual MAI is found to be more accurate than those that are presented in [Yoo93] and [Hui98] where the variance was given as $\text{var}[V_{j\zeta}^{Total}[f]] = 4\rho^{(j)}[f-1] \text{var}[V_{j\zeta}]$. This is shown in Appendix B. Therefore,

$$\gamma^{Total}[f] = \left[\frac{2(K-1)q(L, \delta) \left(4Q[\sqrt{\gamma[f-1]q(\delta, M)}]\right)}{3N} + \frac{[q(L, \delta) - 1]}{N} + \frac{N_0}{\Omega_1 PT} \right]^{-1} \quad (2.26)$$

With an assumption of perfect channel gain estimation, the average BER for the total PIC receiver can therefore be expressed as

$$\rho^{(j)} = \frac{1}{\pi} \int_0^{\frac{\pi}{2}} \frac{\sin^{2m_T} \theta d\theta}{(\sin^2 \theta + \gamma_{Total}'[f])^{m_T}} \quad (2.27)$$

$$\text{where } \gamma_{Total}'[f] = \frac{\gamma^{Total}[f] \Omega_T}{2m_T}.$$

2.4.3 Weighted PIC.

The decision statistics at the end of the f^{th} stage of a weighted PIC receiver can be expressed as

$$X_j = \sum_{\zeta=1}^M \left\{ U_{j\zeta} + V_{j\zeta}^{Weighted}[f] + W_{j\zeta} + N_{\zeta} \right\} \quad (2.28)$$

where $V_{j\zeta}^{Weighted}[f] = V_{j\zeta} - \lambda_f \hat{V}_{j\zeta}[f]$. Also, the variance of the residual MAI component of the f^{th} stage can be shown to be

$\text{var}[V_{j\zeta}^{Weighted}[f]] = \left((\lambda_f - 1)^2 + 4\lambda_f Q \left[\sqrt{\gamma^{Weighted}[f-1]q(M, \delta)} \right] \right) \text{var}[V_{j\zeta}]$ therefore

$$\gamma^{Weighted}[f] = \left[\frac{2(K-1)q(L, \delta) \left((\lambda_f - 1)^2 + 4\lambda_f Q \left[\sqrt{\gamma^{Weighted}[f-1]q(M, \delta)} \right] \right)}{3N} + \frac{[q(L, \delta) - 1]}{N} + \frac{N_0}{\Omega_1 PT} \right]^{-1} \quad (2.29)$$

With an assumption of perfect channel gain estimation, the average BER for the weighted PIC receiver can therefore be expressed as

$$\rho^{(j)} = \frac{1}{\pi} \int_0^{\frac{\pi}{2}} \frac{\sin^{2m_T} \theta d\theta}{(\sin^2 \theta + \gamma_{Weighted}^{(j)})^{m_T}} \quad (2.30)$$

where $\gamma_{Weighted}^{(j)} = \frac{\gamma^{Weighted}[f] \Omega_T}{2m_T}$.

2.5 Optimal Weights Determination for the Weighted PIC Receiver.

To avoid an arbitrary selection of the cancellation weights in the weighted PIC receiver, it is expedient to determine expressions for the values of the weights that will produce optimum performance with changing channel parameters and system loading. In this Section therefore, we used the Minimum Mean Square Error (MMSE) criterion to determine these optimal weights. The procedure is to minimize the mean square error at a given stage for each of the receivers with respect to the cancellation weights.

The received baseband signal is given by

$$r(t) = \sum_{k=1}^K \sqrt{2P_k} \sum_{l=1}^L \beta_{lk} a_k(t - \tau_{lk}) b_k(t - \tau_{lk}) \cos(\psi_{lk}) + n(t) \quad (2.31)$$

At the f^{th} cancellation stage, the estimate of the received signal will be

$$\hat{r}_f(t) = \sum_{k=1}^K \sqrt{2P_k} \sum_{l=1}^L \beta_{lk} a_k(t - \tau_{lk}) \hat{b}_{k,f-1}(t - \tau_{lk}) \cos(\psi_{lk}) \quad (2.32)$$

where $\hat{b}_{k,f-1}(t - \tau_{lk})$ is the estimate of $b_k(t - \tau_{lk})$ at the end of the $(f-1)^{\text{th}}$ stage. We, therefore, need to obtain the value of cancellation weights that minimizes the mean square error between the original received signal and its estimate. That is, $\min_{\lambda_f} E[(r(t) - \lambda_f \hat{r}_f(t))^2]$. The optimal weight can then be obtained by differentiating

$E[(r(t) - \lambda_f \hat{r}_f(t))^2]$ with respect to λ_f and equating the differential to zero, that

$$\text{is } \frac{dE[(r(t) - \lambda_f \hat{r}_f(t))^2]}{d\lambda_f} = 0.$$

Therefore, $\lambda_f^{\text{opt}} = \frac{E[r(t)\hat{r}_f(t)]}{E[(\hat{r}_f(t))^2]}$. But $E[(r_f(t))^2] = \frac{K\Omega_1 q(L, \delta)}{8}$ conditioned on the

message bit and $E[(\hat{r}_f(t))^2] = \frac{K\Omega_1 q(L, \delta)(1 - 2Q[\sqrt{\gamma[f-1]q(M, \delta)}])}{8}$ also conditioned

on the message bit. Therefore

$$\lambda_f^{\text{opt}} = 1 - 2Q[\sqrt{\gamma[f-1]q(M, \delta)}] \quad (2.33)$$

for any given cancellation stage f .

2.6 Discussion of Numerical Results.

In this Section, we determine the accuracy of the analytical models that are presented in this Chapter by comparing them with results that are obtained through computer simulations. We then used the analytical models in determining the effects of changes in channel parameters on the performances of the PIC receivers. For computer simulations we define the SNR as $\frac{\Omega_1 PT}{N_o}$. The unit energy constraint is applied in all the computer simulations.

2.6.1 PIC receivers with no channel estimation error.

We begin by determining the accuracy of the analytical models that are developed for the conventional RAKE receiver, the total PIC receivers and the weighted PIC receivers. Figure 2.13 compares analytical results using equation (2.24) that is developed in this dissertation and simulation results for the RAKE reception stage. For various numbers of users and processing gains, the number of multipath is three and the MIP decay factor is taken as 0.2. High degrees of agreement could be observed. This shows the accuracy of the analytical model. Figures 2.14 and 2.15 compare analytical results and simulation results for two stages of the total PIC receiver. The processing gain is 15 and the number of users in the system is 10. The exponential MIP decay factor is taken to be 0.2. This is typical of the urban mobile communication system [Row98]. It can be seen that the proposed analytical model is accurate for the PIC receivers. In Figure 2.14 for instance, the model that is proposed in this Chapter is labeled as “Total PIC-1 (Ana)” and “Total PIC-2 (Ana)” for the first and the second cancellation stages respectively. The model that has been reported in the literature is labeled as “Total PIC-1 (Old Ana)” and “Total PIC-2 (Old Ana)” for the first and the second cancellation stages respectively. It can be observed that the model that is developed in this work has better agreement with simulation results (labeled as “Total PIC-1 (Sim)” and “Total PIC-2 (Sim)” for the first and the second cancellation stages respectively). This is further articulated in appendix B. Figures 2.16 and 2.17 compare the analytical and simulation results for the weighted PIC receiver.

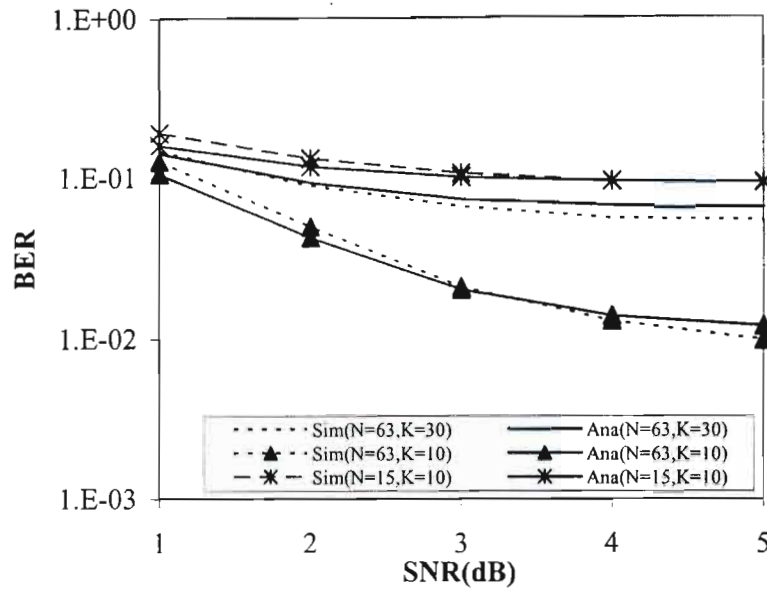


Figure 2.13: BER results to show the accuracy of the proposed analytical model for the RAKE receiver.

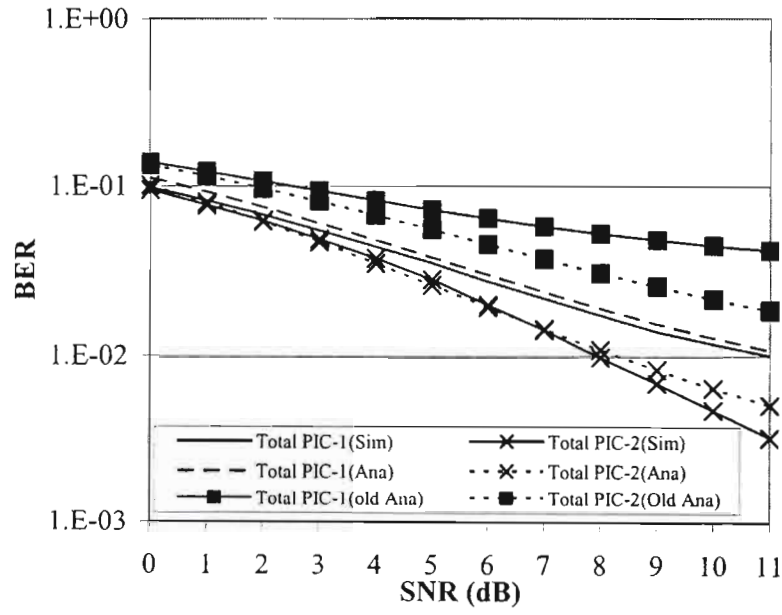


Figure 2.14: BER vs SNR for RAKE receiver and the total PIC receiver. $L=3, M=3, m=1, \delta=0.2, k=10, N=15$.

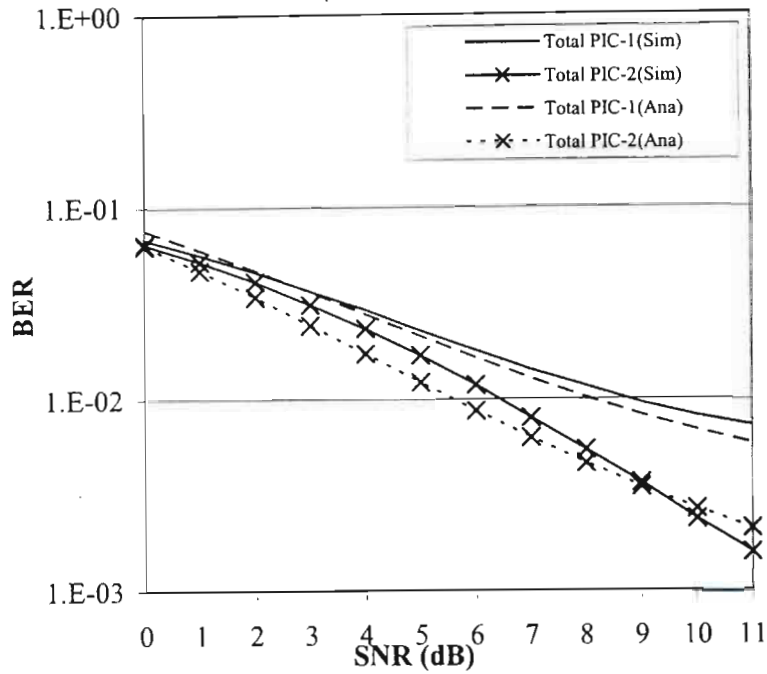


Figure 2.15: BER vs SNR for RAKE receiver and the total PIC receiver. $L=5$, $M=5$, $m=1$, $\delta=0.2$, $k=10$, $N=15$.

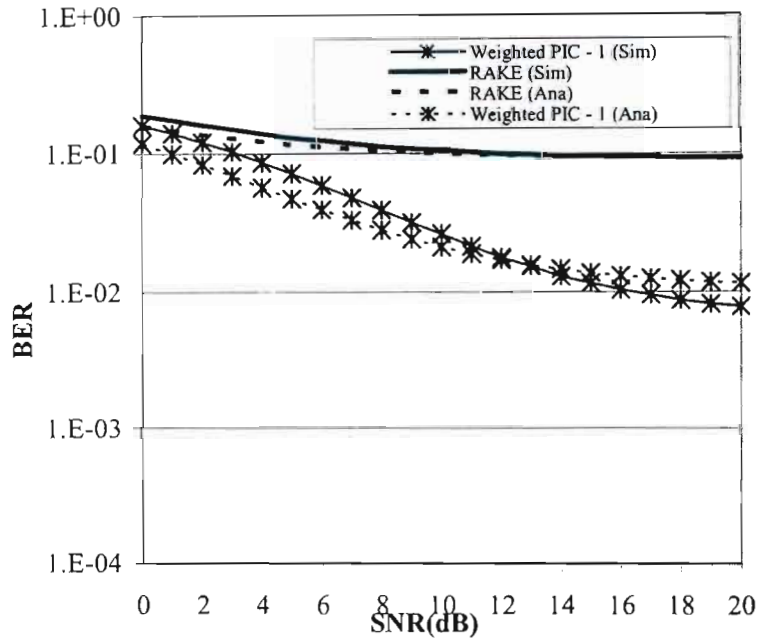


Figure 2.16: BER vs SNR for RAKE receiver and the first stage of weighted PIC receiver. $L=3$, $M=3$, $m=1$, $\delta=0.2$, $k=10$, $N=15$. Cancellation weight = 0.7.

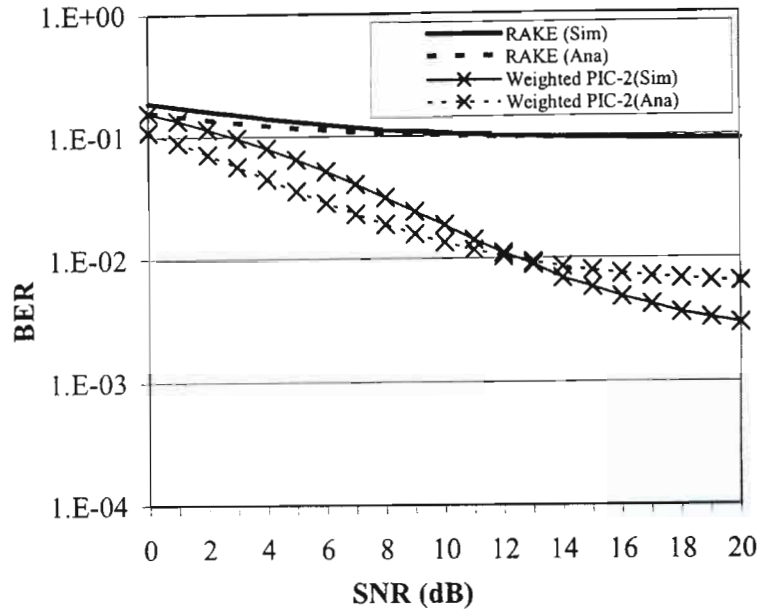


Figure 2.17: BER vs SNR for RAKE receiver and the two stages of weighted PIC receiver. $L=3$, $M=3$, $m=1$, $\delta=0.2$, $k=10$, $N=15$. Cancellation weight = 0.7.

2.6.3 Weighted PIC receiver with optimal cancellation weights.

In this Section we present results for the weighted PIC receiver using various cancellation weights and compare those results with the result obtained using the optimal cancellation weights. BER performances for various channel fading conditions and cancellation weights are presented. The objective of the Section is to determine effects of using the optimal cancellation weights as opposed to selecting the cancellation weights arbitrarily.

In Figure 2.18 we show error rate results for the weighted PIC receiver in the multipath fading channel with three propagation paths. The m parameter for the Nakagami fading channel is taken to be 0.75. It will be observed that the receiver that uses the optimum cancellation weight has the best performances. The need for cancellation weight selection is obvious with the un-predictable manner in which the error rate performances of the weighted PIC receiver changes with various arbitrarily selected cancellation weights. A method for selecting cancellation weights that are as close to the optimum weight as

much as possible is by the use of an adaptive algorithm. This is the subject of discussion in the next Chapter.

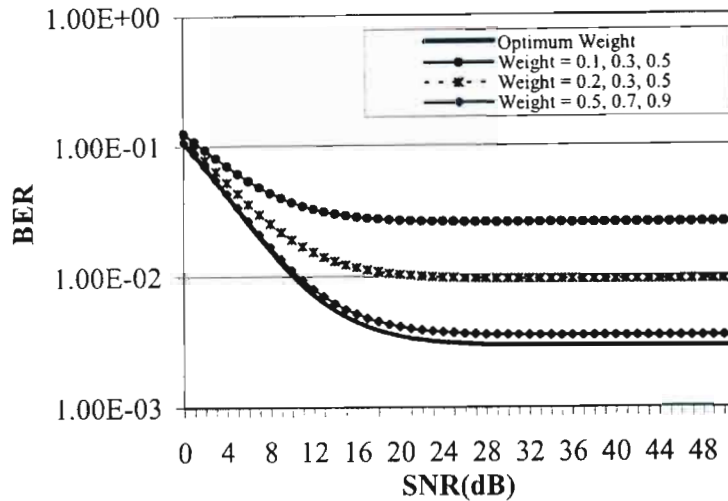


Figure 2.18: BER vs SNR for three stages of weighted PIC receiver. $L=3$, $M=3$, $m=0.75$, $\delta=0.2$, $k=10$, $N=15$.

2.7 Conclusions.

This chapter began with a detailed description of PIC receiver types that have been proposed in the literature. A motivation was also made for the need to investigate the performance of these receivers in the Nakagami multipath fading channel with exponential MIP. The SD-PIC and the HD-PIC receiver types were also introduced.

The HD-PIC receiver was shown to have better BER performance when compared with the SD-PIC receiver. The additional hard decision devices can introduce some delay in the HD-PIC system but the capacity gain of the HD-PIC receiver over the SD-PIC receiver justifies the use of the tentative decision devices.

An accurate analytical model for the evaluation of the BER of the MRC-based RAKE receiver for the DS-CDMA system in the Nakagami multipath fading channel was presented in this channel. The developed model is based on the Gaussian approximation method. The Gaussian approximation approach is accurate in the multipath fading

channel and the Gaussian assumption becomes more accurate with increase in the number of RAKE fingers. The level of the accuracy of the model shows that the model is useful for CDMA system design. Analytical models were also presented for the BER evaluation of the total and the weighted PIC receivers. It was observed that the models that are developed in this work for the total and the weighted PIC receivers have better agreement with simulation results than models that are already proposed in the literature.

The optimal cancellation weight for the weighted PIC receiver was also determined. The observation that the weight selected based on the MMSE criterion gives optimal BER performance in the weighted PIC receiver is a motivation for the need to adaptively estimate the cancellation weight as the channel condition changes. Adaptive PIC receiver is the subject of discussion in Chapter 3.

Finally the substantial capacity gain of the PIC receivers over the ordinary RAKE receiver is seen in many of the results that were presented in this chapter. This definitely explains the wide acceptance of PIC receivers in the wireless communication community.

Chapter 3

Adaptive Parallel Interference Cancellation Receivers for DS-CDMA.

3.1 Introduction.

It was observed in Chapter 2 of this dissertation that the selection of optimal cancellation weights for the weighted PIC receiver is necessary in order to have the best possible receiver performance for any channel condition or for any level of system loading. There is, therefore, a need to have a method of selecting the optimal weights in a way that adapts to changes in channel conditions and system parameter variations. This is the subject of this Chapter.

The use of adaptive algorithms for parameter estimation is a well established field of knowledge [Din97]. There are also many adaptive algorithm types that have been developed and well researched. A good overview of adaptive algorithms can be found in [Hay01]. Our main activity in this Chapter will be to adopt one of the existing adaptive algorithms for PIC reception. The selection of the appropriate algorithm shall be based on its suitability for the wireless communication scenario and its peculiar characteristics. Any adaptive algorithm that is used for any purpose in wireless communication will have to consider power consumption and computational complexity as these are the major constraints.

For the PIC receiver, the adaptive algorithm that should be selected should not have a high computational overhead so as not to negate one of the reasons why PIC receivers are very attractive; their low computational complexity. At the same time, such algorithms

should still be able to estimate the receiver parameter reliably. One adaptive algorithm that seems to meet this requirement is the Least Mean Square (LMS) algorithm.

The Least Mean Square (LMS) algorithm has been used for the estimation of the cancellation weights for the weighted PIC receiver in [Xue99][Wan01]. The LMS algorithm was selected in these works because of its low computational complexity. This is desirable in wireless systems design where low power consumption, which is related to the computational overhead of algorithms, is very important. We will be using the LMS algorithm in our work for the same reasons. In previous works in [Xue99]and [Wan01] only simulation results are presented. Our focus in this Chapter will therefore be to present analytical models for the performance analysis of the adaptive weighted PIC receiver.

Our analysis of the adaptive PIC receiver will be to perform the BER evaluation for the receivers when the adaptive algorithm has reached the steady-state situation. In steady-state there will be some noise in the estimation which can be quantified by the excess mean square error. We present expressions for the excess mean square error of the adaptive receiver and presented the effects of the error on the BER performances of the receiver.

The rest of the Chapter is organized as follows: Section 3.2 gives the LMS implementation of the adaptive PIC receiver. Error rate performance analysis of the adaptive receiver is presented in Section 3.3. Section 3.4 concludes the Chapter.

3.2 LMS implementation of adaptive PIC receiver.

The system that is considered in this chapter is also the asynchronous DS-CDMA system in a multipath fading channel. The fading variates are taken to have the Nakagami distribution. Therefore, in order to avoid repetitions, the channel and system models that

are presented in Chapter 2 are also used in this Chapter. We will use the system model of [Xue99] in the implementation of LMS-based weighted PIC receiver. In [Xue99] the received signal is sampled at the chip rate before using it in the LMS algorithm. The sampled received signal can therefore be written as

$$R(n) = \sum_{k=1}^K \sqrt{2P_k} \sum_{l=1}^L \beta_{lk} a_k(n) b_k(n) \cos(\psi_{lk}) + \Xi(n) \quad (3.1)$$

where $a_k(n)$ and $b_k(n)$ represents the sampled version of the spreading sequence and the message bits respectively. Notation $\Xi(n)$ represents the sampled version of the AWGN. The sampled version of the estimated received signal can also be written as

$$R_f(n) = \sum_{k=1}^K \lambda_{fk}(n) \sqrt{2P_k} \sum_{l=1}^L \beta_{lk} a_k(n) \hat{b}_{k,f-1}(n) \cos(\psi_{lk}) \quad (3.2)$$

The error in the estimation of the received signal at the f^{th} stage is therefore

$$e_f(n) = R(n) - R_f(n) \quad (3.3)$$

The cancellation weight adaptation by the normalized LMS algorithm can be expressed as

$$\lambda_{f(n+1)} = \lambda_{f(n)} + \frac{2\mu e_f(n) \mathbf{X}_f(n)}{\|\mathbf{X}_f(n)\|^2} \quad (3.4)$$

where $\mathbf{X}_f(n)$ is the input vector to the LMS algorithm at instance n and stage f . Notation μ represents the step size of the adaptive algorithm. The k^{th} component of $\mathbf{X}_f(n)$ can be expressed as

$$X_f^k(n) = \sum_{l=1}^L \sqrt{2P_k} \beta_{lk} a_k(n) b_{k,f-1}(n) \cos(\Psi_{lk}) \quad (3.5)$$

Notation $\lambda_f(n)$ is the weight vector of the LMS algorithm at instance n and stage f . The k^{th} component of $\lambda_f(n)$ can be represented as $\lambda_{fk}(n)$. The normalized LMS algorithm is employed in order to have a faster convergence [Din97]. For each bit, $\lambda_{fk}(N-1)$ is then used as the cancellation weight. Therefore, the new expression for the residual MAI will be:

$$V_{j\zeta}^{Adaptive}[f] = V_{j\zeta} - \lambda_{fk}(N-1) \hat{V}_{j\zeta}[f] \quad (3.6)$$

and the more reliable decision on the signal of the user of interest will be $\text{sgn}[X_j^{(f)}]$

where

$$X_j^{(f)} = \sum_{\zeta=1}^M \left\{ U_{\zeta j} + V_{j\zeta}^{Adaptive}[f] + W_{\zeta j} + \eta_{\zeta} \right\} \quad (3.7)$$

3.3 Error Rate Performance of the Adaptive PIC Receiver.

Cancellation weights estimated by the LMS algorithm tend to converge to the optimal value. Despite the fact that the algorithm converges to the optimum value on an average, there are instantaneous deviations which can be quantified as $\Delta\lambda_{fk}(n) = \lambda_{fk}(n) - \lambda_{fk}^{opt}$. Notation λ_{fk}^{opt} represents the optimum cancellation weight. We can model this noise term as a Gaussian noise of zero mean and variance of σ_{λ}^2 [Din97] [Ber96a] [Ber96b].

By using an approach that is similar to the one that is presented in [Din97], the variance of the noise term can be computed. Determination of the excess mean square error in

LMS algorithm is well documented in [Din97]. It was shown in [Din97] that the excess of mean square error for the LMS algorithm at steady state will be $\xi_{exc} \approx \mu(\kappa - 1)\sigma_n^2\sigma_x^2$ where κ is the number of stages and σ_x^2 is the variance of the input to the LMS algorithm. When applied specifically to the LMS-based PIC receiver we have

$$\xi_{exc} \approx \mu'(K - 1)\sigma_n^2\sigma_x^2 \quad (3.8)$$

where $\sigma_n^2 = \frac{N_o}{2}$ (as applied to the system model that is presented in this Chapter) and σ_x^2 is the variance of the input to the LMS algorithm which is obtained by taking the second moment of (3.5) and can be given as

$$\sigma_x^2 = PT\Omega_1q(L, \delta) \quad (3.9)$$

μ is the step size of the classical LMS algorithm (without normalization). With the normalized LMS algorithm that is presented in this Chapter, then $\mu' = \frac{\mu}{\|\mathbf{X}_f(n)\|^2}$ which is a random variable. Therefore the expectation of μ' shall be used in equation (3.8). The expectation of μ' then is

$$E[\mu'] = E\left[\frac{\mu}{\|\mathbf{X}_f(n)\|^2}\right] = \frac{\mu}{KPT\Omega_1q(L, \delta)} \quad (3.10)$$

Hence,

$$\sigma_\lambda^2 = \xi_{exc} \approx \frac{\mu(K - 1)N_o}{2K} \quad (3.11)$$

Equation (3.12) shows the relationship between the excess of mean square error and the step size of the adaptive algorithm. It can be seen that the step size should be selected as small as possible in order to minimize the value of the excess of mean square error. A tradeoff will have to be reached though on the selection of the value of the step size because if a very small value is selected, the algorithm will converge very slowly.

The variance of the residual MAI component, $V_{j\zeta}^{Adaptive}[f]$, can be determined as follows.

$$\begin{aligned}
\text{var}[V_{j\zeta}^{Adaptive}[f]] &= \left(1 - 2E[\lambda_f \hat{b}_{0,k}^{(f-1)}] + E[\lambda_f^2 (\hat{b}_{0,k}^{(f-1)})^2] \right) \text{var}[V_{j\zeta}] \\
&= \left(1 - 2E[\hat{b}_{0,k}^{(f-1)}] E[\lambda_f] + E[(\hat{b}_{0,k}^{(f-1)})^2] \text{var}[\lambda_f^2] \right) \text{var}[V_{j\zeta}] \\
&= \left(1 - 2E[\hat{b}_{0,k}^{(f-1)}] \lambda_{fk}^{(opt)} + E[(\hat{b}_{0,k}^{(f-1)})^2] (\sigma_\lambda^2 + (\lambda_{fk}^{(opt)})^2) \right) \text{var}[V_{j\zeta}] \\
&= \left(1 - 2E[\hat{b}_{0,k}^{(f-1)}] \lambda_{fk}^{(opt)} + E[(\hat{b}_{0,k}^{(f-1)})^2] (\sigma_\lambda^2 + (\lambda_{fk}^{(opt)})^2) \right) \text{var}[V_{j\zeta}] \\
&= \left(1 - 2\lambda_f^{opt} \left(1 - 2Q \left[\sqrt{\gamma^{Adaptive}[f-1]q(\delta, M)} \right] \right) + \sigma_\lambda^2 + (\lambda_f^{opt})^2 \right) \text{var}[V_{j\zeta}]
\end{aligned} \tag{3.13}$$

where

$$\gamma^{Adaptive}[f] = \left[\frac{(K-1)q(L, \delta) \left(1 - 2\lambda_f^{opt} \left(1 - 2Q \left[\sqrt{\gamma^{Adaptive}[f-1]q(\delta, M)} \right] \right) + \sigma_\lambda^2 + (\lambda_f^{opt})^2 \right)}{6N} + \frac{[q(L, \delta) - 1]}{4N} + \frac{N_0}{4\Omega_1 PT} \right]^{-1} \tag{3.14}$$

for the situation where we incorporate the cancellation weight estimation error term.

The expression for the BER of the adaptive PIC receiver will, therefore, be given as:

$$\rho^{(j)} = \frac{1}{\pi} \int_0^{\frac{\pi}{2}} \frac{\sin^{2m_T} \theta d\theta}{(\sin^2 \theta + \gamma'_{Adaptive}[f])^{m_T}} \quad (3.15)$$

$$\text{where } \gamma'_{Adaptive}[f] = \frac{\gamma^{Adaptive}[f] \Omega_T}{2m_T}$$

The analytical model that is presented in this Chapter is compared with results that are obtained through computer simulations in order to determine the accuracy of the analytical models. The processing gain for the system is selected as 63. This value of the processing gain is selected because we found that convergence of the LMS algorithm is difficult to achieve at the lower value of processing gain, like the processing gain of 15 that was used in Chapter 2 of this dissertation. We suspect that the processing gain of 63 was used in [Xue99] for the same reason. The step-size for the adaptive algorithm is selected as 1E-2. Random spreading sequences are used for data spreading. The receiver is investigated in the Nakagami multipath fading channel.

Figure 3.1 compares the BER results that are obtained from the developed analytical model and the results that are obtained through computer simulations for a single stage adaptive PIC receiver. The number of active users is 10. The number of multipath is three and the decay factor for the exponential MIP is 0.2. The unit energy constraint is enforced. It could be observed that BER results that are obtained through the use of the developed model are close to results that are obtained through computer simulations.

In Figure 3.2 BER results that are obtained from the developed analytical model and the results that are obtained through computer simulations for a two stage adaptive PIC receiver are compared. The number of active users is 30. The number of multipath is three and the decay factor for the exponential MIP is 0.2. The unit energy constraint is also enforced. It can be seen that BER results that are obtained through the use of the developed model are close to results that are obtained through computer simulations.

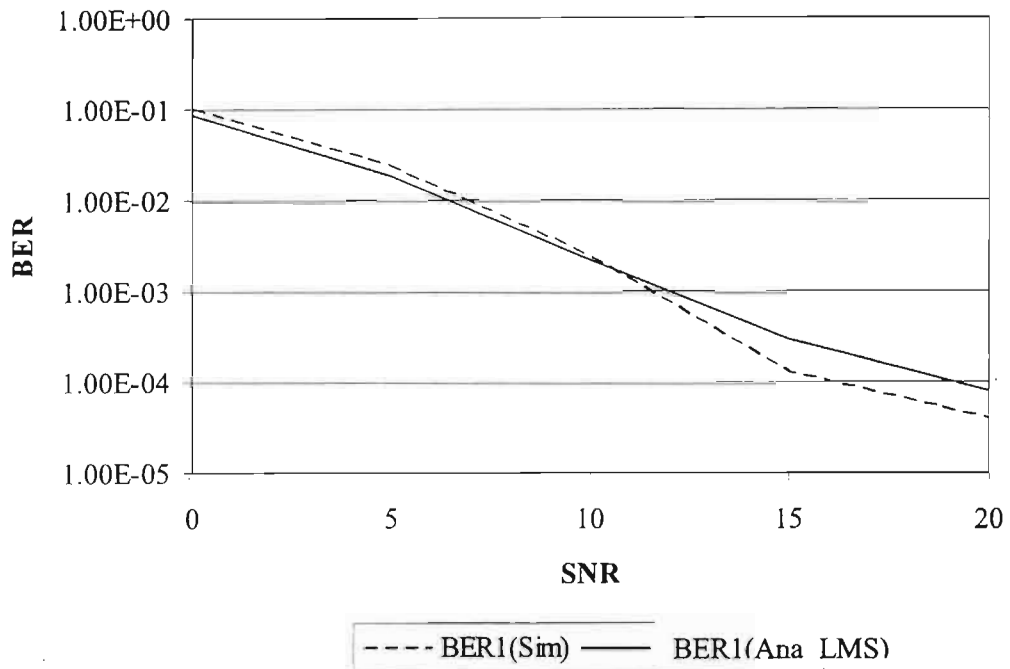


Figure 3.1: BER vs SNR results for the single stage adaptive PIC receiver.

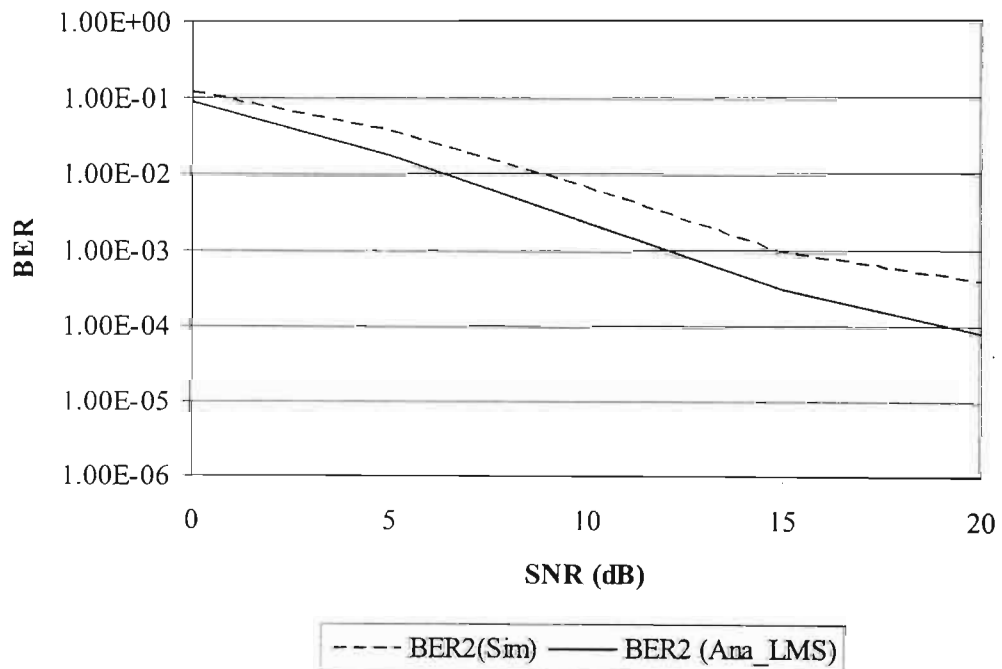


Figure 3.2: BER vs SNR results for the two stage adaptive PIC receiver.

3.4 Conclusion.

This chapter started with a discussion on the need to use a low complexity algorithm to adaptively estimate the optimal cancellation weights for the weighted PIC receiver with changes in channel parameters. The LMS algorithm was then motivated as an appropriate algorithm for the wireless communication scenario. The LMS-PIC receiver's model was then presented.

An analytical expression for the BER analysis of the LMS-based adaptive PIC receiver was then presented. Effects of the selection of the appropriate step-size for the adaptive receiver were also studied. The excess mean square noise was shown to be a function of the step-size and some other receiver and system parameters. In system design of adaptive PIC receivers, the selection of the appropriate step-size for conditions under which the receiver will be operating could be achieved by using equation (3-11) for the excess mean square noise that is presented in this chapter.

Chapter 4

Convergence Analysis of Iterative Interference Cancellation Receivers for Turbo-Coded DS-CDMA Systems

4.1 Introduction

Turbo codes are a class of error correcting codes that are generated from the parallel concatenation of two or more Recursive Systematic Convolutional (RSC) codes [Ber93]. Turbo codes have performances that are very close to the Shannon limit. The good performances of turbo codes at very low values of signal to noise ratio have made them very popular and the subject of very active research in the communication industry. A short but comprehensive overview of turbo codes and the concept of iterative decoding is given in [Rya].

Error correction alone cannot militate against the effects of the multiple access interference. There is the need to combine error correction and multiuser detection in an efficient manner. Multiuser detection and error correction could be combined in a partitioned format (in which the multiuser detection function is performed first and then followed by error correction) or in the integrated manner (in which the error correction and the multiuser detection functionalities are performed in the same “unit”). Combinations of many multiuser detection techniques and error correction in the partitioned manner have been presented in the literature. The Minimum Mean Square Error (MMSE) multiuser detector was combined with the convolutional decoder in [Foe00] and with the turbo decoder in [Tan01]. The parallel interference cancellation receiver was combined in the partitioned manner with the serially concatenated convolutional code in [Shi01]. However, the combination of multiuser detection and the

error correction functionalities in the integrated manner has the potential for better performance and provides the possibility of exchange of soft information.

The iterative decoding concept [Hag97] provides the possibility of designing integrated error correcting and multiuser detection schemes in which information is exchanged and improved upon from one iteration to the other. This type of receiver architecture is often referred to as iterative multiuser detection. Figure 4.1 illustrates the concept of iterative multiuser detection. In this figure, the information at the output of the turbo decoder for each user's system (U_1, U_2, \dots, U_K) are fed back into an multi-user detection unit. Using this information and the knowledge of the spreading codes of each user, the multi-user detection unit estimates and improved channel information for the turbo decoder in the next decoding iteration. This process continues for as many numbers of iterations as it is desired. Many types of multiuser detectors have been combined in an iterative manner with error correction. Examples of the use of the MMSE, the decorrelating, the MAI whitening and the parallel interference cancellation receivers in iterative multiuser detection can be found in [Gam00][Hsu01][Wu01][Mar01b].

Iterative interference cancellers were proposed in [Ale98] for the convolutionally coded DS-CDMA system. Performances of the receiver in different systems has been extensively studied through computer simulations for the AWGN channel in [Moh99][Ker99][Wu01]. In this Chapter, we shall be investigating the behaviour of the iterative interference cancellation receivers in the turbo-coded DS-CDMA systems. Our focus shall be on the convergence analysis of the receivers. We shall be proposing a methodology for the convergence analysis of the iterative interference cancellation receivers. Our method is based on the Gaussian approximation technique of [Gam01]. In the proposed method, analytical expressions for the SNR transfer function of the interference cancellation stage of the receiver is presented. This is in contrast to the semi-analytical approach that was used in [Shi01] to determine the "variance transfer function" of the interference cancellation stage. In the approach of [Shi01], the relationship between the variance of the signal at the input of the interference cancellation unit and at the output of the interference cancellation unit are evaluated by using Gaussian variates

as input to the interference cancellation unit. The variance transfer function is then evaluated by taking the ratio of the variance of the Gaussian variates at the output of the interference cancellation unit and at the input of the interference cancellation unit.

The rest of the Chapter is organized as follows. Section 4.2 gives an overview of the Gaussian approximation approach for the analysis of turbo decoders. Performance of the iterative interference cancellation receiver for turbo-coded DS-CDMA systems is investigated through computer simulations in Section 4.3. The convergence analysis of the iterative interference cancellation receiver is presented in Section 4.4. Section 4.5 concludes the Chapter.

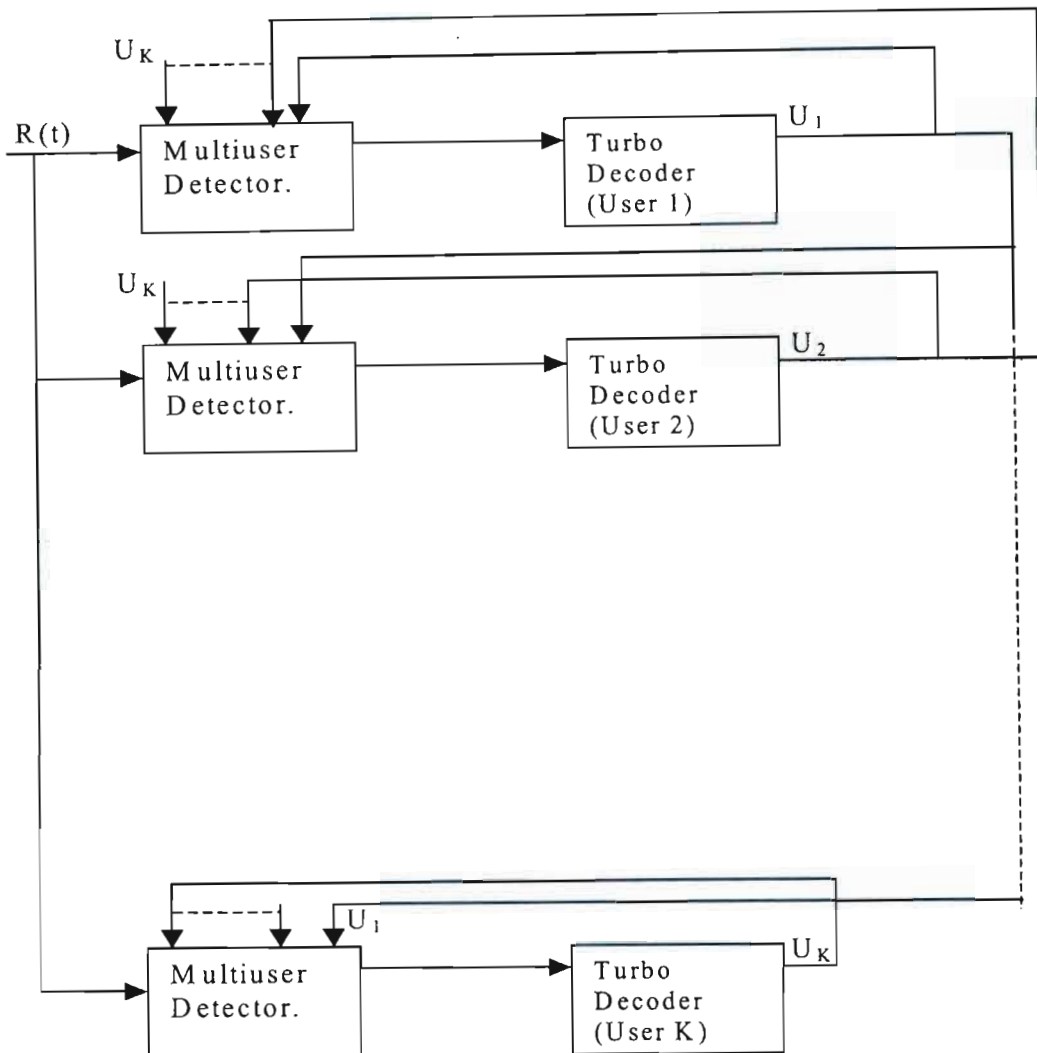


Figure 4.1: Iterative Multiuser Detector for Turbo Coded Systems.

4.2 Gaussian Approximation method for the analysis of Turbo Decoders.

There has been some work on the determination of the convergence behaviour of iterative decoders in recent times. The authors of [Ric01] used the density evolution approach to determine the convergence behaviour of Low Density Parity Check (LDPC) codes. In [Div01a], [Div01b] and [Gam01] the Gaussian approximation approach (based on the

measure of the signal-to-noise ratio) was used. The author of [Bri01] used an approach that is based on the measure of the mutual information.

The density evolution approach involves the computation of density functions as they evolve from one iteration to the next [Gam01]. The Gaussian approximation approach is based on the discovery by Wiberg that the Probability Density Function (PDF) of the extrinsic information of the turbo decoder is Gaussian [Wib96]. It was also shown in [Div01b] that the PDF of the extrinsic information approximates more to the Gaussian distribution function as the number of iterations increases. In the mutual information approach the mutual information between the extrinsic information and the transmitted bit is computed from one iteration to the next.

In this work, we shall use the Gaussian approximation approach based on the SNR measure. We select this approach because of its simplicity. Despite the level of simplicity, results that are amazingly accurate can be obtained by using the Gaussian approximation method

There are two choices for modeling the Gaussian variate. One approach is to determine the mean and the variance of the extrinsic information and then use the determined parameters in modeling the Gaussian variate. The second approach is to use the mean only, assuming that the variate is both Gaussian and consistent, the variance can be determined as two times the mean [Div01a], [Div01b], [Bri01]. The second approach has been found to be more accurate than the first approach [Bri01]. In the AWGN channel the intrinsic information and the extrinsic information to the turbo decoder at the input are independently Gaussian [Gam01] and the BER at the output of the decoder can therefore be computed as $Q[2\text{SNR}_{\text{total}}]$, where $\text{SNR}_{\text{total}}$ is the sum SNR of the intrinsic and the extrinsic information.

4.2.1. Dynamic Model of Turbo Decoding

The turbo decoder can be viewed as a density propagating unit in which the parameters of the density function of the extrinsic information changes from one iteration to the next [Mce98]. Since the extrinsic information is Gaussian, a parameter that could be monitored is the signal-to-noise ratio (SNR) of the extrinsic information. The ratio relates the mean of the extrinsic information to the variance of the extrinsic information.

For each of the component decoders of the turbo decoder, there is a non-linear function that relates the SNR of the extrinsic information at the input to the extrinsic information at the output of the decoder [Div01a][Div01b][Gam01]. This is illustrated in Figure 4.2 for each of the component decoders. Following the convention of [Div01a] we represent the SNR transfer functions as G_1 and G_2 . Apart from depending on the SNR of the extrinsic information at the input of the decoder, G_1 and G_2 also depend on the SNR of the channel information. For the sake of clarity, we shall make the following parameter definitions: Let $\text{SNR}_{\text{in},1}$ and $\text{SNR}_{\text{in},2}$ represent the signal-to-noise ratio of the extrinsic information at the input of the first and second decoders respectively. Let $\text{SNR}_{\text{out},1}$ and $\text{SNR}_{\text{out},2}$ represent the SNR of the extrinsic information at the output of the first and the second decoders respectively. Let SNR_{chn} represent the signal-to-noise ratio of the channel information. Let $(\text{SNR}_{\text{chn}})_{\text{db}}$ represent the value of SNR_{chn} in dB.

The functions G_1 and G_2 can be evaluated through computer simulation by using the Monte Carlo method. The Gaussian assumption about the extrinsic information becomes more valid with longer framelength. For symmetric turbo codes, the functions G_1 and G_2 are identical.

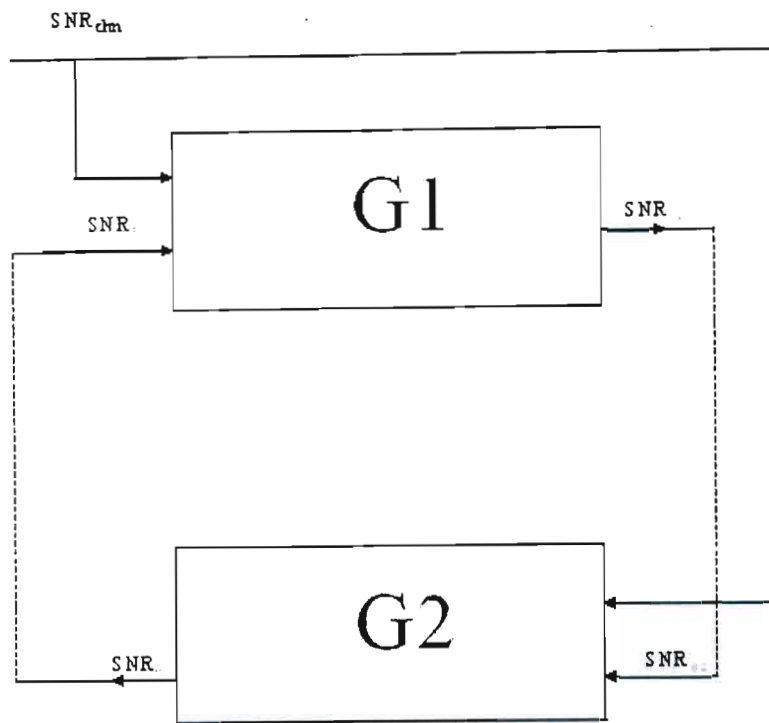


Figure 4.2: The nonlinear dynamic model of the turbo decoder.

Since the extrinsic information at the output of the first decoder becomes the a prior information for the second MAP decoder, the SNR of the extrinsic information are traced from the transfer function curve of the first decoder to the transfer function curve of the second decoder. The evolution of the SNR of the extrinsic information is traced as the iteration increases.

The density evolution approach has been used to explain some behaviour of the turbo decoder in the literature. The role of the systematic bits, the role of the RSC codes, the role of the primitive polynomial and the role of the state complexity were explained in [Div01a] and [Div01b]. The transmitted signal to noise ratio at which there will be convergence was determined in [Gam01] [Div01a] and in many other works by using the SNR transfer function curves of the decoders. The Gaussian approximation technique is, therefore, very useful in code selection and in convergence analysis.

The “noise figure” of the decoder is used in the convergence analysis of the turbo decoder. The noise figure can be defined as the ratio of the SNR of the extrinsic information at the input of the decoder to the SNR of the extrinsic information at the output of the decoder [Div01a]. This is computed from one iteration to the other. Since the SNR of the extrinsic information at the input side of the decoder will initially be zero, the noise figure will start from zero and increase at subsequent iterations. The decoder will not converge for any transmitted SNR at which the noise figure of the decoder gets to one. Any SNR for which the noise figure is just below one will be the value at which the decoder will converge.

4.2.2. Convergence Analysis of Turbo coded DS-CDMA Systems.

The procedure that was presented in Section 4.2.1 is used to explain the convergence analysis of the turbo-coded DS-CDMA system in this sub-section. We shall begin with the definition of the system model of the DS-CDMA system.

Let us consider a turbo coded asynchronous BPSK modulated DS-CDMA system in an AWGN channel. The received signal at the receiver in a multiuser system will be

$$r(t) = \sum_{k=1}^K \sqrt{2P} a_k(t) b_k(t) \cos(\omega_c t + \phi_k) + n(t) \quad (4.1)$$

where K represents the total number of active users, P represents the transmitted power of each active user, $a_k(t)$ represents the spreading code’s waveform of user k , $b_k(t)$ represents the message waveform of user k . Notation ϕ_k represents the phase shift of the signal of user k and $n(t)$ represents the AWGN that has a power spectral density (PSD) of $\frac{N_o}{2}$.

If user j is taken as the user of interest, the signal at the output of a matched filter that is matched to the spreading code of user j can be expressed as

$$U_j = \sqrt{PT}b_{j,0} + \sum_{\substack{k=1 \\ k \neq j}}^K \sqrt{\frac{P}{T}}(b_{k,0}R_{jk}(\tau_{jk}) + b_{k,-1}\hat{R}_{jk}(\tau_{jk}))\cos(\varphi_{jk}) + \int_0^T n(t)\sqrt{\frac{2}{T}}a_j(t)\cos(w_c t)dt \quad (4.2)$$

where $R_{ab}(\tau) = \int_0^\tau a_a(t-\tau)a_b(t)dt$ and $\hat{R}_{ab}(\tau) = \int_\tau^{T_b} a_a(t-\tau)a_b(t)dt$. Notations φ_{jk} and τ_{jk} represent the phase shift and delay respectively between the signals of user j and user k . Notation T represents the message bit duration of the user of interest. Notation $b_{k,0}$ denotes the transmitted coded bit of user k at the current instance and $b_{k,-1}$ denotes the transmitted coded bit of user k at the immediately previous instance.

It is well understood that U_j can be modeled as a Gaussian random variate with a mean value of \sqrt{PT} and a variance of $\frac{(K-1)PT}{3N} + \frac{N_o}{2}$ [Jul02]. The mean and the variance are computed, conditioned on the transmitted message bit. The SNR of U_j that is seen by the turbo decoder will therefore be

$$\text{SNR}_{\text{chn}} = \frac{PT}{\left(\frac{PT(K-1)}{3N} + \frac{N_o}{2}\right)} \quad (4.3)$$

and in decibel as

$$(\text{SNR}_{\text{chn}})_{\text{db}} = 10 \log_{10} \left(\frac{PT}{\left(\frac{PT(K-1)}{3N} + \frac{N_o}{2}\right)} \right) \quad (4.4)$$

In the convergence analysis of the turbo coded DS-CDMA system the iteration trajectories will be traced on the SNR transfer function curve that correspond to the SNR as calculated with equation (4.4). The signal to noise ratio is not $\frac{PT}{N_o}$ as is the case with the narrowband system.

4.3 Error Rate Performances of Iterative Interference Cancellation Receivers.

The iterative interference cancellation for a turbo coded system is illustrated in Figure 4.3. The output of the matched filter is received by the decoders. The multiple access interference cancellation is carried out through the subtraction of the estimate of the MAI from the received signal as shown in the Figure 4.3. The improved received signal then goes to the matched filter and subsequently the turbo decoder. The estimation of the MAI is made by adding the re-spread version of the detected message bits of all the other users in the channel (apart from user j) together.

The iterative interference cancellation receiver was proposed in [Ale98] for the convolutionally coded DS-CDMA system. In this receiver, the estimated MAI is subtracted directly from the received signal of the user of interest as is illustrated in Figure 4.3. This receiver is essentially the iterative combination of the parallel interference cancellation receiver that was discussed in Chapter 2 of this dissertation and the turbo decoder. Performance of the receiver have been investigated in [Ker99] [Moh99] [Ale98] for the convolutionally coded system. In this sub-Section we shall present simulation results on the performance of the iterative interference cancellation receiver for turbo coded DS-CDMA systems.

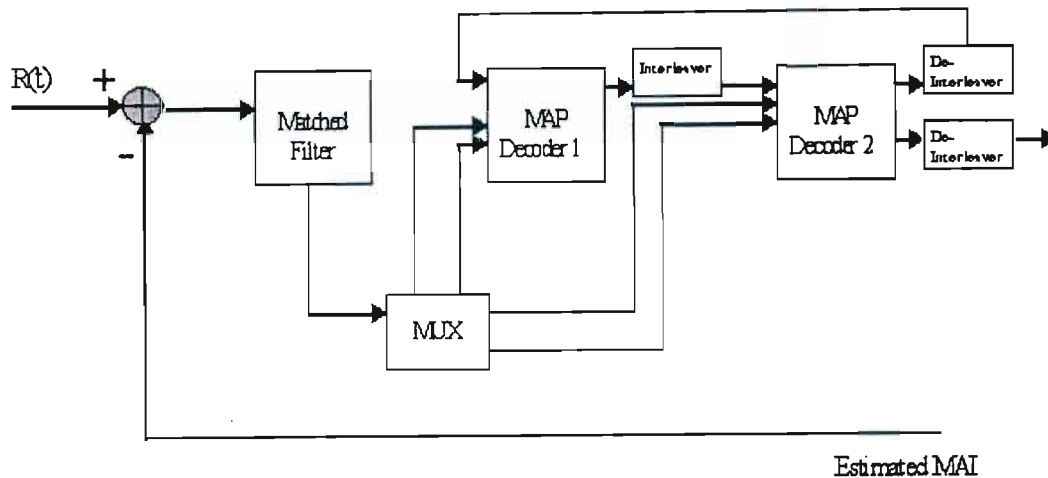


Figure 4.3: Functional block diagram of the iterative interference cancellation receiver.

For the simulation, at the transmitter we have the message bits encoded by a turbo encoder that is constituted by two (1,5/7) RSC codes that are separated by a random iterative. The notation that is used in this thesis to represent the constituent encoders is $(1, G_1/G_0)$, where G_0 is the feedback polynomial and G_1 is the feedforward polynomial. The processing gain of the DS-CDMA system is 15 and we have 10 active users.

Figure 4.4 illustrates performances of the iterative interference cancellation receiver with variations in the number of iterations. When compared with the turbo decoder without interference cancellation, a high level of error rate performance improvement is obtained. It should be noted though that the performance of the iterative interference cancellation receiver will not converge to the single user performance. This is because the residual interference cannot be totally removed from the received signal [Hon99].

4.4 Convergence Analysis.

It could be observed that the value of the SNR_{chn} as presented in equation (4.3) depends on the number of active users that are on the common channel. Therefore, the SNR_{chn} that will be seen by the turbo decoder will change as the number of users changes.

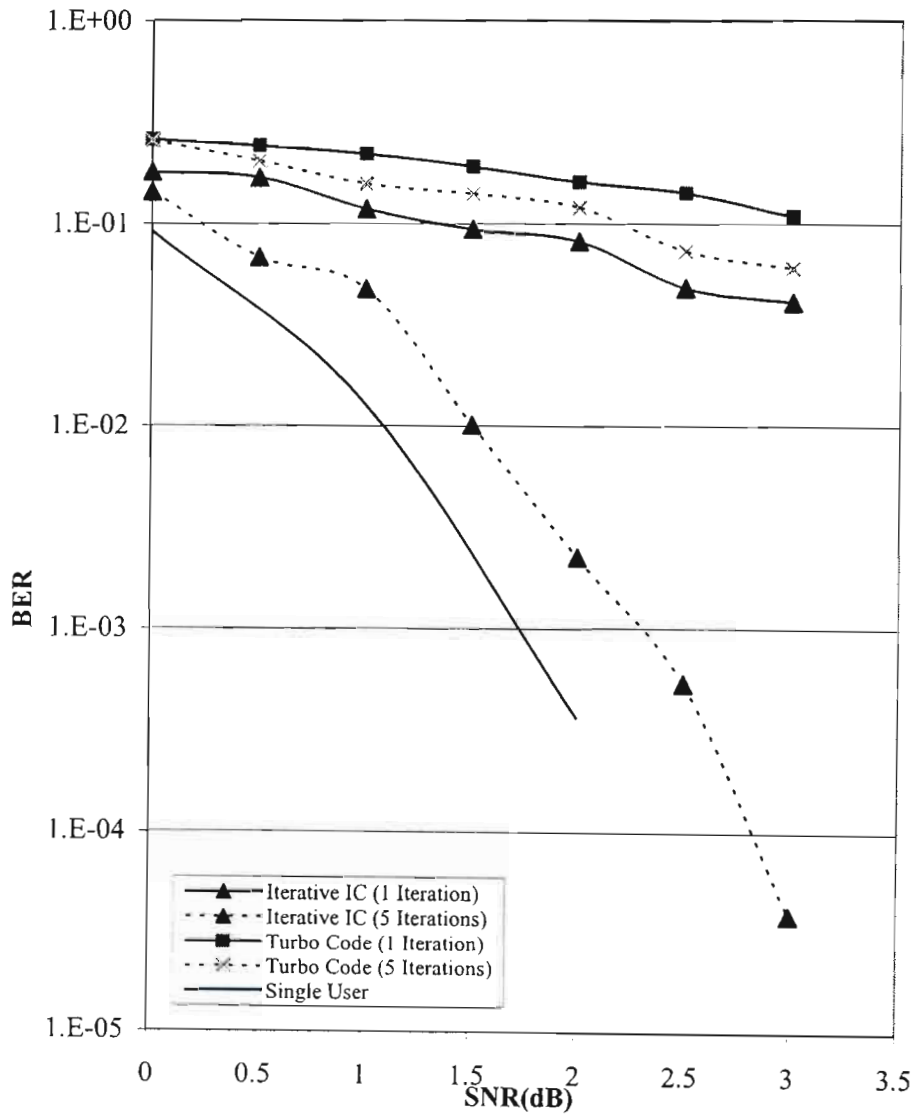


Figure 4.4: Error rate performances of the iterative interference cancellation receiver. Framelength=200.

With the interference cancellation operation included, the output of the matched filter at the f^{th} iteration becomes:

$$\begin{aligned}
 U_{j,f} = & \sqrt{PT}b_{o,j} + \sum_{\substack{k=1 \\ k \neq j}}^K \sqrt{\frac{P}{T}} \left\{ (b_{-1,k} - \hat{b}_{-1,k}^{(f-1)})R_{kj}(\tau_k - \tau_j) + (b_{0,k} - \hat{b}_{0,k}^{(f-1)})\hat{R}_{kj}(\tau_k - \tau_j) \right\} \cos(\psi_k - \psi_j) \\
 & + \int_0^T n(t) \sqrt{\frac{2}{T}} a_j(t - \tau_j) \cos(\omega_c t) dt
 \end{aligned} \tag{4.5}$$

Where $\hat{b}_{-1,k}^{(f-1)}$ and $\hat{b}_{0,k}^{(f-1)}$ are the estimate bit for user K after the $(f-1)^{\text{th}}$ iteration at the present and the immediately past instances respectively. The variance of $U_{j,f}$ will

then be $\frac{4PTQ(\text{SNR}_{\text{chn}}^{f-1})(K-1)}{3N} + \frac{N_o}{2}$. The signal to noise ratio of the channel information at the f^{th} iteration will therefore be

$$\text{SNR}_{\text{chn}}^f = \frac{PT}{\left(\frac{4PTQ(\text{SNR}_{\text{chn}}^{f-1})(K-1)}{3N} + \frac{N_o}{2} \right)} \tag{4.6}$$

The expression for the SNR_{chn} in equation (4.6) depends on the number of users and the iterations.

The iterative schedule for the iterative interference cancellation receiver will be as illustrated in Figure 4.5 for three iterations for a turbo coded DS-CDMA that has a processing gain of 15 and 10 users. The turbo code is constructed from RSC code (1,5/7). This Figure illustrates the variation in SNR_{chn} from iteration to iteration. Different curves that are equivalent to different SNR_{chn} values are used in each of the three iteration. This is unlike in the case of a system with no interference cancellation where SNR_{chn} remains

constant throughout the decoding operation. The SNR of the a posteriori information at the output of the turbo decoder can, therefore, be expressed as

$$\text{SNR}_{\text{aposteriori}} = \text{SNR}_{\text{chn}} + \text{SNR}_{\text{out}}^{(1)} + \text{SNR}_{\text{out}}^{(2)} \quad (4.7)$$

This procedure is repeated for the number of iterations required. The accuracy of this measure is checked by computing the BER of the a posteriori information is computed as $Q(\text{SNR}_{\text{aposteriori}})$. Where the function $Q(\cdot)$ is the Q – Function. The results obtained are then compared through computer simulations, some of such results are presented in Figures 4.6, 4.7, and 4.8 for a turbo coded DS–CDMA systems with the components RSC codes (1,5/7). The PG is 15 and the number of users is 10.

For the convergence analysis we have a DS–CDMA system that has a PG of 15. The number of users is 10 and the component codes for the turbo encoder are the RSC code (1,5/7). The noise figure of the turbo decoder is determined for $\left(\frac{PT}{N_o}\right)_{dB}$ of 0dB to

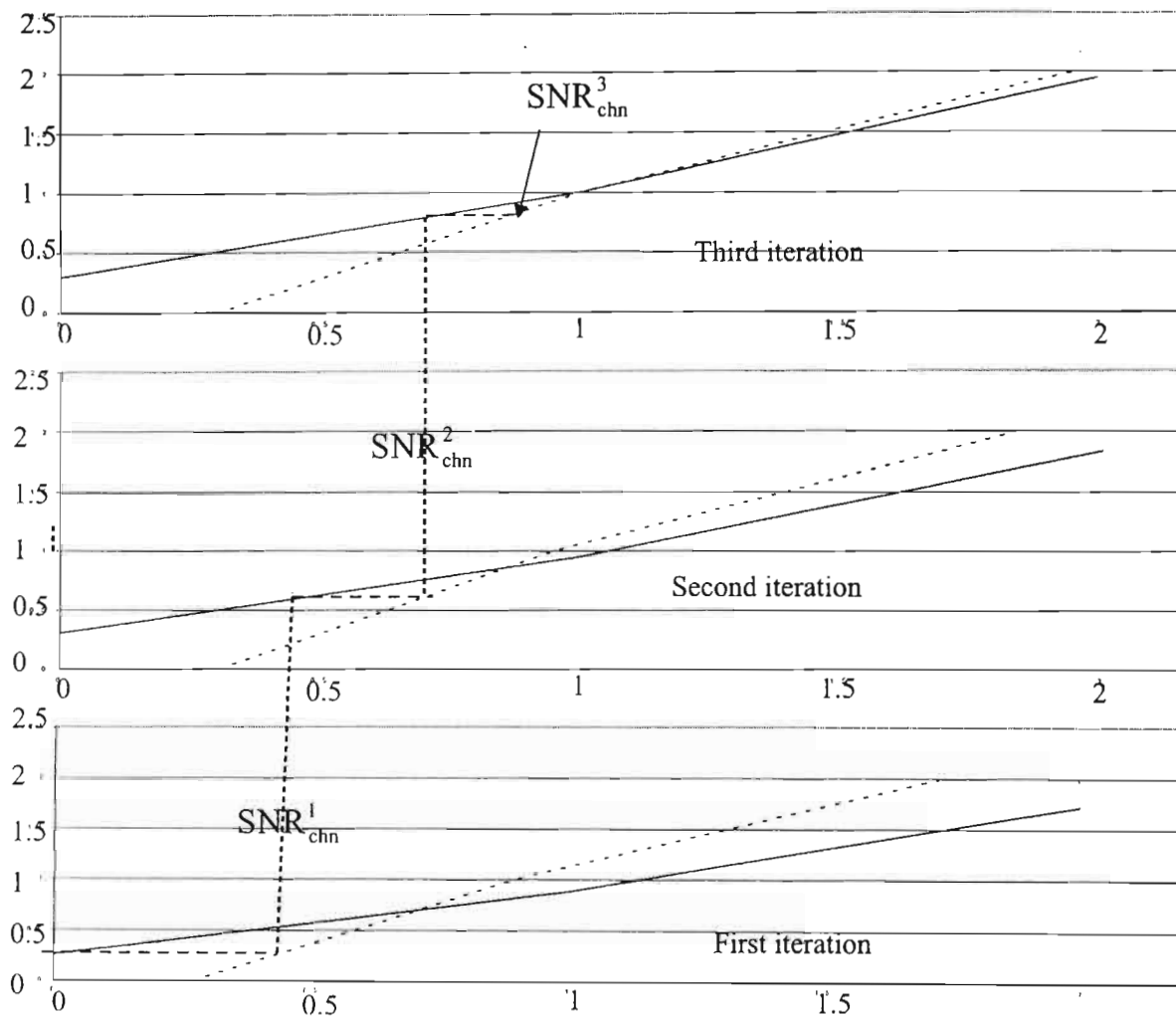


Figure 4.5: Iteration Schedule for the iterative interference cancellation receiver.

4dB and it is observed that convergence will occur between 2.5dB and 3dB. This is shown in Figure 4.9(a). The noise figure of the decoder is also done in the interval 2.5dB to 3dB using finer selection of intervals. The $\left(\frac{PT}{N_o}\right)_{dB}$ at which convergence will occur is found to be 2.64dB. The noise figure computation is computed noting that the SNR_{chn} for the iterative interference cancellation receiver varies from iteration to iteration.

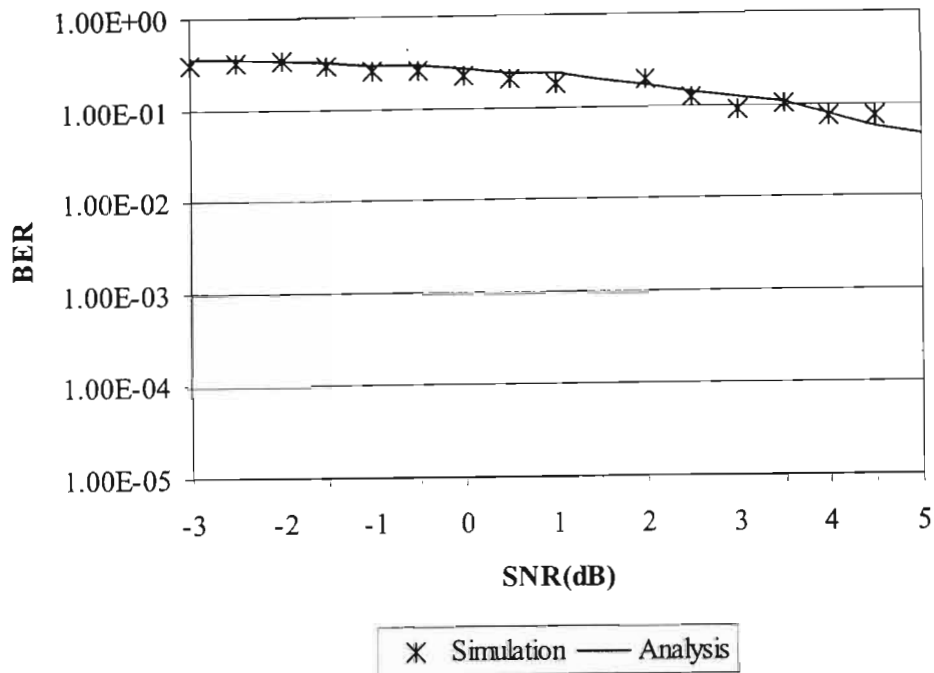


Figure 4.6: Error rate performance of the iterative interference cancellation receiver after one iteration.

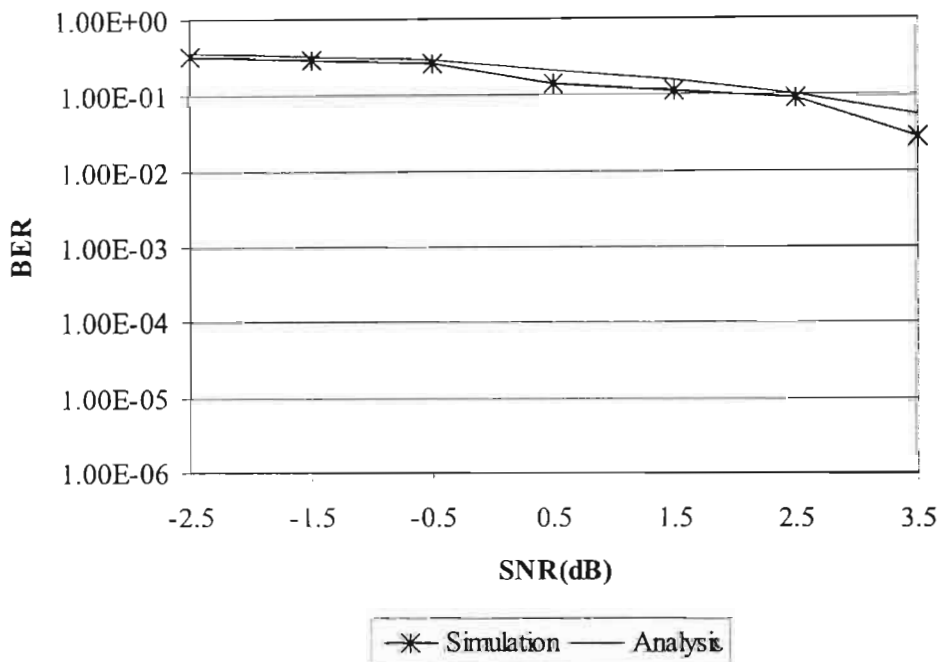


Figure 4.7: Error rate performance of the iterative interference cancellation receiver after two iterations.

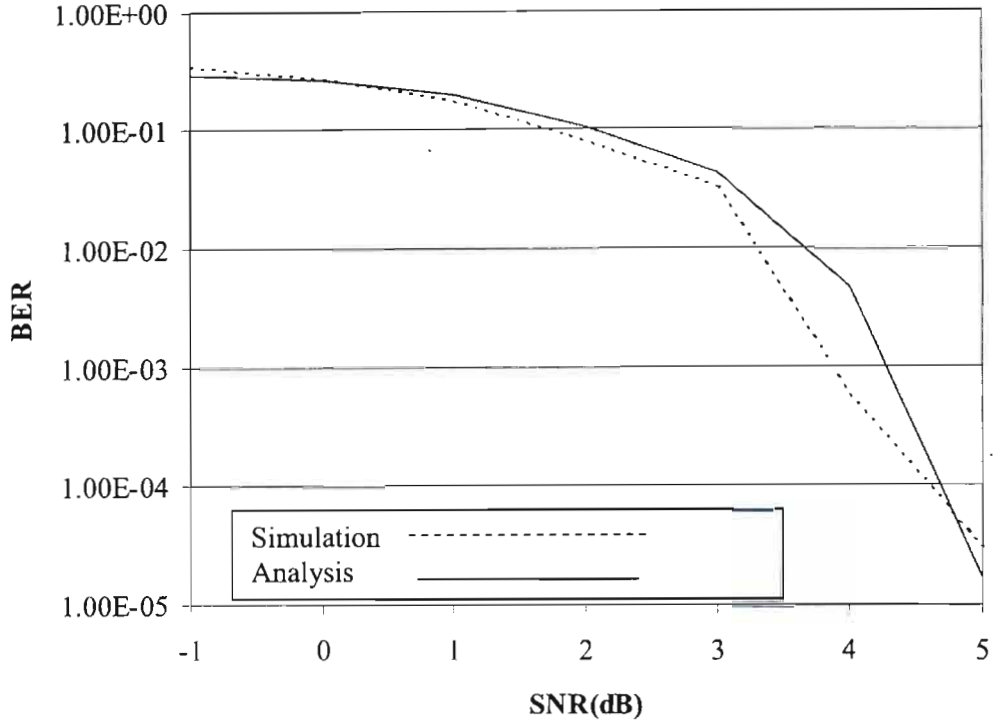


Figure 4.8: Error rate performance of the iterative interference cancellation receiver after three iterations. Dashed line for simulation results. Solid line for Analytical results.

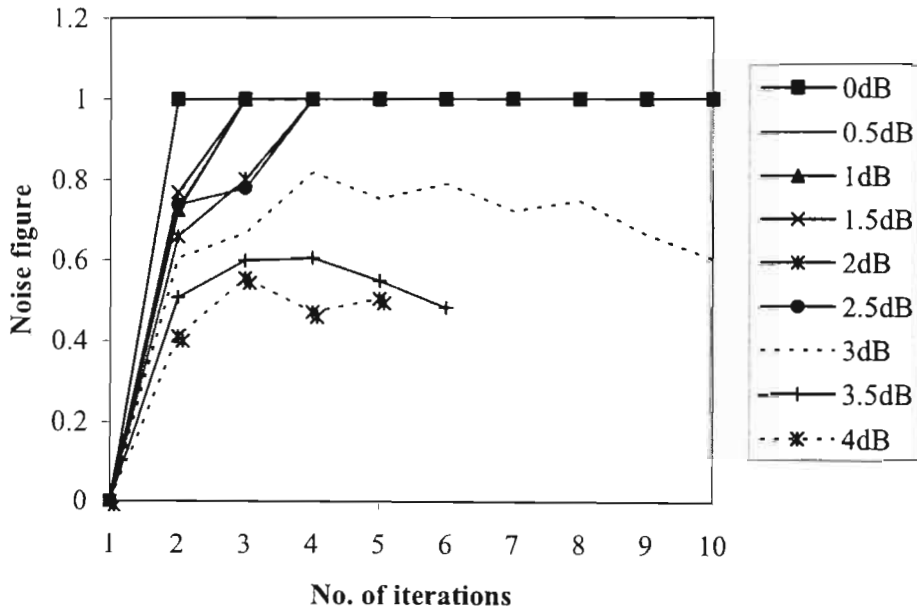


Figure 4.9(a): The noise figure of the turbo decoder over $\left(\frac{PT}{N_0}\right)_{dB}$ of 0dB to 4dB.

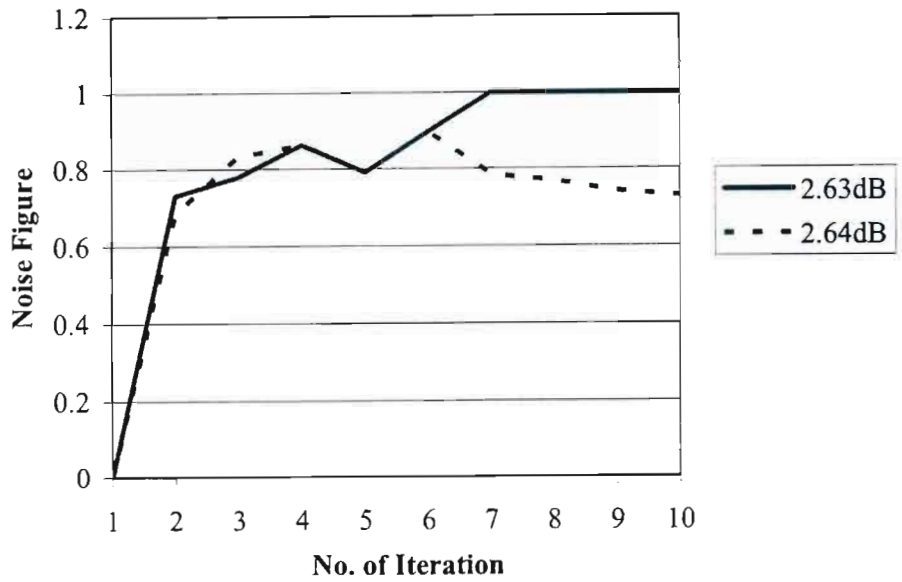


Figure 4.9(b): The noise figure of the turbo decoder over $\left(\frac{PT}{N_o}\right)_{dB}$ of 2.5dB to 3dB.

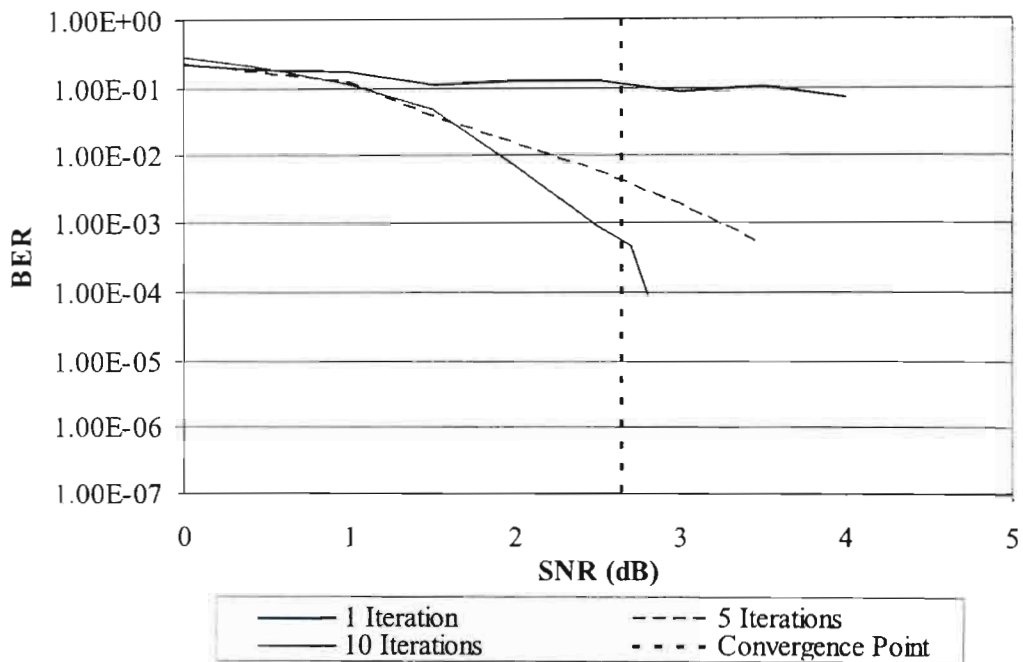


Figure 4.10: Convergence Analysis of the Iterative Interference Cancellation Receiver.

The accuracy of the convergence analysis is verified through computer simulation of the iterative interference cancellation receiver for a framelength of 20000. Results of the simulations and their comparison with the convergence point predicted through analysis are presented in Figure 4.10. The degree of accuracy of the analytical result shows that the methodology that is presented in this Chapter is very accurate despite its simplicity.

4.5 Conclusions.

A methodology for the convergence analysis of the iterative interference cancellation receiver for the turbo coded DS-CDMA system is presented in this Chapter. Analytical expressions are used for the determination of the SNR evolution of the interference cancellation module. This is in contrast to the semi analytical approach that has been used in the literature. Simulation results confirm that the convergence analysis technique is accurate in predicting the point of convergence of the iterative interference cancellation receiver for turbo-coded DS-CDMA systems.

Chapter 5

An Iterative Multiuser Detector for Turbo Coded DS-CDMA Systems

5.1 Introduction

In this Chapter, an iterative multiuser detector for Turbo coded Direct Sequence Code Division Multiple Access (DS-CDMA) systems is proposed. The receiver is derived from the Maximum a-Posteriori (MAP) estimation of the single user's transmitted data, conditioned on information about the estimate of the Multiple Access Interference (MAI) and the received signal from the channel. A direct subtraction of the estimated MAI from the received signal is avoided in the proposed iterative receiver. The motivation for this is the fact that the multiple access interference estimation error could lead to erroneous detection if subtracted directly from the received signal.

The proposed detection paradigm is compared with an earlier proposed detection type that is based on the direct cancellation of the estimated MAI from the received signal prior to channel decoding [Ale98][Ker99]. This type of receiver is discussed in Chapter 4. The multiuser detector proposed in this Chapter has a better performance when the received powers of all active users are equal. The detector is also found to be resilient against the near-far effect.

The complexity of the proposed receiver increases linearly with the number of users. Performances that are close to the single user bound are also obtained after a few number of detection iterations.

The rest of this Chapter is organized as follows. In Section 5.2 the CDMA system model is presented. The proposed iterative multiuser detector is developed in Section 5.3. Issues on implementing the proposed detector are discussed in Section 5.4. The performance of the proposed detector is investigated by simulation for the AWGN channel in Section 5.5.1. The near-far performance of the detector is investigated by simulation in Section 5.5.2. The performance of the multiuser receiver in an asynchronous DS-CDMA system is presented in Section 5.5.3. Section 5.6 concludes the Chapter.

5.2 System Model

5.2.1. Received Signal Model

A Turbo coded synchronous BPSK modulated DS/CDMA system is considered in this Chapter (Figure 5.1). The system transmits over an AWGN channel. In a multiple access system, the signal transmitted by a user k can be represented as:

$$S_k(t) = \sqrt{2P_k} a_k(t) c_k(t) \cos(\omega_c t) \quad (5.1)$$

where $c_k(t)$ stands for the signal of the code bit of user k . Notation $a_k(t)$ represents the signature waveform of user k of period equal to the code bit interval, T , and it is given by [Qui01]

$$a_k(t) = \frac{1}{\sqrt{N}} \sum_{m=0}^{N-1} a_k[m] \text{rect}(t - mT_c) \quad (5.2)$$

where $\text{rect}(t)$ denotes the rectangular chip waveform, N is the processing gain, T_c is the chip duration $\left(T_c = \frac{T}{N}\right)$. Notation P_k represents the power of the transmitted coded

bit of user k . $P_k = \frac{RE_b}{T}$ where R is the coding rate and E_b is the energy of the un-coded information bit. Notation ω_c represents the carrier frequency.

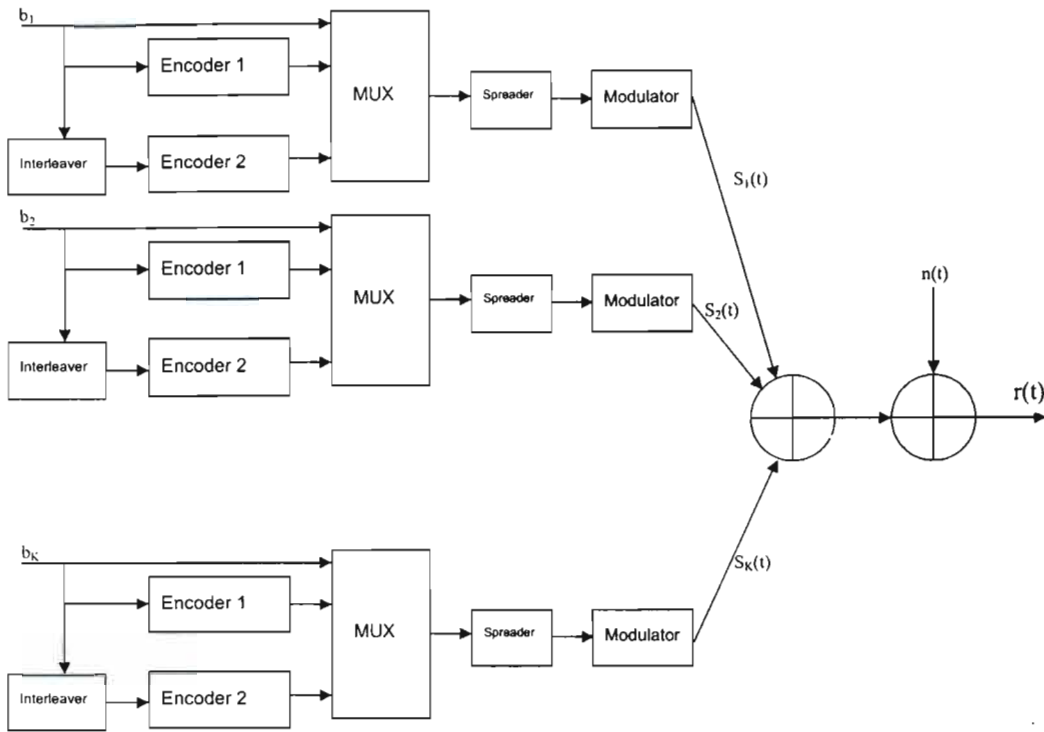


Figure 5.1: A Turbo Coded CDMA transmission System.

The overall transmitted signal on a common channel in a multiple access situation with K number of active users can be expressed as

$$S(t) = \sum_{k=1}^K \sqrt{2P_k} a_k(t) c_k(t) \cos(\omega_c t) \quad (5.3)$$

When transmitted over an AWGN channel, the received signal at the receiver can be expressed as

$$r(t) = \sum_{k=1}^K \sqrt{2P_k} a_k(t) c_k(t) \cos(\omega_c t) + n(t) \quad (5.4)$$

where $n(t)$ represents the AWGN with a double sided spectral density of $\frac{N_0}{2}$.

Without loss of generality, user h is taken as the user of interest. The received signal at the output of the matched filter that is matched to the signature waveform of user h is given by

$$\begin{aligned} U_h &= \int_0^T r(t) \sqrt{\frac{2}{T}} a_h(t) \cos(\omega_c t) dt \\ &= \sqrt{P_h T} c_{h,0} + \sum_{\substack{k=1 \\ k \neq h}}^K \sqrt{\frac{P_k}{T}} c_{k,0} R_{h,k} + \int_0^T n(t) \sqrt{\frac{2}{T}} a_h(t) \cos(\omega_c t) dt \end{aligned} \quad (5.5)$$

The first term of equation (5.5) represents the desired user's component, the second term represents the multiple access interference component and the third term represents the AWGN component. The transmitted coded bit of user k at the current instance is denoted by $c_{k,0}$. The cross correlation between user h and user k is $R_{h,k}$. The matched filter output is a sufficient statistics in detecting the transmitted signal of user h [Qui01].

The Turbo codes considered in this paper are composed of two recursive systematic convolutional codes (RSC) separated by a random interleaver.

5.2.2 Channel Model

In order to investigate the performance of the iterative MUD that is developed in this Chapter with increasing values of cross correlation between users, we will define the K-symmetric channel [Moh98a]. The K-symmetric channel has also been used in

[Ker99],[Hsu01] and [Wan99]. In the K-symmetric channel, the cross-correlation value between different users' signal on the channel is the same. To illustrate the K-symmetric channel, let us represent equation (5.5) in the matrix form as:

$$\mathbf{U} = \mathbf{A}\mathbf{R}\mathbf{C} + \mathbf{N} \quad (5.6)$$

where \mathbf{A} is the diagonal amplitude matrix, \mathbf{C} is the coded bit vector, \mathbf{R} is the correlation matrix and \mathbf{N} is the Gaussian noise vector.

The correlation matrix, \mathbf{R} , can be represented as:

$$\mathbf{R} = \begin{bmatrix} 1 & \rho & \rho & \cdots & \cdots & \rho \\ \rho & 1 & \rho & \cdots & \cdots & \rho \\ \rho & \rho & 1 & & & \\ \vdots & \vdots & & \ddots & & \\ \vdots & \vdots & & & \ddots & \\ \rho & \rho & \rho & \cdots & \cdots & 1 \end{bmatrix} \quad (5.7)$$

All the entries in the correlation, except the diagonal elements are equal to ρ , where ρ is the correlation between users. Note that for the correlation matrix of (5.7), $R_{h,k} = T\rho$ for all $h \neq k$

5.3 The Iterative Multiuser Detector

Figure 5.2 illustrates the concept of the detector being developed in this Section. The estimate of the MAI is not subtracted directly from the received signal. The philosophy behind this approach is that the estimation noise in the estimated MAI can bias the

resultant decision statistics after the cancellation adversely. Therefore, a Maximum a-Posteriori (MAP) estimation of the transmitted bit of the user of interest, given the received baseband signal and the estimate of the MAI is done in this Section. In doing this, the following parameter definitions are made. Let s' represent the immediately previous state on the trellis and let s represent the present state. Let the input bit into the encoder of user h be represented by b_h . Furthermore let the received sequence be represented by \underline{Y} , let the received sequence associated with the immediately previous transition be represented by \underline{Y}_{j-1} , let the received sequence associated with the present transition be represented by \underline{Y}_j and let the received sequence associated with the transition immediately after the present transition be represented by \underline{Y}_{j+1} .

The MAP algorithm performs the estimation by selecting the value of the code bit that maximizes the probability $P(\underline{Y}, \underline{I} | b_h)$. The log-likelihood ratio $L(b_h | \underline{Y}, \underline{I})$, stated in equation (5.8), is a reliable tool for this selection. Notation \underline{I} represents the sequence of the estimated MAI. Let the following definition also be made about the sequence of the estimated MAI. Let the sequence of the estimated MAI associated with the immediately previous transition be represented by \underline{I}_{j-1} , let the sequence of the estimated MAI associated with the present transition be represented by \underline{I}_j and let sequence of the estimated MAI associated with the transition immediately after the present transition be represented by \underline{I}_{j+1} .

Therefore,

$$\begin{aligned}
 L(b_h | \underline{Y}, \underline{I}) &= \ln \left(\frac{P(b_h = +1 | \underline{Y}, \underline{I})}{P(b_h = -1 | \underline{Y}, \underline{I})} \right) \\
 &= \ln \left(\frac{\sum_{\substack{b_h = +1 \\ (s, s')}} P(s, s', \underline{Y}, \underline{I})}{\sum_{\substack{b_h = -1 \\ (s, s')}} P(s, s', \underline{Y}, \underline{I})} \right) \tag{5.8}
 \end{aligned}$$

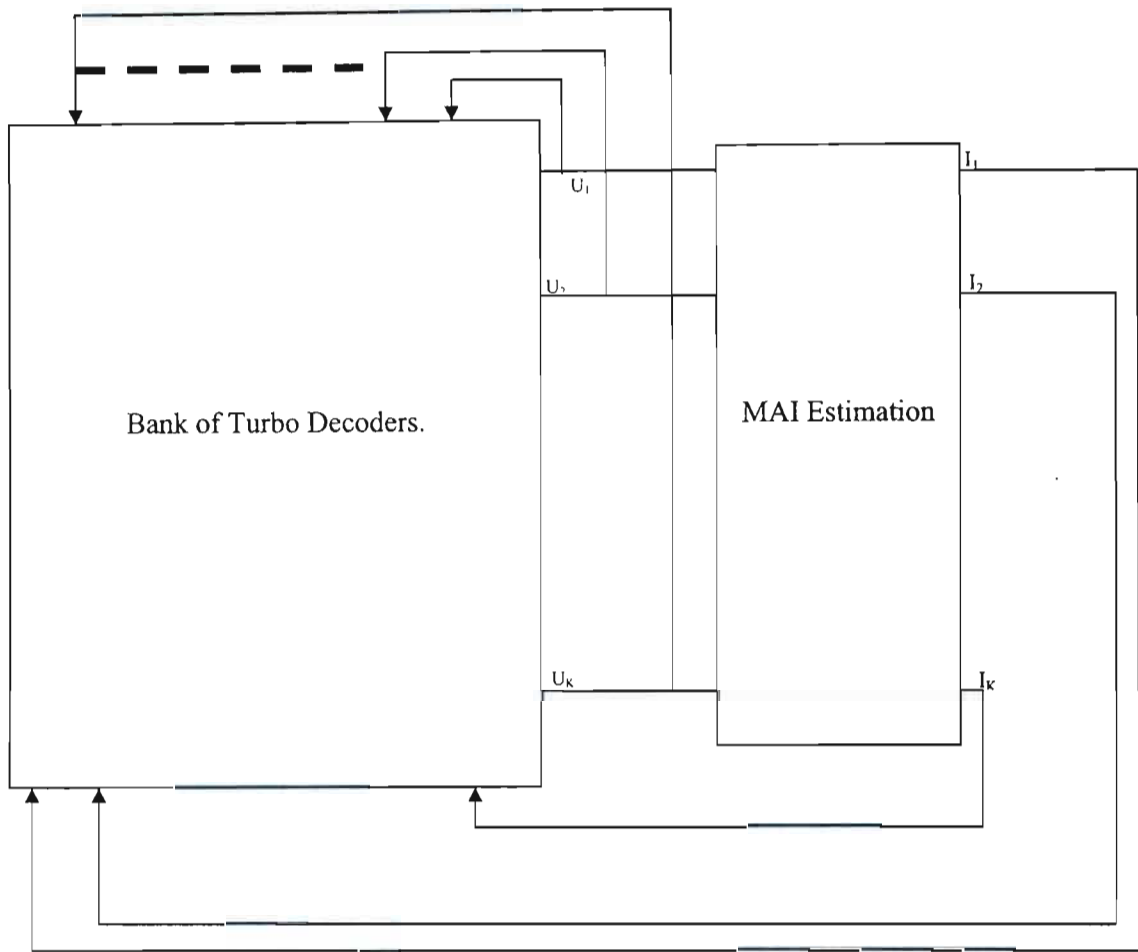


Figure 5.2: The Proposed Iterative Multiuser Detector.

$P(s, s', \underline{Y}, \underline{I})$ can be simplified using the Baye's rule and the Markov property (that say that if s is known, events after time j do not depend on s' or \underline{Y}_j) as:

$$\begin{aligned}
P(s, s', \underline{Y}, \underline{I}) &= P(\underline{Y}_{j-1}, \underline{Y}_j, \underline{Y}_{j+1}, \underline{I}_{j-1}, \underline{I}_j, \underline{I}_{j+1}, s, s') \\
&= P(\underline{Y}_{j+1}, \underline{I}_{j+1} | \underline{Y}_{j-1}, \underline{Y}_j, \underline{I}_{j-1}, \underline{I}_j, s, s') P(\underline{Y}_{j-1}, \underline{Y}_j, \underline{I}_{j-1}, \underline{I}_j, s, s') \\
&= P(\underline{Y}_{j+1}, \underline{I}_{j+1} | s) P(\underline{Y}_{j-1}, \underline{Y}_j, \underline{I}_{j-1}, \underline{I}_j, s, s') \\
&= P(\underline{Y}_{j+1}, \underline{I}_{j+1} | s) \cdot P(s, \underline{Y}_j, \underline{I}_j | \underline{Y}_{j-1}, \underline{I}_{j-1}, s') \cdot P(\underline{Y}_{j-1}, \underline{I}_{j-1}, s') \\
&= P(\underline{Y}_{j+1}, \underline{I}_{j+1} | s) \cdot P(s, \underline{Y}_j, \underline{I}_j | s') \cdot P(\underline{Y}_{j-1}, \underline{I}_{j-1}, s') \\
&= \beta'_j(s) \gamma'_j(s, s') \alpha'_{j-1}(s')
\end{aligned} \tag{5.9}$$

where $\alpha'_{j-1}(s')$, $\beta'_j(s)$ and $\gamma'_j(s, s')$ are defined as:

$$\alpha'_{j-1}(s') = P(\underline{Y}_{j-1}, \underline{I}_{j-1}, s') \tag{5.10}$$

$$\beta'_j(s) = P(\underline{Y}_{j+1}, \underline{I}_{j+1} | s) \tag{5.11}$$

$$\gamma'_j(s, s') = P(s, \underline{Y}_j, \underline{I}_j | s') \tag{5.12}$$

$$\begin{aligned}
\alpha'_j(s) &= P(\underline{Y}_j, \underline{I}_j, s') \\
&= \sum_{\text{all } s'} P(s, \underline{Y}_j, \underline{I}_j, s') \\
&= \sum_{\text{all } s'} P(s, \underline{Y}_j, \underline{Y}_{j-1}, \underline{I}_j, \underline{I}_{j-1}, s') \\
&= \sum_{\text{all } s'} P(s, \underline{Y}_{j-1}, \underline{I}_{j-1}) P(s, \underline{Y}_j, \underline{I}_j, | s', \underline{Y}_{j-1}, \underline{I}_{j-1}) \\
&= \sum_{\text{all } s'} P(s, \underline{Y}_{j-1}, \underline{I}_{j-1}) P(s, \underline{Y}_j, \underline{I}_j, | s') \\
\alpha'_j(s) &= \sum_{\text{all } s'} \alpha'_{j-1}(s') \gamma'_j(s, s')
\end{aligned} \tag{5.13}$$

$$\begin{aligned}
\beta'_j(s) &= P(\underline{Y}_{j+1}, \underline{I}_{j+1} | s) \\
&= \sum_{\text{all } s'} P(s', \underline{Y}_{j+1}, \underline{I}_{j+1} | s) \\
&= \sum_{\text{all } s'} \frac{P(s', \underline{Y}_{j+1}, \underline{I}_{j+1}, s)}{P(s)} \\
&= \sum_{\text{all } s'} \frac{P(s', \underline{Y}_{j+1}, \underline{I}_{j+1}, \underline{Y}_{j+2}, \underline{I}_{j+2}, s)}{P(s)} \\
&= \sum_{\text{all } s'} \frac{P(\underline{Y}_{j+2}, \underline{I}_{j+2} | s', \underline{Y}_{j+1}, \underline{I}_{j+1}, s) P(s', s)}{P(s)} \\
&= \sum_{\text{all } s'} \frac{P(\underline{Y}_{j+2}, \underline{I}_{j+2} | s') P(s', \underline{Y}_{j+1}, \underline{I}_{j+1} | s) P(s)}{P(s)} \\
&= \sum_{\text{all } s'} P(\underline{Y}_{j+2}, \underline{I}_{j+2} | s') P(s', \underline{Y}_{j+1}, \underline{I}_{j+1} | s) \\
&= \sum_{\text{all } s'} \beta'_{j+1}(s') P(s', \underline{Y}_{j+1}, \underline{I}_{j+1} | s) \\
\beta'_j(s) &= \sum_{\text{all } s'} \beta'_{j+1}(s') \gamma'_{j+1}(s, s')
\end{aligned} \tag{5.14}$$

and

$$\begin{aligned}
\gamma'_j(s, s') &= P(s, \underline{Y}_j, \underline{I}_j | s') \\
&= P(\underline{Y}_j, \underline{I}_j | s, s') P(s | s') \\
\gamma'_j(s, s') &= P(\underline{Y}_j, \underline{I}_j | x_k) \cdot P(b_h)
\end{aligned} \tag{5.15}$$

where b_h stands for the input bit that is necessary to cause the transition from state s' to state s . Notation x_k represents the transmitted codeword associated with this transition. $\alpha'_{j-1}(s')$ is the forward recursion coefficient, $\beta'_j(s)$ is the backward recursion coefficient and $\gamma'_j(s, s')$ is the transition coefficient (Figure 5.3). Implementing the MAP recursive algorithm as stated in equations (5.13) and (5.14) leads to a numerically

unstable algorithm [Rya][Hag96][Qui01]. To ensure stability, these quantities must be

$$\text{normalized as } \tilde{\alpha}'_j(s') = \frac{\alpha'_j(s')}{\sum_{\text{all } s'} \alpha'_j(s')} \text{ and } \tilde{\beta}'_j(s) = \frac{\beta'_j(s)}{\sum_{\text{all } s'} \alpha'_j(s')} .$$

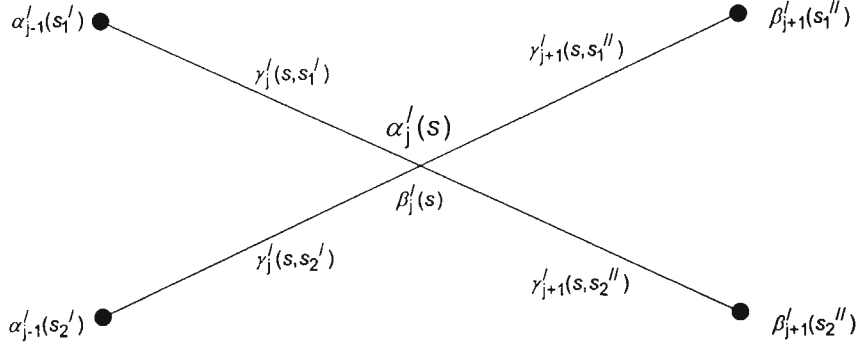


Figure 5.3: Forward and reverse state probability recursions.

The log-likelihood ratio can, thus, be calculated from

$$L(b_h | \underline{Y}, \underline{I}) = \ln \left(\frac{\sum_{\substack{b_h=+1 \\ (s, s')}} \tilde{\alpha}'_{j-1}(s') \tilde{\beta}'_j(s) \gamma'_j(s, s')}{\sum_{\substack{b_h=-1 \\ (s, s')}} \tilde{\alpha}'_{j-1}(s') \tilde{\beta}'_j(s) \gamma'_j(s, s')} \right) \quad (5.16)$$

The estimated MAI sequence and the received signal sequence are not independent variables. They are mutually correlated. As the number of user increases, the two sequences can be taken to have a probability density function (PDF) that is jointly Gaussian. The joint PDF of the received sequence and the sequence of the estimated MAI given the transmitted coded sequence is therefore given as [Pap84]

$$\begin{aligned}
P(\underline{Y}_j, \underline{I}_j | x_k) &= \prod_{l=1}^n \left\{ \frac{1}{2\prod \sigma_1 \sigma_2 \sqrt{1-r^2}} \cdot \left[\exp \left(- \left(\frac{(Y_{jl} - X_{jl})^2}{\sigma_1^2} - \frac{2r(Y_{jl} - X_{jl})I_{jl}}{\sigma_1 \sigma_2} + \frac{I_{jl}^2}{\sigma_2^2} \right) \right) \right]^{\frac{1}{2(1-r^2)}} \right\} \\
&= A.B \prod_{l=1}^n \left\{ \left[\exp \left(\frac{2Y_{jl}X_{jl}}{\sigma_1^2} + \frac{2r(Y_{jl} - X_{jl})I_{jl}}{\sigma_1 \sigma_2} \right) \right]^{\frac{1}{2(1-r^2)}} \right\}
\end{aligned} \tag{5.17}$$

where $A = \frac{1}{2\prod \sigma_1 \sigma_2 \sqrt{1-r^2}}$ and $B = \prod_{l=1}^n \left\{ \left[\exp \left(\frac{-Y_{jl}^2 - X_{jl}^2 - I_{jl}^2}{\sigma_1^2} - \frac{I_{jl}^2}{\sigma_2^2} \right) \right]^{\frac{1}{2(1-r^2)}} \right\}$. The

variable r stands for the value of the correlation between the received signal (Y) and the estimate of the MAI (I), σ_1^2 stands for the variance of the received signal and σ_2^2 stands for the variance of the estimate of the MAI. From [Hag96], it is shown that

$$\begin{aligned}
P(b_h) &= \left(\frac{\exp[-L^e(b_h)/2]}{1 + \exp[-L^e(b_h)]} \right) \cdot \exp[b_h L^e(b_h)/2] \\
&= D_j \exp[b_h L^e(b_h)/2]
\end{aligned} \tag{5.18}$$

where $L^e(b_h) \triangleq \log \left(\frac{P(b_h = +1)}{P(b_h = -1)} \right)$ and $D_k = \left(\frac{\exp[-L^e(b_h)/2]}{1 + \exp[-L^e(b_h)]} \right)$. Then,

$$\gamma'_j(s, s') = ABD_j \exp \left(\frac{b_h L^e(b_h)}{2} \right) \cdot \prod_{l=1}^n \left\{ \left[\exp \left(\frac{2Y_{jl}X_{jl}}{\sigma_1^2} \right) \right]^{\frac{1}{2(1-r^2)}} \left[\exp \left(\frac{2r(Y_{jl} - X_{jl})I_{jl}}{\sigma_1 \sigma_2} \right) \right]^{\frac{1}{2(1-r^2)}} \right\} \tag{5.19}$$

Since $\gamma'_k(s, s')$ appears both in the numerator and the denominator of equation(5.16), factor A , B and D_j will be cancelled out as they are independent of b_h . $\gamma'_j(s, s')$ can be represented by

$$\gamma'_j(s, s') \sim \exp\left(\frac{b_h L^e(b_h)}{2}\right) \cdot \prod_{l=1}^n \left\{ \left[\exp\left(\frac{2Y_{jl}X_{jl}}{\sigma_1^2}\right) \right]^{\frac{1}{2(1-r^2)}} \left[\exp\left(\frac{2r(Y_{jl}-X_{jl})I_{jl}}{\sigma_1\sigma_2}\right) \right]^{\frac{1}{2(1-r^2)}} \right\} \quad (5.20)$$

For the case of a turbo coding with coding rate 1/3 that is considered in this paper, $\gamma'_j(s, s')$ can be represented as

$$\begin{aligned} \gamma'_j(s, s') &\sim \exp(b_h L^e(b_h)/2) \cdot \left(\exp\left(\frac{2Y_{j1}b_h}{\sigma_1^2} + \frac{2rY_{j1}I_{j1}}{\sigma_1\sigma_2} - \frac{2rb_h I_{j1}}{\sigma_1\sigma_2}\right) \right)^{\frac{1}{2(1-r^2)}} \\ &\quad \cdot \left(\exp\left(\frac{2Y_{jp}X_{jp}}{\sigma_1^2} + \frac{2rY_{jp}I_{jp}}{\sigma_1\sigma_2} - \frac{2rX_{jp}I_{jp}}{\sigma_1\sigma_2}\right) \right)^{\frac{1}{2(1-r^2)}} \quad (5.21) \\ &= \exp(b_h L^e(b_h)/2) \cdot \left(\exp\left(\frac{2Y_{j1}b_h}{\sigma_1^2} + \frac{2rY_{j1}I_{j1}}{\sigma_1\sigma_2} - \frac{2rb_h I_{j1}}{\sigma_1\sigma_2}\right) \right)^{\frac{1}{2(1-r^2)}} \cdot \chi_j^e(s, s') \end{aligned}$$

where $\chi_j^e(s, s') = \left(\exp\left(\frac{2Y_{jp}X_{jp}}{\sigma_1^2} + \frac{2rY_{jp}I_{jp}}{\sigma_1\sigma_2} - \frac{2rX_{jp}I_{jp}}{\sigma_1\sigma_2}\right) \right)^{\frac{1}{2(1-r^2)}}$. The log likelihood ratio of equation (5.8) can then be simplified as

$$L(b_h) = L^e(b_h) + \frac{2Y_{j1}}{(1-r^2)\sigma_1^2} - \frac{2rI_{j1}}{(1-r^2)\sigma_1\sigma_2} + \ln \left(\frac{\sum_{\substack{(s,s') \\ b_j=+1}} \alpha'_{j-1}(s') \chi_j^e(s,s') \beta'_j(s)}{\sum_{\substack{(s,s') \\ b_j=-1}} \alpha'_{j-1}(s') \chi_j^e(s,s') \beta'_j(s)} \right) \quad (5.22)$$

This log-likelihood ratio (taken for each user) is the reliable information that is used in the estimation of the multiple access interference sequence.

5.4 Implementing the Iterative Detector

A detailed functional diagram of the iterative receiver is illustrated in Figure 5.4. The estimated MAI is multiplexed into decoders 1 and 2 such that I_{j1} and I_{j2} are sent to decoder 1 while I_{j1} and I_{j3} are sent into decoder 2. These information are used as added knowledge in the MAP estimation of the transmitted bits in each decoder. The MAP decoder is adapted to estimate the coded bit instead of the information bit. This is done in order to avoid re-encoding the decoded information sequence before the interference estimation. Another advantage of this approach is that different types of tentative decision technique could be used apart from the hard decision.

After the hard tentative decision has been taken, each bit is re-spread and multiplied by the transmitted power. This power should have been estimated by an algorithm that is, however, not a subject of this paper. The estimated interference on the user of interest is the summation of all the re-spread and signal from all the other users.

$$\hat{U}_{mai} = \sum_{\substack{k=1 \\ k \neq j}}^K \sqrt{P_k T_b} \hat{c}_k R_{j,k} \quad (5.23)$$

\hat{c}_k is the decoded bit of user k .

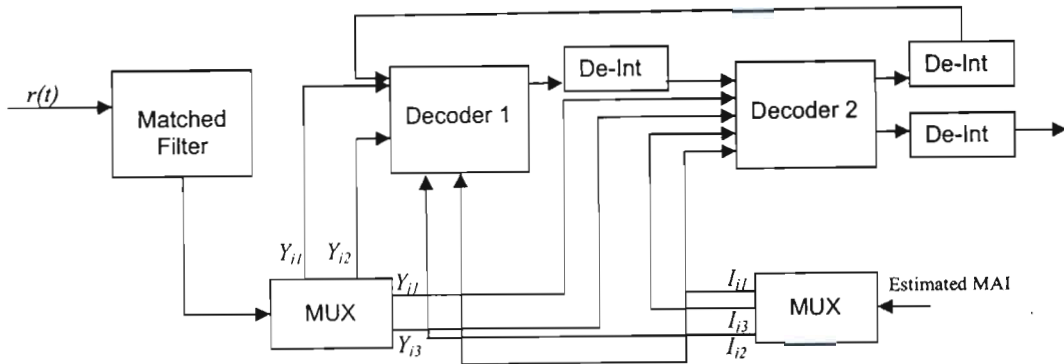


Figure 5.4: Functional diagram of the proposed iterative multiuser detector.

The estimated interference is input into the two component decoders through a multiplexer. The multiplexer ensures that the estimated interference bit due to interfering information bit is sent to both decoders (with the sequence sent to the second decoder interleaved). The estimated interference due to the interfering parity bits is sent to the appropriate component decoder.

5.5 Performance Discussion

The performance results of the proposed system are discussed in this Section. Both simulation and analytical results are given. The developed system is compared with the conventional iterative receiver system through simulations. By the conventional iterative receiver system we mean the approach in which the estimated interference is subtracted from the received signal prior to channel decoding. This type of receiver is discussed in [Ale98][Ker99].

5.5.1 Simulation Results in K-Symmetric AWGN Channel

The component encoder used in the simulations is the recursive systematic convolutional encoder (1,5/7). Each encoder is separated by a random interleaver. The coding rate is 1/3. The simulations were performed for frame length of 200. The signal-to-noise ratio is defined as $\frac{E_b}{N_0}$.

The cross correlation between adjacent users in a DS-CDMA system is typically low. If the orthogonal Hadamard code is used a cross correlation value of zero could be obtained [Moh98a]. Using the Gold code generated from polynomials of order z for instance, a

maximum cross correlation values of $\frac{2^{\frac{(z+1)}{2}} + 1}{2^z - 1}$ is obtained when the value of z is odd

and $\frac{2^{\frac{(z+2)}{2}} + 1}{2^z - 1}$ is obtained when the value of z is even [Ser80]. This translates to a

maximum cross correlation value of 0.29 for a system with a processing gain of 31; 0.27 for a system with a processing gain of 63 and 0.13 for a system with a processing gain of 127. Therefore, for practical DS-CDMA applications, the value of the cross correlation between adjacent signals is not expected to be very high. In our simulations therefore, cross correlation values of 0.25, 0.3 and 0.35 are used.

Figure 5.5 and 5.6 show the comparison of the bit-error-rate performances of the iterative receiver developed in this paper and the conventional iterative interference canceller. The number of users is 10 and all users have an equal received power. For a low cross correlation value of 0.25, the performance of our system is better than the performance of the conventional interference canceller. Also, our receiver converged after the 6th iteration and the conventional iterative receiver converged after the 8th iteration. It can be seen, though, that the proposed receiver converged to a better value than the conventional receiver. The margin of improvement in the performance of our system becomes more obvious at a higher value of cross correlation (0.3). In fact at a cross correlation value of 0.3, the performance of the conventional iterative interference canceller breaks down. This same phenomenon is observed in [Ker99] for the conventional interference canceller with weighted MAI estimate.

At a cross correlation value of 0.25 and after three iterations, our receiver has a dB gain of about 2.5dB at a BER of 1×10^{-3} over the conventional interference canceller. When

the cross correlation value was increased to 0.3 the conventional iterative interference canceller stops converging. Our iterative multiuser detector still converges at low SNR values when the cross correlation value was increased to 0.35. This is illustrated in Figure 5.7.

Figure 5.8 shows the performance of the iterative multiuser detector with 1, 10 and 15 users at a cross correlation value of 0.3. The number of iteration is 3. The low sensitivity of the multiuser detector to channel loading is evident from the small degradation in system performance when the number of users was increased from 1 to 15.

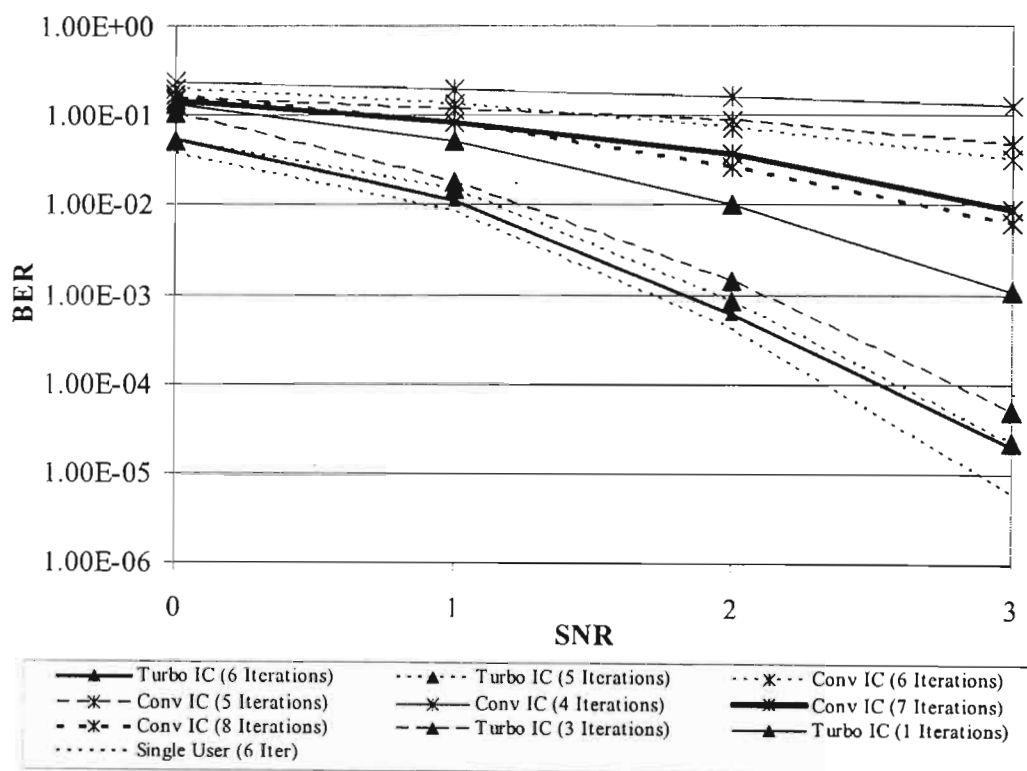


Figure 5.5: Comparison of the performance of the “Turbo IC” and the Conventional Iterative Interference Canceller. Cross-Correlation = 0.25, K=10, Framelength=200.

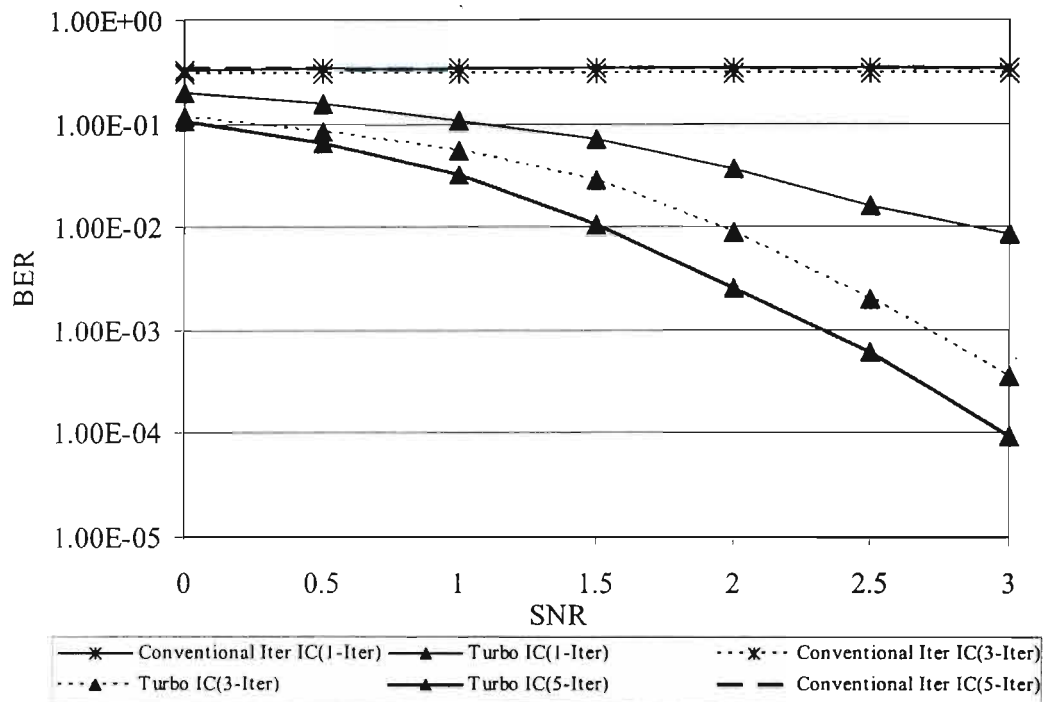


Figure 5.6: Comparison of the performance of the “Turbo IC” and the Conventional Iterative Interference Canceller. Cross-Correlation = 0.3, K=10, Framelength=200.

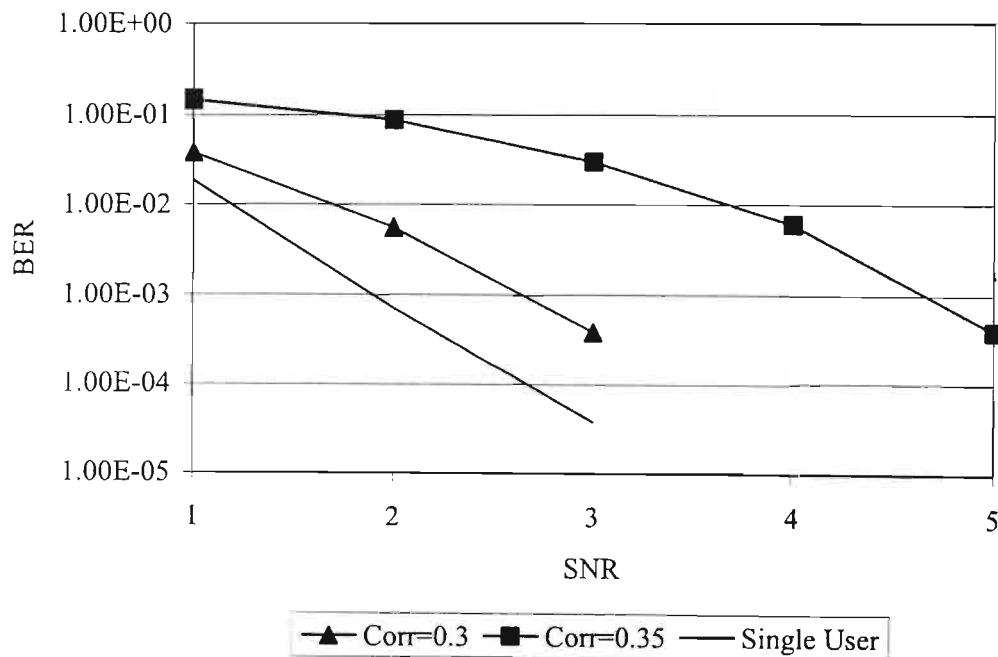


Figure 5.7: Performance of the “Turbo IC” with various cross-correlation values K=10, Framelength=200.

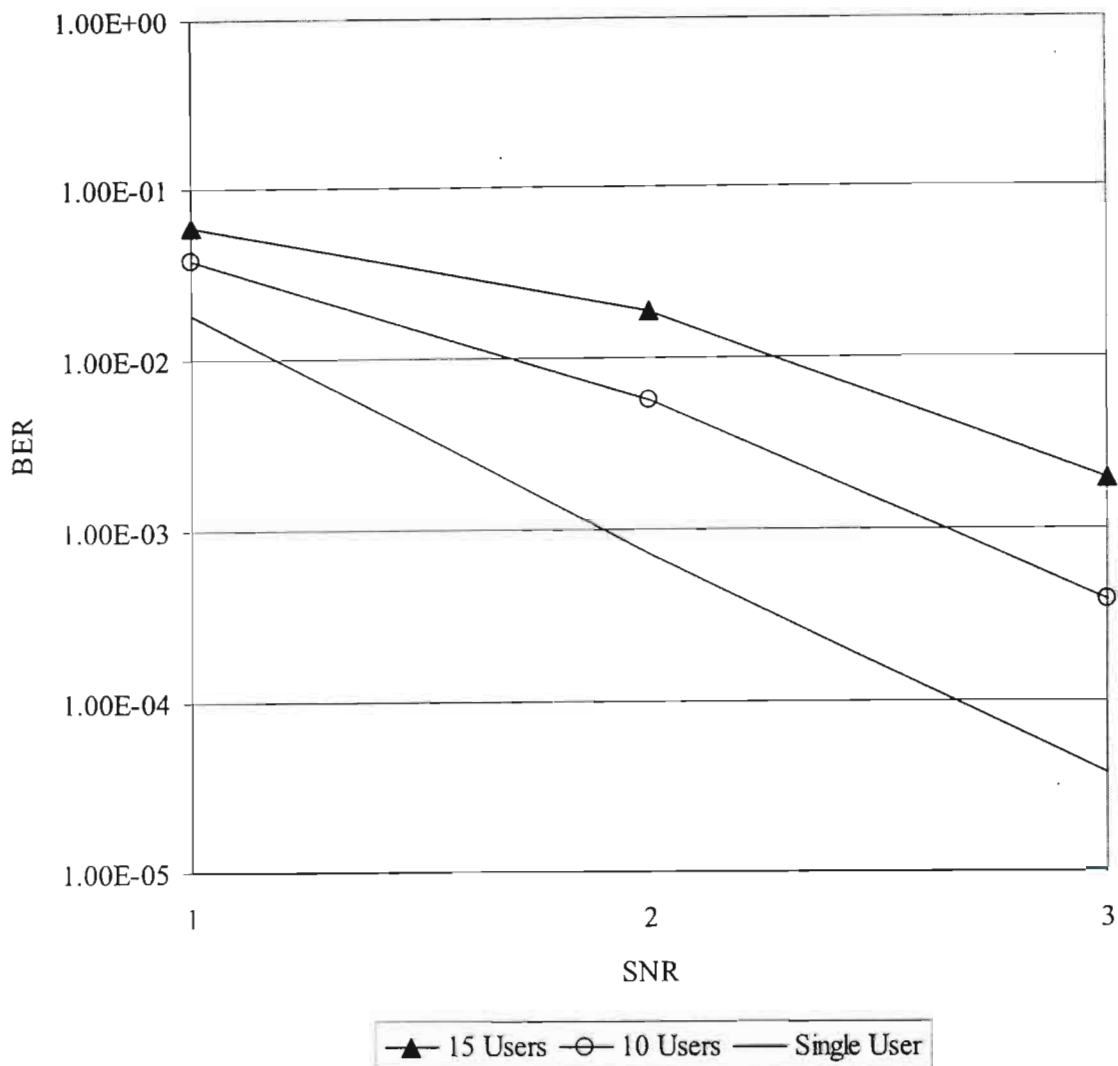


Figure 5.8: Performance of the “Turbo IC” with various numbers of users. Cross-correlation=0.3, Framelength=200. 3 iterations.

5.5.2 Near-Far Performance

The performance of the “Turbo IC” in the near-far scenario is studied in this Section. To perform this study we use 10 users out of which five users transmit at powers that are 3.01dB and 4.8dB stronger than the other five. Our user of interest is taken to be among the five “weaker” users in both cases. The cross-correlation between users is taken to be 0.3 and the framelength is 200. Figure 5.9 shows that the performance of the user of interest improves after one iteration in the near-far scenario when compared with the equal power scenario. This same phenomenon was observed in [Wan99] and [Ale98]. This phenomenon disappears as the number of iteration increases. After three iterations, it can be noticed that there is only a slight degradation in the performance of the “Turbo

IC” as the difference in SNR between the signals of the strong and the weak interferers increases from 0dB to 3.01dB and finally to 4.8dB.

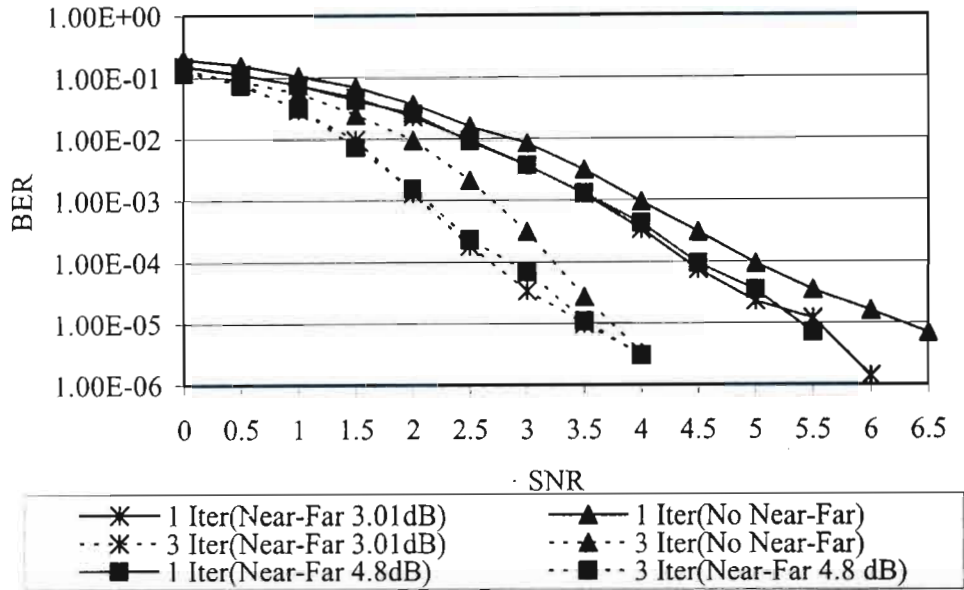


Figure 5.9: Performance of the “Turbo IC” in near-far scenarios. Cross-correlation=0.3, Framelength=200.

5.5.3 Performance in the asynchronous DS-CDMA system.

We investigate the performance of the developed multiuser detector in the asynchronous DS-CDMA system in this Section. The output of the transmitter of a given user k is still as stated in equation(5.1). The received signal at the receiver in an Additive White Gaussian Noise (AWGN) channel can be expressed as

$$r(t) = \sum_{k=1}^K \sqrt{2P_k} a_k(t) c_k(t) \cos(\omega_c t + \varphi_k) + n(t) \quad (5.24)$$

where φ_k is the phase shift of the signal of user k with respect to a reference. In this case user 1’s signal could be selected as that reference and $0 \leq \varphi_k \leq 2\pi$.

If we again take user h as our user of interest and if $r(t)$ is detected by a matched filter that is matched to the signature sequence of user h then the output of the matched filter can be expressed as:

$$\begin{aligned}
 U_h &= \int_0^T r(t) \sqrt{\frac{2}{T}} a_h(t) \cos(\omega_c t) dt \\
 &= \sqrt{P_h T} c_{h,0} + \sum_{\substack{k=1 \\ k \neq h}}^K \sqrt{\frac{P_k}{T}} (c_{k,-1} R_{h,k}(\tau_{h,k}) + c_{k,0} \hat{R}_{h,k}(\tau_{h,k})) \cos \phi_{h,k} \\
 &\quad + \int_0^T n(t) \sqrt{\frac{2}{T}} a_h(t) \cos(\omega_c t) dt
 \end{aligned} \tag{5.25}$$

where $\phi_{h,k} = \varphi_h - \varphi_k$. $R_{ab}(\tau) = \int_0^\tau a_a(t-\tau) a_b(t) dt$ and $\hat{R}_{ab}(\tau) = \int_\tau^T a_a(t-\tau) a_b(t) dt$.

Notation T represents the message bit duration of the user of interest.

Figure 5.10 shows the bit error rate performance of the developed system in a turbo coded system having a component encoder RSC (1,5/7). The framelength is 200, the processing gains are 15 and 31 respectively. The number of users is 10 and the number of iterations is three.

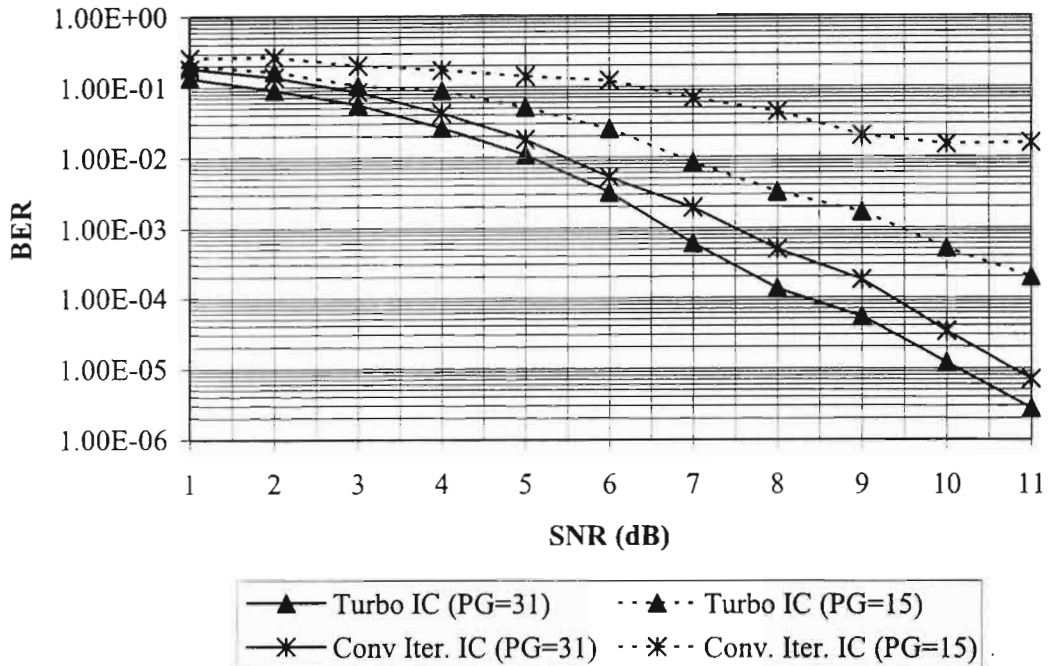


Figure 5.10: Performance of the “Turbo IC” in the asynchronous DS-CDMA system.

It will be observed that the multiuser detector that is developed in this Chapter has error rate performances that are better than those of the conventional iterative interference canceller. The margin of the performance superiority reduces, however, as the processing gain increases.

5.6 Conclusion

In this Chapter, a low complexity iterative interference canceller for Turbo coded CDMA systems has been presented. The developed receiver was compared with the receiver of [Ale98] under various cross-correlation conditions in the AWGN channel. The performance of the proposed detector is found to be superior to those of the receiver of [Ale98].

As the cross-correlation between users in a synchronous CDMA systems increases from the medium value of 0.25 to a higher value of 0.35 we observed the breakdown in performance of the detector of [Ale98]. Our proposed receiver, however, continues to perform in this range of cross-correlation values, albeit with some performance changes. The proposed system was found to be very close to the single user bound within a few numbers of iterations. The proposed receiver is also found to be resilient against the near-far effect.

The complexity of the proposed receiver is linear with the number of users. This level of complexity of the proposed receiver and its performance advantage over the conventional iterative interference canceller of [Ale98] makes the proposed receiver suitable for use in CDMA systems.

Chapter 6

Performance of the Iterative Multiuser Detection in Multirate DS-CDMA Systems.

6.1 Introduction

In the integrated wireless personal communication scenario, there is the need to provide different classes of services to different types of traffic on the channel. For example, the voice traffic requires more stringent transmission rate than the data traffic in order to provide acceptable voice quality at the receiver side of the transmission. Therefore there is the need for the ability to provide wireless communication systems that can handle different types of traffic seamlessly. That means the integration of emerging networks should be able to provide different data transmission rates for different types of traffic. For the DS-CDMA system that is the subject of this dissertation (and that is a major candidate technology in the emerging wireless communication systems), one of the ways of achieving the objective of providing a variable transmission rate is by employing multirate DS-CDMA transmission.

For CDMA systems, the selection of the FEC coding rate, the modulation type and the processing gain determines the transmission rate of the system [Hot96]. All the methods of transmission rate selection stated above have been used extensively in CDMA systems and have been reported in the literature [Oja96] [Joh96][Cho02]. The variable transmission rate based on the selection of variable processing gain is used in this

Chapter because the implementation of a system changing from one processing gain value to the other while transmission is in progress is easier than the implementation of the system involving changes in modulation type. Also, the search for the optimum puncturing pattern is not required as is the case with variable FEC coding rate. CDMA systems having variable processing gains are referred to as the multirate CDMA.

The implementation of the multirate CDMA could be static or dynamic. By static multirate CDMA is meant a situation where the processing gain is negotiated before the commencement of transmission. The negotiated processing gain is then left unchanged for the duration of the transmission. This type of multirate system has been used with interference cancellation multiuser receivers in [Oja96] [Joh96] [Mah99] [Mee99]. In the dynamic multirate CDMA, the processing gain for a particular type of traffic could change while the transmission is in progress. The dynamic multirate CDMA system is used in [Cho02] for the adaptive MMSE multiuser receiver.

Performance of the iterative multiuser receiver that was developed in Chapter 5 in the multirate CDMA scenario is investigated in this Chapter. The performance penalty suffered by traffic that is transmitted with lower processing gain is investigated and results will show that the iterative multiuser detector is suitable for variable traffic transmission using the multirate CDMA approach.

In Section 6.2 the models of the multirate CDMA system are presented. Simulation parameters for the multirate CDMA are presented in Section 6.3. Discussion of results is presented in Section 6.4. Section 6.5 concludes the Chapter.

6.2 Multirate CDMA System Model.

In investigating the performance of the iterative receiver in the multirate CDMA system, we shall begin by defining the system model. In the multirate CDMA system, different classes of signals are spread, at the transmitter, with different lengths of spreading codes. The transmitted information by a given user k is as given in equation (5.1) and the signal received at the receiver can be expressed as in equation (5.4).

We consider a multirate CDMA system with two different processing gains. Random spreading codes are used in the simulation. We want to investigate the performance of the iterative multiuser detector when the user of interest has a processing gain that is the higher of the two processing gains and when the user of interest has a processing gain that is the lower of the two processing gains. It should be mentioned, however, that the multirate CDMA systems that are discussed in this Chapter could be extended to cases having more than two processing gains easily. At the receiver, to detect the transmitted signal when the user of interest has the longer spreading sequence, the output of the matched filter will be

$$\begin{aligned}
 U_h &= \int_0^T r(t) \sqrt{\frac{2}{T}} a_h(t) \cos(\omega_c t) dt \\
 &= \sqrt{P_h T} c_{h,0} + \sum_{\substack{k=1 \\ k \neq h}}^{K_m} \sqrt{\frac{P_k}{T}} (c_{k,-1} R_{h,k}(\tau_{h,k}) + c_{k,0} \bar{R}_{h,k}(\tau_{h,k})) \cos \phi_{h,k} \\
 &\quad + \sum_{g=1}^{K_n} \sqrt{\frac{P_g}{T}} (c_{g,-2} R_{h,g}(\tau_{h,g}) + c_{g,-1} \bar{R}_{h,g}(\tau_{h,g}) + c_{g,0} \bar{R}_{h,g}(\tau_{h,g})) \cos \phi_{h,g} \\
 &\quad + \int_0^T n(t) \sqrt{\frac{2}{T}} a_h(t) \cos(\omega_c t) dt
 \end{aligned} \tag{6.1}$$

Symbol $\tau_{h,g}$ is the time delay between the information bits of users h (the user of interest that has the larger processing gain) and user g (a user that has the lower

processing gain). $\tau_{h,g} \leq T \left(\frac{PG_{low}}{PG_{high}} \right)$ and PG_{low} is the lower processing gain while PG_{high} is the higher processing gain. $\tau_{h,k} \leq T$. Notation K_m stands for the number of users having the same processing gain as the user of interest. Notation K_n stands for the number of users having different processing gain from that of the user of interest. Figure 6.1(a) illustrates the interaction between interfering bits for the case where the user of interest has the higher processing gain.

To detect the transmitted signal when the user of interest has the shorter spreading sequence, the output of the matched filter will be

$$\begin{aligned}
 U_h &= \int_0^T r(t) \sqrt{\frac{2}{T}} a_h(t) \cos(\omega_c t) dt \\
 &= \sqrt{P_h T} c_{h,0} + \sum_{\substack{k=1 \\ k \neq h}}^{K_m} \sqrt{\frac{P_k}{T}} (c_{k,-1} R_{h,k}(\tau_{h,k}) + c_{k,0} \hat{R}_{h,k}(\tau_{h,k})) \cos \phi_{h,k} \\
 &+ \sum_{g=1}^{K_n} \sqrt{\frac{P_g}{T}} (c_{g,-1} R_{h,g}(\tau_{h,g}) + c_{g,0} \hat{R}_{h,g}(\tau_{h,g})) \cos \phi_{h,g} \\
 &+ \int_0^T n(t) \sqrt{\frac{2}{T_b}} a_h(t) \cos(\omega_c t) dt
 \end{aligned} \tag{6.2}$$

For this case, $\tau_{h,g} \leq T \left(\frac{PG_{low}}{PG_{high}} \right)$ and $\tau_{h,k} \leq T \left(\frac{PG_{low}}{PG_{high}} \right)$ too. PG_{low} is the lower processing gain while PG_{high} is the higher processing gain. Figure 6.1(b) illustrates the interaction between interfering bits for the case where the user of interest has the lower processing gain.

$R_{ab}(\tau) = \int_0^\tau a_a(t-\tau) a_b(t) dt$ and $\hat{R}_{ab}(\tau) = \int_\tau^T a_a(t-\tau) a_b(t) dt$. Notation T represents the message bit duration of the user of interest.

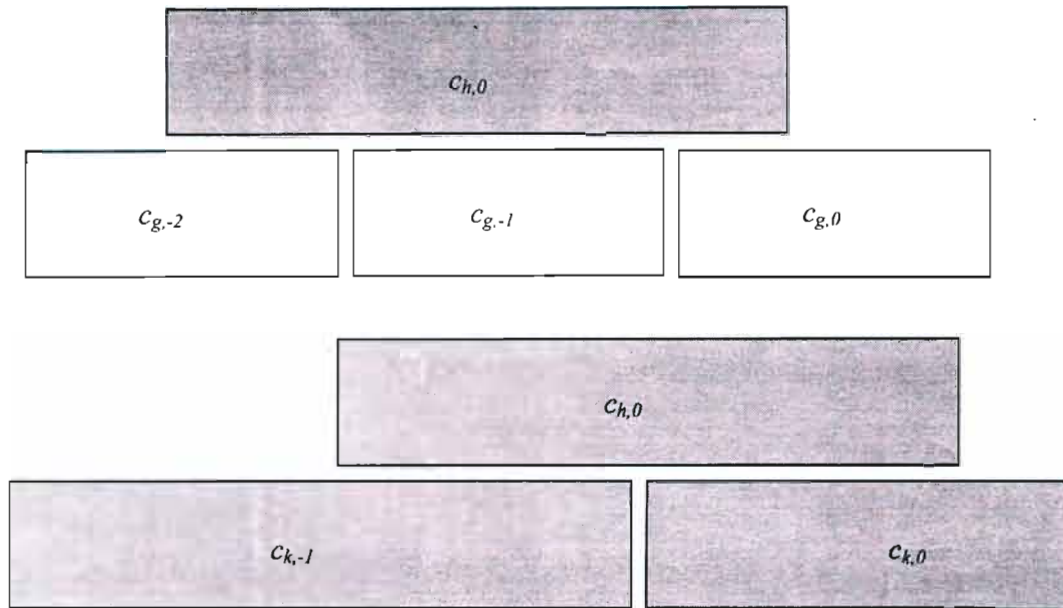


Figure 6.1(a): Illustration of the bit interaction of interfering bits in a dual multirate CDMA system when the user of interest has the higher processing gain.

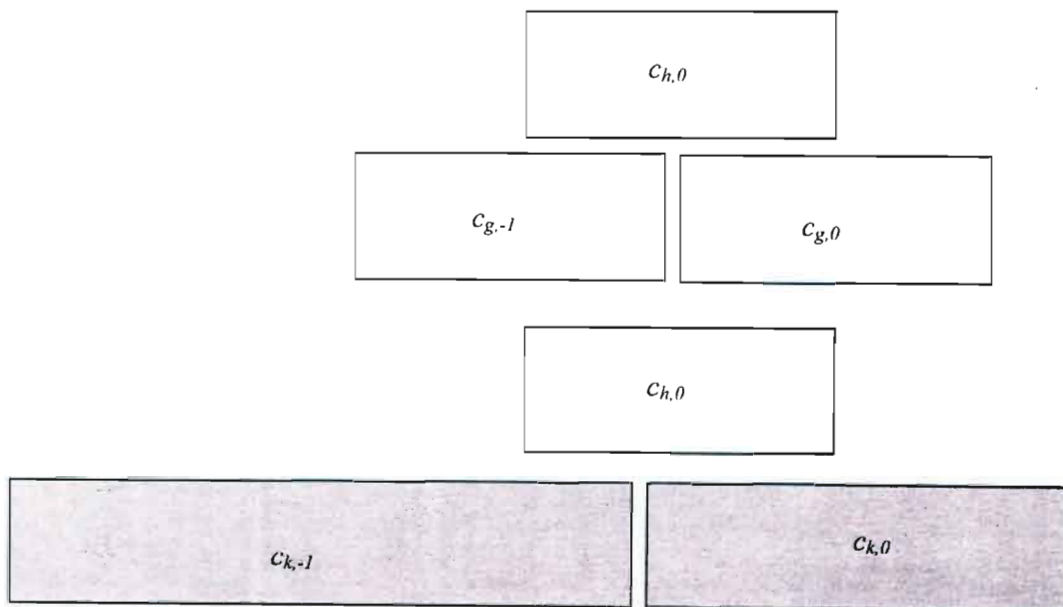


Figure 6.1(b): Illustration of the bit interaction of interfering bits in a dual multirate CDMA system when the user of interest has the lower processing gain.

6.3 Simulation Model of Multirate CDMA

We consider a turbo coded BPSK modulated asynchronous CDMA system with random spreading codes. The lower processing gain is 16 and the higher processing gain is 32. The data rate of the system that has the higher processing gain is 64Kbps and the data rate for the system that has the lower processing gain is 128Kbps. Simulations were performed for multirate CDMA systems with various values of framelength and for various number of detection iterations for the (1,5/7) component RSC code corresponding to four coding states. The objective of doing these is to be able to observe performances of the multiuser detector over a wide range of situations.

6.4 Discussion of Results.

In the results that are presented in this Section some expressions are used in describing the system that is under investigation. "Multirate CDMA (High)" refers to the multirate CDMA system having the higher processing gain while "Multirate CDMA (Low)" refers to the multirate CDMA system having the lower processing gain. As could be observed in Figures 6.2, 6.3 and 6.4 the error rate performance of systems having the lower processing gain are poorer than those of systems having the higher processing gain for all situations that were studied.

In Figure 6.2 in particular the same trend is observed where the performance of the "Multirate CDMA (Low)" is poorer than that of "Multirate CDMA (High)". Curiously, it could be observed that the performance of "Multirate CDMA (High)" after one detection iteration is even better than the performance of "Multirate CDMA (low)" after three detection iterations. We attribute this to the increased "virtual near-far phenomenon" that is experienced by "Multirate CDMA (Low)".

In Figure 6.3, the performances of the multiuser detector in multirate CDMA system with variations in the coding framelength is investigated. The better performance of

“Multirate CDMA (High)” when compared with “Multirate CDMA (Low)” is still noticed even when the framelength was changed from 500 to 1024.

Figure 6.4 shows that the performances of the multiuser detector in either the “Multirate CDMA (High)” or the “Multirate CDMA (Low)” system is still better than the situation where there is no multiuser detection. In Figure 6.4 there are 10 active users and the processing gain for “Multirate CDMA (High)” is 32 while the processing gain for “Multirate CDMA (Low)” is 16. The frame length is 200 and the octal representation of the constituent RSC code is $(7,5)_{\text{octal}}$. The number of iterations is three. Capacity gain can be made when the multiuser detector is used in a multirate CDMA system to provide differentiated performances. The penalty paid for higher data rate, however, is a reduction in error rate performance.

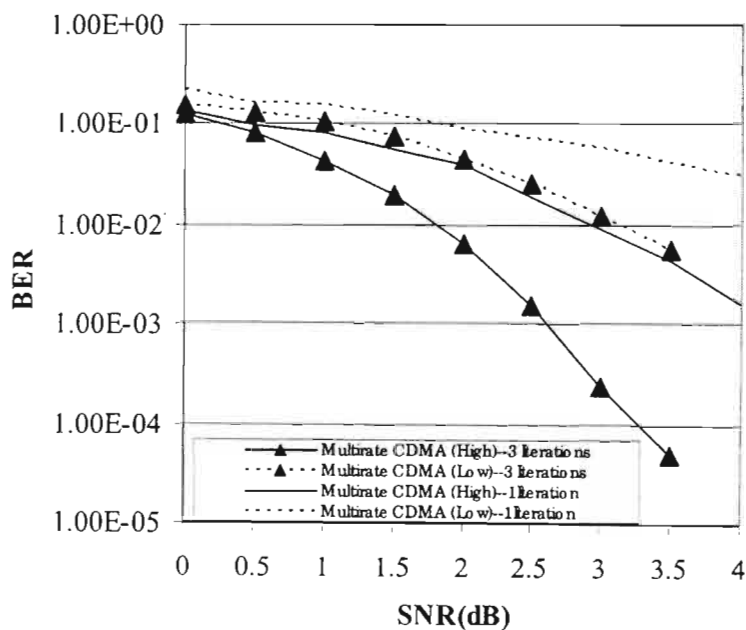


Figure 6.2: BER performance of the multiuser detector in the multirate CDMA system with variations in the number of detection iterations.

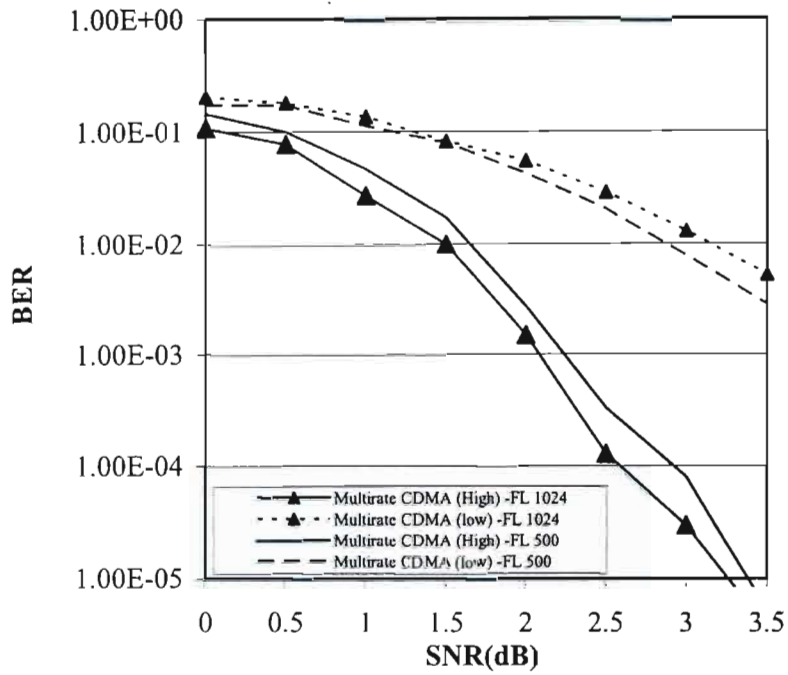


Figure 6.3: BER performance of the multiuser detector in the multirate CDMA system with variations in the size of the framelength.

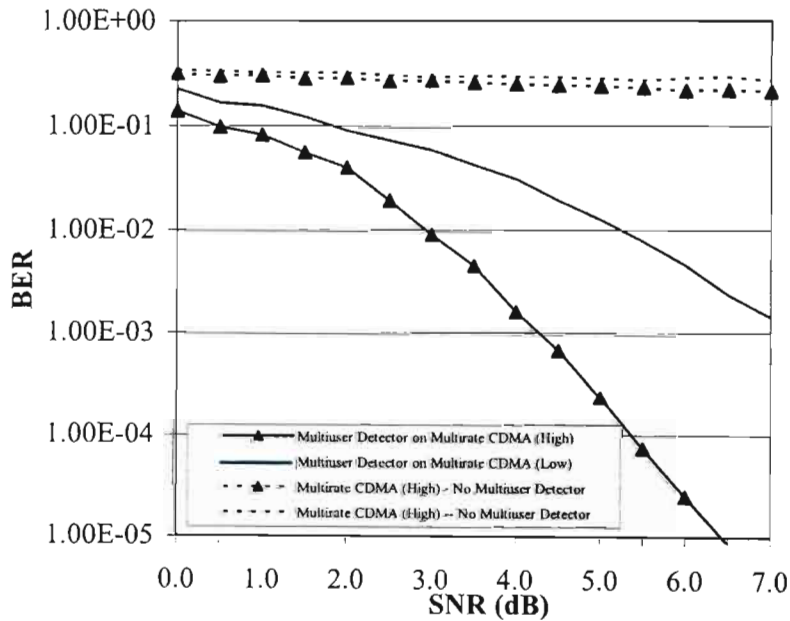


Figure 6.4: Comparison of the BER performance of the multiuser detector and the Turbo decoder in the multirate CDMA system. Number of iteration is one. Frame Length = 200.

6.5 Conclusion.

In the Chapter we investigated the performance of the iterative multiuser detector that was developed in Chapter 5 in the multirate CDMA system. The proposed multiuser detector was demonstrated to be able to support multiple users with different data rates. It has been shown that the performance of the receiver still remained superior to that of the ordinary Turbo decoder in the multirate CDMA system. It was also noted that increasing the number of detection iteration is a way of reducing the performance degradation in systems that operate on the lower processing gain.

Chapter 7

Conclusion.

This dissertation discusses interference cancellation in both the channel coded (with emphasis on the turbo code) and the uncoded DS-CDMA systems. We presented models for the error rate analysis of PIC receivers, presented a methodology for the analysis of iterative interference cancellation receivers for turbo coded DS-CDMA systems and developed an iterative multiuser detector that has performances that are close to the single user's bound after a few iterations.

In Chapter 2, we presented analytical expressions for the error rate performance evaluation of the total and the weighted PIC receivers in the Nakagami multipath fading channel. We derived new expressions for the variance of the residual MAI of the PIC receivers. We showed that the derived expressions are more accurate than the expressions that have already been reported in the literature. An integral part of the results provided is the expression for evaluating the error rate performance of the MRC-based RAKE receivers for DS-CDMA system in the Nakagami multipath fading channel. Expressions were also obtained for the optimal cancellation weights for the weighted PIC receivers.

There is a need to adaptively estimate the optimal cancellation weights for the weighted PIC receiver as the channel condition changes. We gave a motivation for the use of the LMS algorithm for the weights estimation in chapter 3. We then analysed the error rate performance of the LMS-based adaptive PIC receiver. Results show that the adaptive PIC receiver has better performances than the non-adaptive PIC receiver. Also, results of the error rate analysis of the receivers and results that are obtained from computer simulations of the receivers show a high level of agreement.

The rest of the dissertation discussed the iterative multiuser detector for turbo-coded DS-CDMA systems. We used the density evolution method to perform the convergence analysis of the iterative interference cancellation receiver in Chapter 4. Results show a high degree of agreement between predicted convergence points and convergence points that were observed during computer simulation of the system. The proposed methodology is useful in predicting the point of convergence of iterative interference cancellation receivers thereby removing the need for lengthy computer simulations in the determination of the point of convergence.

Finally, a novel iterative multiuser detector was developed for the turbo-coded DS-CDMA system in Chapter 5. The developed receiver avoided a direct subtraction of the estimated multiple access interference from the received signal of the user of interest. Rather, the estimated multiple access interference was used as added information in the detection process. Results show that the proposed detection paradigm performs better than the receiver that is based on direct subtraction of the estimated multiple access interference. The proposed detector was found to have performances that are close to those of the single user performance. The detector is also resilient against the near-far phenomenon.

An application of the detector in the multirate CDMA system in Chapter 6 shows that the detector can handle multiple users with different processing gains. Communication systems in emerging technologies are expected to deliver multiple services of heterogeneous nature in an integrated manner. Multirate CDMA is an enabling technique in achieving this objective.

This dissertation examined multiuser detection in the uplink channel of a CDMA system. However, it was not our objective to examine the effects of user mobility and cell design on multiuser detector in cellular CDMA systems. It will be interesting, for future work, to investigate the effects of the adoption of the iterative multiuser receiver that was developed in Chapter 5 of this dissertation on capacity, coverage and system sensitivity in a cellular CDMA system with consideration for outer-cell interference and user

mobility. The feasibility of deploying the developed receiver in practical CDMA systems requires system-level evaluation. The feasibility of combining the receiver with channel estimation algorithms, power control schemes etc will have to be investigated.

Capacity of wireless systems can be improved with the use of multiple transmit and receive antenna (Multiple Input Multiple Output (MIMO) systems). For future work, novel techniques of combining space-time detection and iterative multiuser detection can be explored.

Issues about the hardware implementation of the iterative multiuser detector have to be addressed. Performances of fixed-point implementation, sequence variance estimation and correlation computation are needed to be addressed and should be studied in a future work.

References.

- [Ale97] P. D. Alexander, L. K. Rasmussen and C. B. Schlegel, "A Linear Receiver for Coded Multiuser CDMA," *IEEE Transactions on Communications*, vol. 45, no.5, pp. 605-610, May 1997.
- [Ale98] P.A Alexander , A. J Grant and M.C Reed "Iterative Detection in Code-Division Multiple-Access With Error Control Coding" *European Transaction on Telecommunications special issues on CDMA Techniques for Wireless Communications Systems*. Vol 9, pp 419-425,Sept./ Oct. 1998.
- [Ale99] P. D. Alexander, M. C. Reed, J. A. Asenstorfer and C. B. Schlegel, "Iterative Multiuser Interference Reduction: Turbo CDMA," *IEEE Transactions on Communications*, vol. 47, no. 7, pp. 1008-1014, July 1999.
- [Alh85] E. K. Al-Hussaini and A.Z. Al-Bassiouni, " Performance of MRC Diversity Systems for the Detection of Signals with Nakagami Fading," *IEEE Transactions on Communications*, vol. COM-33, no.12, pp. 1315-1319. December 1985.
- [And02] J. G. Andrews, " Successive Interference Cancellation for Uplink CDMA". PhD dissertation, Stanford University, June 2002.
- [Bej00] E O Bejide and F Takawira, "Performance of Parallel Interference Cancellation Receivers for DS-CDMA in Frequency-Selective Fading Channels. In: *SATCAM 2000 Proceedings of the Communications and Signal Processing Chapter of the SA Section of the IEEE*, pp. 48-53, Somerset West. (CD-Rom. ISBN: 0-620-26497-7)
- [Bej01] E O Bejide and F Takawira, "Error Probabilities of Parallel Interference Cancellers for CDMA in Nakagami Multipath Fading Channel with an Imperfect Channel Estimation" *South Africa Telecommunication and Networking Conference (SATNAC)*, 2-5 September 2001, pp. 147-151 (CD-Rom. ISBN: 0-620-27769-6).
- [Bej03] E. Oluremi Bejide and F. Takawira, "An Iterative Multiuser Detector for DS-CDMA.". *South Africa Telecommunication and Networking Conference (SATNAC)*, 7-10 September 2003. Conference CD-ROM.
- [Ben95} S.Benedetto and G.Montorsi," Design of Parallel Concatenated Convolutional Codes" *IEEE Transactions on Communications*,pp.1-26,October 4, 1995

- [Ben97] S. Benedetto, D. Divsalar, G. Montorsi and F. Pollara, "A Soft-Input Soft-Output APP Module for Iterative Decoding of Concatenated Codes," IEEE Communications Letters, vol. 1, no. 1, pp.22-24, January 1997.
- [Ber93] C. Berrou, A. Glavieux and P. Thitimajshima, "Near Shannon limit error-correcting coding and decoding: Turbo codes," Proceedings of IEEE International Conference on Communications, pp 1064-1070, Geneva, Switzerland, May 1993.
- [Ber96a] J.C.M. Bermudez and N.J. Bershad, "A Nonlinear Analytical Model for the Quantized LMS Algorithm-The Arbitrary Step Size Case." IEEE Transactions on Signal Processing, Vol. 44, No. 5. Pp. 1175-1183. May 1996
- [Ber96b] J.C.M. Bermudez and N.J. Bershad, "A Nonlinear Analytical Model for the Quantized LMS Algorithm-The Power-of-two Step Size Case." IEEE Transactions on Signal Processing, Vol. 44, No. 11. Pp. 2895-2900. November 1996
- [Bri01] S. ten Brink, "Convergence Behavior of Iteratively Decoded Parallel Concatenated Codes," IEEE Transactions on Communications, vol. 49, no. 10, pp. 1727-1737, October 2001.
- [Bue99] R. M. Buehrer and S. P. Nicoloso, "Comments on "Partial Parallel Interference Cancellation for CDMA"," IEEE Transactions on Communications, vol. 47, no. 5, pp. 658-661, May 1999.
- [Chi92] S.Chia, "The Universal Mobile Telecommunication System," IEEE Communication Magazine, pp. 54-62, December 1992.
- [Cho02] J. Choi and S. R. Kim "Adaptive MMSE Receiver for Multirate CDMA Systems" IEEE Transactions On Signal Processing, Vol.50, No.12. Pp. 3098-3106. December 2002.
- [Cor99] N.S Correal, R.M Buehrerand B.D. Woerner "A DSP-Based DS-CDMA Multiuser Receiver Employing Partial Parallel Interference Cancellation" IEEE Journal On Selected Areas In Communications, Vol. 17, 4. Pp. 613-630. April 1999.
- [Din97] P.S.R. Diniz, "Adaptive Filtering. Algorithms and Practical Implementation." Kluwer Academic Publishers.1997.
- [Div01a] D.Divsalar,S.Dolinar and F.Pollara," Iterative Turbo Decoder Analysis Based on Density Evolution," TMO Progress Report 42-144,pp.1-33,February15,2001
- [Div01b] D. Divsalar, S. Dolinar and F. Pollara, "Iterative Turbo Decoder Analysis Based on

- Density Evolution,” IEEE Journal on Selected Areas in Communications, vol. 19, no. 5, pp. 891-907, May 2001.
- [Div95] D. Divsalar, M. K. Simon, “CDMA with Interference Cancellation for Multiprobe Missions,” TDA Progress Report 42-120, pp. 40-53, February 15, 1995.
- [Div98] D. Divsalar, M. K. Simon and D. Raphaeli, “Improved Parallel Interference Cancellation for CDMA,” IEEE Transactions on Communications, vol. 46, no.2, pp. 258-268, February 1998.
- [Dol95] S.Dolinar and D.Divsalar,” Weight Distributions for turbo Codes Using Random and nonrandom Permutations”TDA Progress Report 42-122,pp.56-65,August 15,1995
- [Dum98] T.M. Duman and M.Salehi,” New Performance Bounds for Turbo Codes” IEEE Transactions on Communications, Vol. 46, no. 6,pp.717-723, June 1998
- [Eft97] G. P. Eftymoglou, V. A. Aalo and H. Helmken “Performance Analysis of Coherent DS-CDMA Systems in a Nakagami Fading Channel With Arbitrary Parameters” IEEE Transactions On Vehicle Technology, Vol.46,No.2. Pp. 289 – 297. May 1997.
- [Eng95] T. Eng and L. B. Milstein, “Coherent DS-CDMA Performance in Nakagami Multipath Fading,” IEEE Transactions on Communications, vol. 43, no.2/3/4, pp. 1134-1143, February/March/April 1995.
- [Eng97] T. Eng and L. B. Milstein, “Partially Coherent DS-SS Performance in Frequency Selective Multipath Fading,” IEEE Transactions on Communications, vol. 45, no.1, pp. 110-118, January 1997.
- [Faw95] U. Fawer and B. Aazhang, “A Multiuser Receiver for Code Division Multiple Access Communications over Multipath Channels,” IEEE Transactions on Communications, vol. 43, no. 2/3/4, pp. 1556-1565, February/March/April 1995.
- [Foe00] J. R. Foerster and L. B. Milstein “Coding for a Coherent DS-CDMA System Employing an MMSE Receiver in a Rayleigh Fading Channel” IEEE Transactions On Communications ,Vol.48, No.6. Pp. 1012-1021. June 2000.
- [Fre99] P.Frenger, “ Turbo decoding on Rayleigh Fading Channels With Noisy Channels Estimates” Vehicular technology Conference Record,vol.1/3,pp.884-888,Houston Texas,USA,May 16-19,1999

- [Gam00] H. E. Gamal, E. Geraniotis, "Iterative Multiuser Detection for Coded CDMA Signals in AWGN and Fading Channels," *IEEE Journal on Selected Areas in Communications*, vol. 18, no. 1, pp. 30-41, January 2000.
- [Gam01] H. E. Gamal and A. R. Hammons, "Analyzing the Turbo Decoder Using the Gaussian Approximation," *IEEE Transactions on Information Theory*, vol. 47, no. 2, pp. 671-686, February 2001.
- [Gar97] V.K. Garg, K.F. Smolik and J.E. Wilkes, "Applications of CDMA in Wireless/Personal Communications" .Prentice Hall Inc, New Jersey, 1997.
- [Ger82] E. A. Geraniotis and M. B. Pursley, "Error Probability for Direct-Sequence Spread-Spectrum Multiple-Access Communications—Part II: Approximations," *IEEE Transactions on Communications*, vol. COM-30, n0. 5, pp. 985-995, May 1982.
- [Gia96a] T. R. Giallorenzi and S. G. Wilson, "Multiuser ML sequence estimator for convolutionally coded asynchronous DS-CDMA systems," *IEEE Transactions on Communications*, vol. 44, no.8, pp. 997--1008, August 1996.
- [Gia96b] T. R. Giallorenzi and S. G. Wilson, "Suboptimum multiuser receiver for convolutionally coded asynchronous DS-CDMA systems," *IEEE Transactions on Communications*, vol. 44, no.9, pp. 1183-1196, Sept. 1996.
- [Goh01] R.H. Gohary,H.M.Mourad and E.K. AlHussaini "An Adaptive Parallel Interference Cancellation System Employing Soft Decisions For Asynchronous DS/CDMA Multipath Fading Channels" *IEEE Global Telecommunications Conference*,Vol.5,pp.3145-3147, San Antonio, Texas, USA, November 25-29,2001
- [Gra95] S. D. Gray, M. Kocic and D. Brady, "Multiuser Detection in Mismatched Multiple-Access Channels," *IEEE Transactions on Communications*, vol. 43, no. 12, pp. 3080-3089, December 1995.
- [Guo98] D.Guo, L.K Rasmussen,S.Sun, T.J Lim and C.Cheah, "MMSE-Based Linear Parallel Interference Cancellation in CDMA" *IEEE Fifth International Symposium on Spread Spectrum Techniques & Applications*,vol.3/3,pp.917-921,Sun City, South Africa, September 2-4,1998
- [Guo99] D. Guo, L. K. Rasmussen and T. J. Lim, "Linear Parallel Interference Cancellation in Long-Code CDMA Multiuser Detection," *IEEE Journal on Selected Areas in Communications*, vol. 17, no. 12, pp. 2074-2081, December 1999.

- [Ha99] N.H.Ha and E.Shwedyk," Performance of Turbo Codes on Frequency-Selective Rayleigh Fading Channels with Joint Data and Channel Estimation" IEEE International Conference on Communications, vol.1/3,pp.98-102,Vancouver,BC,Canada, 6-10June 1999
- [Hag96] J.Hagenauer, E. Offer and L.Papke " Iterative Decoding of Binary Block and Convolutional Codes" IEE Transactions on Information Theory, Vol.42, no.2, pp.429-445, March 1996
- [Hag97] J.Hagenauer," The Turbo Principle: Tutorials Introduction and State of the Art" International Symposium on Turbo Codes, pp.1-11, Breast-France,3-5 September, 1997
- [Hay01] S. Haykins, "Adaptive Signal Processing". Prentice Hall; 4th edition 2001.
- [Hol92] J. M. Holtzman, "On Using Perturbation Analysis to do Sensitivity Analysis: Derivatives versus Differences," IEEE Transactions on Automatic Control, vol. 37, no. 2, pp. 243-247, February 1992.
- [Hol92] J. M. Holtzman, "A Simple, Accurate Method to Calculate Spread-Spectrum Multiple-Access Error Probabilities," IEEE Transactions on Communications, vol. 40, no. 3, pp. 461-464, March 1992.
- [Hon00] M.Honig and M.K. Tsatsanis," Adaptive Techniques for Multiuser CDMA Receivers" IEEE Signal Processing Magazine, pp.49-61, May, 2000
- [Hon95] M. Honig, U. Madhow and S. Verdu "Blind Adaptive Multiuser Detection" IEEE Transactions On Information Theory, Vol. 41, No.4. Pp. 944 – 960. July 1995.
- [Hon99] D. Hong, Y. You and C. Kang, "Asymptotic Performance Limit of a DS/CDMA RAKE receiver with a multistage interference cancellation scheme." IEEE Wireless Communications and Networking Conference. Pp. 95-98, 1999.
- [Hot96] A.Hottinen, H. Holma and A.Toskala " Multiuser Detection for Multirate CDMA Communications". IEEE International Conference on Communications, 1996. ICC 96, Conference Record, Volume: 3 , 23-27 Jun 1996 Page(s): 1819 -1823 vol.3
- [Hsu01] J. M. Hsu and C. Wang, "A Low-Complexity Iterative Multiuser Receiver for Turbo-Coded DS-CDMA Systems," IEEE Journal on Selected Areas in Communications, vol. 19, no. 9, pp. 1775-1783, September 2001.
- [Hui98] A.L.C. Hui and K.B. Letaief "Successive Interference Cancellation for Multiuser

- Asynchronous DS/CDMA Detectors in Multipath Fading Links" IEEE Transactions On Communications, Vol.46, No. 3. Pp. 384 – 391. March 1998.
- [Hwa98] K. C. Hwang and K. B. Lee, "Performance Analysis of Low Processing Gain DS/CDMA Systems with Random Spreading Sequences," IEEE Communications Letters, vol. 2, no.12, pp. 315-317, December 1998.
- [Joh96] A.Johnansson , T. Ottosson and A.Svensson "On Multirate DS/CDMA with interference cancellation for wireless multimedia applications" IEEE International Conference on Personal Wireless Communications, 19-21 Feb 1996 Pp: 102 -107
- [Jul02] J.Cheng and N.C.Beaulieu "Accurate DS-CDMA Bit-Error Probability Calculation in Rayleigh Fading" IEEE Transactions On Wireless Communications Vol.1, No.1. Pp. 3 – 15. January 2000.
- [Jun98a] M.J.Junti," Performance of parallel Interference cancellation for CDMA in Estimated Fading Channels with Delay Mismatch" IEEE Fifth International Symposium on Spread Spectrum Techniques & Applications,vol.3/3,pp.936-940,Sun City, South Africa, September 2-4, 1998
- [Jun98b] M.J.Junti " Multiuser Detector Performance Comparisons in multirate CDMA Systems" IEEE VTS Vehicular Technology Conference, Vol. 1, pp. 31 – 35, 1998.
- [Jun99a] M.Junti and O.Kaurahalmel," Performance of Parallel Interference Cancellation for CDMA With Channel Coding" 49th IEEE Vehicular Technology Conference,pp1440-1444,Houston,Texas,USA,May16-20,1999
- [Jun99b] M.Junti,M.Latva-aho and K.kansanen, "Performance of Parallel Interference Cancellation for CDMA with Delay Estimation" IEEE 49th Vehicular Technology Conference,pp.1633,Houston,Texas,USA, May 16-20,1999
- [Ker99] R. W. Kerr, P. S. Guinand and M. Moher,"An Iterative Multi-user Decoder with Soft-interference Cancellation," IEEE International Conference on Communications (ICC), pp.46-50, Vancouver, BC, Canada, 6-10 June, 1999.
- [Kim99] S.R. Kim, Y.G.Jeong, J.G. Lee and I. Choi, "Incorporation of Adaptive Interference Cancellation into Parallel Interference Cancellation" 49th IEEE Vehicular Technology Conference, pp.1242-1245, Houston, Texas, USA, May 16-20
- [Kou98] D. Koulakiotis and A. H. Aghvami, "Evaluation of a DS/CDMA Multiuser

- Receiver Employing a Hybrid Form of Interference Cancellation in Rayleigh-Fading Channels,” IEEE Communications Letters, vol.2, no. 3, pp. 61-63, March 1998
- [Lat99] M.Latva-aho,M.Junti and K.Kansanen,” Residual Interference Suppression in Parallel Interference Cancellation Receivers” IEEE International Conference on Communications,vol.1,pp.927-931,Vancouver ,BC,Canada,6-10 June 1999
- [Lee00] L.Lee, A.R. Hammons,F.Sun and M.Eros,” Application and Standardization of Turbo Codes in Third-Generations High-Speed Wireless Data services” IEEE Transactions on Vehicular Technology,Vol.49,no.6,pp.2198-2207,November 2000
- [Leh87] J. S. Lehnert and M. B. Pursley, “Error Probabilities for Binary Direct-Sequence Spread Spectrum Communications with Random Signature Sequences,” IEEE Transactions on Communications, vol. COM-35, no.1, pp. 87-98, January 1987.
- [Leh89] J. S. Lehnert, “An Efficient Technique for Evaluating Direct-Sequence Spread-Spectrum Multiple-Access Communications,” IEEE Transactions on Communications, vol. 37, no. 8, pp. 851-858, August 1989.
- [Len87] J. S. Lehnert and M. B. Pursley, “Error Probabilities for Binary Direct-Sequence Spread-Spectrum Communications with Random Signature Sequences,” IEEE Transactions on Communications, vol. COM-35, no. 1, pp. 87-98, January 1987.
- [Let97] K. B. Letaief, “Efficient Evaluation of the Error Probabilities of Spread-Spectrum Multiple-Access Communications,” IEEE Transactions on Communications, vol. 45, no. 2, pp.239-246, February 1997.
- [Lom99] P. Lambardo, G. Fedele and M. M. Rao, “MRC Performance for Binary Signals in Nakagami Fading with General Branch Correlation,” IEEE Transactions on Communications, vol. 47, no.1, pp.44-52, January 1999.
- [Mag94] D.T Magill, F.D.Nataliand G.P.Edwards. “Spread-Spectrum Technology for Commercial Applications” Proceedings of the IEEE Vol.82 No.4. Pp. 572 – 584. April 1994.
- [Mah99] M. Alam, T. Ojanpera and R. Prasad “Near-Far Resistance of Parallel Interference Cancellation Detector in a Multirate DS-CDMA Systems “IEEE VTS 50th Vehicular Technology Conference (VTC 1999). vol.3,1830 – 1834, 1999.
- [Mar01a] S. Marinkovic, B. S. Vucetic and J. Evans “Improved Iterative Parallel Interference

- Cancellation For Coded CDMA Systems” International Symposium on Information Theory (ISIT) June 24-29 2001, Pp 34.
- [Mar01b] S.Marinkovic, B.Vucetic and A.Ushirokawa “Space-Time Iterative and Multistage Receiver Structures for CDMA Mobile Communication Systems” IEEE Journal on Selected Areas In Communications Vol.19.No.8. Pp. 1594 – 1604. August 2001.
- [Mce98] R.J.McEliece,D.J.C.Mackay and J. Cheng “Turbo Decoding as an Instance of Pearl’s “Belief Propagation” Algorithm” IEEE Journal On Selected Areas In Communications , vol. 16. No 2. Pp. 140 – 152. February 1998.
- [Mee99] A.F. Van Meeteren, T. Ojanpera, H. Nikookar and R. Prasad “Groupwise Weighted Parallel Interference Cancellation for Asynchronous Multirate DS-CDMA” IEEE VTS 50th Vehicular Technology Conference, vol.3, pp. 1820 - 1824 1999.
- [Moh98a] M. Moher, “An Iterative Multiuser Decoder for Near-Capacity Communications,” IEEE Transactions on Communications, vol. 46, no. 7, pp. 870-880, July 1998.
- [Moh98b] M. Moher and T. A. Gulliver, “Cross-Entropy and Iterative Decoding,” IEEE Transactions on Information Theory, vol. 44, no. 7, pp. 3097-3104, November 1998.
- [Moh99] M. Mohammad, k. Howlader and B.D. Woerner, “Iterative Interference Cancellation and Decoding for DS-CDMA”. Proc. IEEE VTC. Pp. 1815-1819. 1999.
- [Mor89] R. K. Morrow and J. S. Lehnert, “Bit-to-Bit Error Dependence in Slotted DS/SSMA Packet Systems with Random Signature Sequences,” IEEE Transactions on Communications, vol. 37, no. 10, pp. 1052-1061, October 1989.
- [Mor92] J. M. Morris, “Burst Error Statistics of Simulated Viterbi Decoded BPSK on Fading and Scintillating Channels,” IEEE Transactions on Communications, vol. 40, no. 1, pp. 34-41, January 1992.
- [Mos96] S.Moshavi,” Multi-User Detection for DS-CDMA Communications” IEEE Communication magazine,pp.124-135,October 1996
- [Nam99] R. Nambiar and A. Goldsmith,” Iterative Weighted Interference Cancellation For CDMA System with Rake Reception” 49th IEEE Vehicular Technology

Conference, pp.1232-1236, Houston, Texas, USA, May 16-20

- [Oja96] T. Ojanpera, "Design of a 3rd Generation Multirate CDMA System With Multiuser Detection, MUD-CDMA". IEEE 4th International Symposium on Spread Spectrum Techniques and Applications Proceedings, 1996. Volume: 1 , 22-25 Sep 1996
Page(s): 334 -338 vol.1
- [Pap84] A. Papoulis, "Probability, Random Variables and Stochastic Process." McGraw Hill Inc. 1984.
- [Pra98] R. Prasad, T. Ojanpera, "An Overview of CDMA Evolution Towards Wideband CDMA," IEEE Communications Surveys, vol.1, no. 1, pp. 2-29, Fourth Quarter 1998.
- [Pro01] J.G Proakis "Digital Communications ". McGraw-Hill Higher Education. 4th Edition 2000.
- [Pur77] M. B. Pursley, "Performance Evaluation for Phase-Coded Spread-Spectrum Multiple-Access Communication—Part 1: System Analysis," IEEE Transactions on Communications, vol. COM-25, no. 8, pp. 795-799, August 1977.
- [Pur82] M. B. Pursley, D. V. Sarwate and W. E. Stark, "Error Probability for Direct-Sequence Spread-Spectrum Multiple-Access Communications—Part 1: Upper and Lower Bounds," IEEE Transactions on Communications, vol. COM-30, no.5, pp. 975-984, May 1982.
- [Puz99] Z. Pu, W. Haifeng, X. You and S.Cheng. "Improved Partial Parallel Interference Cancellation For Direct Sequence CDMA Communications" IEEE, The 10th International symposium on personal, indoor and Mobile Radio Communications. September 12-15 1999. Pp1320-1324.
- [Qin01] Z. Qin, K. C. The and E. Gunawan, "Iterative Multiuser Detection for Asynchronous CDMA with Concatenated Convolutional Coding," IEEE Journal on Selected Areas in Communications, vol. 19, no. 9, pp. 1784-1792, September 2001.
- [Ras98] L.K.Rasmussen, S.Sun, T.J. Lim and H. Sugimoto," Impact of Estimated Errors on Multiuser Detection in CDMA" 48th IEEE Vehicular Technology Conference, pp.1844-1848, Westin Hotel, Ottawa, Canada, 18-21 May 1998
- [Ray82] R.L.Pickholtz, D.L.Schilling and L.B. Milstein, "Theory of Spread-Spectrum Communications--- A Tutorial " IEEE Transactions on Communications,

- Vol.Com-30, no5, pp. 855-884, May 1982.
- [Ree98] M. C. Reed, C. B. Schlegel, P. D. Alexander, J. A. Asenstorfer, "Iterative Multiuser Detection for CDMA with FEC: Near-Single-User Performance," *IEEE Transactions on Communications*, vol. 46, no.12, pp. 1693-1699, December 1998.
- [Ric01] T. Richardson and R. Urbanke "The Capacity of Low-Density Parity Check Codes Under Message-Passing Decoding" *IEEE Transaction Information Theory*, Vol.47 pp 599-618 Feb 2001.
- [Row98] D. N. Rowitch, "Convolutional and Turbo Coded Multicarrier Direct Sequence CDMA, and Applications of Turbo Codes to Hybrid ARQ Communication Systems," PhD dissertation, Univ. of California at San Diego, La Jolla, CA, June 1998.
- [Rya] W.E. Ryan "A Turbo Code Tutorial" Unpublished work.
- [San96] Y. Sanada and Q. Wang, "A Co-Channel Interference Cancellation Technique Using Orthogonal Convolutional Codes," *IEEE Transactions on Communications*, vol. 44, no.5, pp. 549-556, May 1996.
- [Sch77] R.A. Scholtz, "The Spread Spectrum Concept" *IEEE Transactions on Communications*, Vol. Com-25, no.8, pp.748-755, August 1977.
- [Sch99] P. Schramm and R. R. Muller, "Spectral Efficiency of CDMA Systems with Linear MMSE Interference Suppression," *IEEE Transactions on Communications*, vol. 47, no.5, pp. 722-731, May 1999.
- [Ser80] Sarwate, D.V., and M.B. Pursley, "Crosscorrelation Properties of Pseudorandom and Related Sequences," *Proc. IEEE*, Vol. 68, No. 5, May, 1980, pp. 583-619.
- [Shi01] Z. Shi and C. Schlegel, "Joint Iterative Decoding of Serially Concatenated Error Control Coded CDMA," *IEEE Journal on Selected Areas in Communications*, vol. 19, no. 8, pp. 1646-1653, August 2001.
- [Sim90] S.J. Simmons, "Breadth-First Trellis Decoding with Adaptive Effort." *IEEE Transactions on Communications*, Vol. 38, No. 1, Pp. 3-12. January 1990.
- [Sim98a] M. K. Simon and M. Alouini, "A Unified Approach to the Performance Analysis of Digital Communication over Generalized Fading Channels," *Proceedings of the IEEE*, vol. 86, no. 9, pp. 1860-1877, September 1998.
- [Sim98b] M. K. Simon and D. Divsalar, "Some New Twists to Problems Involving the

- Gaussian Probability Integral," *IEEE Transactions on Communications*, vol. 46, no. 2, pp. 200-210, February 1998.
- [Sk197a] B. Sklar, "Rayleigh Fading Channels in Mobile Digital Communication Systems Part I: Mitigation" *IEEE Communications Magazine*, pp.90-100, July 1997
- [Sk197b] B. Sklar, "Rayleigh Fading Channels in Mobile Digital Communication Systems Part II: Mitigation" *IEEE Communications Magazine*, pp102-109, July 1997
- [Tan01] K. Tang, L. B. Milstein and P. H. Siegel, "Combined MMSE Interference Suppression and Turbo Coding for a Coherent DS-CDMA System," *IEEE Journal on Selected Areas in Communications*, vol. 19, no. 9, pp. 1793-1803, September 2001.
- [Tur72] G. L. Turin et al., "A statistical model for urban radio propagation," *IEEE Trans. Veh. Technol.*, vol. 21, pp. 1--9, Feb. 1972.
- [Var90] M. K. Varanasi and B. Aazhang, "Multistage Detection in Asynchronous Code-Division Multiple-Access Communications," *IEEE Transactions on Communications*, vol. 38, no.4, pp. 509-519, April 1990.
- [Var91] M. K. Varanasi and B. Aazhang, "Near-Optimum Detection in Synchronous Code-Division Multiple-Access Systems," *IEEE Transactions on Communications*, vol. 39, no.5, pp. 725-736, May 1991.
- [Ver86a] S. Verdu, "Optimum Multiuser Asymptotic Efficiency," *IEEE Transactions on Communications*, vol. COM-34, no.9, pp. 890-897, September 1986.
- [Ver86b] S. Verdu "Optimum Multiuser Asymptotic Efficiency. " *IEEE transactions on communications*, Vol.Com-34 No. 9 . Pp. 890 – 897. September 1986.
- [Ver89] S. Verdu "Recent Progress In Multiuser Detection" *Advances in Communication and Signal Processing*. Springer Berlin-Heidelberg 1989.
- [Vit79] A.J. Viterbi," Spread Spectrum Communications—Myths and Realities" *IEEE Communication Magazine*, vol.17, pp.11-18, May 1979
- [Vit90] A. J. Viterbi, "Very Low Rate Convolutional Codes for Maximum Theoretical Performance of Spread-Spectrum Multiple-Access Channels," *IEEE Transactions on Selected Areas in Communications*, vol. 8, no. 4, pp. Pp. 641-649, May 1990.
- [Wan01] Chin-Liang Wang; Kuo-Ming Wu; Ming-Shiang Lai, "On weight initialization for adaptive multistage parallel interference cancellation in CDMA systems."

- IEEE Third Workshop on Signal Processing Advances in Wireless Communications, 2001. Page(s): 194 -197.
- [Wan99] X. Wang and H. V. Poor, "Iterative (Turbo) Soft Interference Cancellation and Decoding for Coded CDMA," IEEE Transactions on Communications, vol. 47, no. 7, pp. 1046-1061, July 1999.
- [Wei97] L. Wei, L. K. Rasmussen and R. Wyrwas, "Near Optimum Tree-Search Detection Schemes for Bit-Synchronous Multiuser CDMA Systems over Gaussian and Two-Path Rayleigh-Fading Channels," IEEE Transactions on Communications, vol. 45, no. 6, pp. 691-700, June 1997.
- [Wen99] J. Weng, G. Xue, T. Le-NGOC and S. Tahar, "Multistage Interference Cancellation With Diversity Reception for QPSK Asynchronous DS/CDMA System Over Multipath Fading Channels," IEEE International Conference on Communications (ICC), pp. 78-82, Vancouver, BC, Canada, 6-10 June 1999.
- [Wib96] N. Wiberg, "Codes and Decoding on General Graphs," Linköping Studies in Science and Technology. Linköping Sweden. Ph.D. dissertation No. 440. 1996.
- [Woj86] A. H. Wojnar, "Unknown Bounds on Performance in Nakagami Channels," IEEE Transactions on Communications, vol. COM-34, no. 1, pp. 22-24, January 1986.
- [Woo00] J.P. Woodard and L. Hanzo, "Comparative study of Turbo Decoding Techniques: An Overview" IEEE transaction on Vehicular Technology, Vol. 49, no. 6, pp. 2208-2233, November 2000
- [Wu01] K. Wu and C Wang, "An Iterative Multiuser Receiver Using Parallel Interference Cancellation for Turbo-coded DS-CDMA System" IEEE Global Telecommunications Conference on Communications (GLOBECOM '96). vol.1, pp. 244 - 248 1996.
- [Xue00a] G. Xue and L. Chengshu, "Performance of Partial Parallel Interference Cancellation in DS-CDMA Systems with Delay Estimation Errors," Proceedings of the IEEE Conference on Personal Indoor and Mobile Radio Communication (PIMRC), pp. 724-727, London, United Kingdom, 18-21 September 2000.
- [Xue00b] G. Xue, J. F. Weng, T. Le-NGOC and S. Tahar, "An Analytical Model for Performance Evaluation of Parallel Interference Cancellers in CDMA Systems," IEEE Communications Letters, vol. 4, no. 6, pp. 184-186, June 2000.

- [Xue99] G. Xue, J. Weng, T. Le-Ngoc and S. Tahar," Adaptive Multistage Parallel Interference Cancellation for CDMA over Multipath Fading Channels" IEEE International Conference on Communications, Vol.1, pp.1251-1255 Vancouver, BC. Canada, 6-10 June,1999
- [Yan98] W.Yan and C.Shixin," An Multiple Access Interference (MAI) Cancellation Detector at the Mobile Terminal in CDMA Systems" IEEE Fifth International Symposium on Spread Spectrum Techniques & Applications, vol.3/3,pp.922-926,Sun City, South Africa, September 2-4,1998
- [Yoo93] Y.C. Yoon, R. Kohno and H. Imai," A Spread-Spectrum Multiaccess System with Cochannel Interference Cancellation for Multipath fading Channels" IEEE Journal on Selected Areas in Communications vol.11 ,no.7,pp.1067-1075,September 1993
- [Zha00] W. Zhang and R. S. Blum, "Iterative Multiuser Detection for Turbo Coded Synchronous CDMA in Gaussian and Non-Gaussian Impulsive noise," Conference on Information Sciences and Systems, Princeton University, 15-17 March 2000.

Appendix A. Derivation of equation (2.24).

The BER can be expressed as $\rho^{(j)} = \left| \int P^{(j)} P(S) dS \right|$, where $P^{(j)}$ is the conditional BER

and is given by $P^{(j)} = Q[\sqrt{S\gamma}] = \frac{1}{\pi} \int_0^{\frac{\pi}{2}} e^{-\left(\frac{S\gamma}{2\sin^2\theta}\right)} d\theta$. $P(S)$ is the PDF of S and is given as:

$$P(S) = \left(\frac{m_T}{\Omega_T} \right)^{m_T} \frac{S^{(m_T-1)}}{\Gamma(m_T)} e^{-\left(\frac{m_T S}{\Omega_T}\right)} \quad (\text{A.1})$$

Therefore,

$$\begin{aligned} \rho^{(j)} &= \left| \int_0^\infty Q[\sqrt{S\gamma}] \left(\frac{m_T}{\Omega_T} \right)^{m_T} \frac{S^{(m_T-1)}}{\Gamma(m_T)} e^{-\left(\frac{m_T S}{\Omega_T}\right)} dS \right| \\ &= \left| \frac{1}{\pi} \int_0^{\frac{\pi}{2}} e^{-\left(\frac{S\gamma}{2\sin^2\theta}\right)} d\theta \left(\frac{m_T}{\Omega_T} \right)^{m_T} \frac{S^{(m_T-1)}}{\Gamma(m_T)} e^{-\left(\frac{m_T S}{\Omega_T}\right)} dS \right| \\ &= \left| \frac{1}{\pi \Gamma(m_T)} \left(\frac{m_T}{\Omega_T} \right)^{m_T} \int_0^{\frac{\pi}{2}} \int_0^\infty S^{(m_T-1)} e^{-\left(\frac{S\gamma}{2\sin^2\theta} + \frac{m_T S}{\Omega_T}\right)} d\theta dS \right| \\ &= \frac{1}{\pi} \int_0^{\frac{\pi}{2}} \frac{\sin^{2m_T} \theta}{(\gamma' + \sin^2 \theta)^{m_T}} d\theta \end{aligned} \quad (\text{A.2})$$

where $\gamma' = \frac{\gamma \Omega_T}{2m_T}$.

Appendix B: Variances of the Residual Multiple Access Interference for the Total and the Weighted Parallel Interference Cancellation Receivers.

We derive the expression for the variances of the residual interference for the PIC receivers in this appendix. The variance of the MAI component of the detected signal is given in equation (2.18) as

$$\text{var}[V_{j\zeta}] = \frac{T^2(\beta_{\zeta j})^2}{6N} \sum_{\substack{k=1 \\ k \neq j}}^K P_k q(L, \delta) \Omega_1 \quad (\text{B.1})$$

For the total PIC receiver, we denote the residual interference at the f^{th} cancellation stage as $V_{j\zeta, \text{total}}^{(f)}$

$$V_{j\zeta, \text{total}}^{(f)} = V_{j\zeta} - \hat{V}_{j\zeta}^{(f)} \quad (\text{B.2})$$

where $\hat{V}_{j\zeta}^{(f)}$ is the estimated MAI at the f^{th} cancellation stage. $\hat{V}_{j\zeta}^{(f)}$ can be expressed as

$$\hat{V}_{j\zeta}^{(f)} = \sum_{\substack{k=1 \\ k \neq j}}^K \sqrt{\frac{P_k}{2}} \sum_{l=1}^L \beta_{\zeta j} \beta_{lk} \left\{ \hat{b}_{-1,k}^{(f-1)} R_{kj}(\tau_{lk} - \tau_{\zeta j}) + \hat{b}_{0,k}^{(f-1)} \hat{R}_{kj}(\tau_{lk} - \tau_{\zeta j}) \right\} \cos(\psi_{lk} - \psi_{\zeta j}) \quad (\text{B.3})$$

where $\hat{b}_{0,k}^{(f-1)}$ and $\hat{b}_{-1,k}^{(f-1)}$ represent the tentative bit of user k that correspond to the present and the immediately past instances respectively. The variance of the residual MAI, $\text{var}[V_{j\zeta, \text{total}}^{(f)}]$, can therefore be expressed as:

$$\text{var}[V_{j\zeta, \text{total}}^{(f)}] = \left(2 - 2E[\hat{b}_{0,k}^{(f-1)}] \right) \text{var}[V_{j\zeta}] \quad (\text{B.4})$$

where $E[\]$ represents the expectation function.

In order to proceed we have to evaluate $E[\hat{b}_{0,k}^{(f-1)}]$. $\hat{b}_{0,k}^{(f-1)}$ is obtained by taking a hard decision on a Gaussian variate. That is, $\hat{b}_{0,k}^{(f-1)} = \text{sgn}(X_j^{(f-1)})$ where $X_j^{(f-1)}$ is a Gaussian variate (as defined in Chapter 2). Hence

$$E[\hat{b}_{0,k}^{(f-1)}] = \frac{1}{\sqrt{2\pi}\sigma_{X_j^{(f-1)}}} \int_{-\infty}^{\infty} \exp\left(-\frac{\left(X_j^{(f-1)} - m_{X_j^{(f-1)}}\right)^2}{2\sigma_{X_j^{(f-1)}}^2}\right) dX_j^{(f-1)} \quad (\text{B.5})$$

where $m_{X_j^{(f-1)}}$ is the mean of $X_j^{(f-1)}$ and $\sigma_{X_j^{(f-1)}}^2$ is the variance of $X_j^{(f-1)}$.

$$\begin{aligned} E[\hat{b}_{0,k}^{(f-1)}] &= \frac{1}{\sqrt{2\pi}\sigma_{X_j^{(f-1)}}} \int_{-\infty}^{\infty} e^{-\frac{\left(X_j^{(f-1)} - m_{X_j^{(f-1)}}\right)^2}{2\sigma_{X_j^{(f-1)}}^2}} dX_j^{(f-1)} \\ &= \left[\frac{1}{\sqrt{2\pi}\sigma_{X_j^{(f-1)}}} \int_0^{\infty} e^{-\frac{\left(X_j^{(f-1)} - m_{X_j^{(f-1)}}\right)^2}{2\sigma_{X_j^{(f-1)}}^2}} dX_j^{(f-1)} \right. \\ &\quad \left. - \frac{1}{\sqrt{2\pi}\sigma_{X_j^{(f-1)}}} \int_{-\infty}^0 e^{-\frac{\left(X_j^{(f-1)} - m_{X_j^{(f-1)}}\right)^2}{2\sigma_{X_j^{(f-1)}}^2}} dX_j^{(f-1)} \right] \quad (\text{B.6}) \end{aligned}$$

$$\text{Let } \frac{\left(X_j^{(f-1)} - m_{X_j^{(f-1)}} \right)}{\sqrt{2\sigma_{X_j^{(f-1)}}}} = Y$$

Therefore $dX_j^{(f-1)} = \sqrt{2}\sigma_{X_j^{(f-1)}} dY$. When $X_j^{(f-1)}=0$, $Y = -\frac{m_{X_j^{(f-1)}}}{\sqrt{2\sigma_{X_j^{(f-1)}}}}$. When

$X_j^{(f-1)} = \infty$, $Y = \infty$. When $X_j^{(f-1)} = -\infty$, $Y = -\infty$.

Therefore,

$$\begin{aligned} E\left[\hat{b}_{0,k}^{(f-1)}\right] &= \frac{1}{\sqrt{2\pi}\sigma_{X_j^{(f-1)}}} \int_{-\infty}^{\infty} e^{-\frac{\left(X_j^{(f-1)} - m_{X_j^{(f-1)}} \right)^2}{2\sigma_{X_j^{(f-1)}}^2}} dX_j^{(f-1)} \\ &= \left(\frac{1}{\sqrt{\pi}} \int_{\frac{m_{X_j^{(f-1)}}}{\sqrt{2\sigma_{X_j^{(f-1)}}}}}{\infty} e^{-Y} dY \right) - \left(\frac{1}{\sqrt{\pi}} \int_{-\infty}^{-\frac{m_{X_j^{(f-1)}}}{\sqrt{2\sigma_{X_j^{(f-1)}}}}} e^{-Y} dY \right) \\ &= \frac{1}{2} \left[\text{erf}(Y) \right]_{\frac{m_{X_j^{(f-1)}}}{\sqrt{2\sigma_{X_j^{(f-1)}}}}}^{\infty} + \frac{1}{2} \left[\text{erf}(Y) \right]_{-\infty}^{-\frac{m_{X_j^{(f-1)}}}{\sqrt{2\sigma_{X_j^{(f-1)}}}}} \\ &= \text{erf} \left(\frac{m_{X_j^{(f-1)}}}{\sqrt{2\sigma_{X_j^{(f-1)}}}} \right) \\ &= 1 - \text{erfc} \left(\frac{m_{X_j^{(f-1)}}}{\sqrt{2\sigma_{X_j^{(f-1)}}}} \right) \\ &= 1 - 2Q \left(\frac{m_{X_j^{(f-1)}}}{\sigma_{X_j^{(f-1)}}} \right) \end{aligned} \tag{B.7}$$

But $\frac{m_{X_j^{(f-1)}}}{\sigma_{X_j^{(f-1)}}} = \sqrt{\gamma \frac{\sum_{\zeta} \beta_{\zeta j}^2}{\Omega_1}}$ which is a random variable. By using the expected value of

$$\frac{m_{X_j^{(f-1)}}}{\sigma_{X_j^{(f-1)}}} \text{ we have } \frac{m_{X_j^{(f-1)}}}{\sigma_{X_j^{(f-1)}}} = \sqrt{\gamma q(\delta, M)}. \text{ Therefore } E[\hat{b}_{0,k}^{(f-1)}] = 1 - 2Q[\sqrt{\gamma q(\delta, M)}].$$

The variance of the residual MAI can then be given as

$$\begin{aligned} \text{var}[V_{j\zeta}^{(f)}] &= \left(2 - 2\left(1 - 2Q[\sqrt{\gamma q(\delta, M)}]\right)\right) \text{var}[V_{j\zeta}] \\ &= 4Q[\sqrt{\gamma q(\delta, M)}] \text{var}[V_{j\zeta}] \end{aligned} \quad (\text{B.8})$$

For the weighted PIC receiver, the residual MAI at the f^{th} stage can be expressed as

$$V_{j\zeta, \text{weighted}}^{(f)} = V_{j\zeta} - \lambda_f \hat{V}_{j\zeta}^{(f)} \quad (\text{B.9})$$

λ_f is the cancellation weight at the f^{th} cancellation stage.

The variance of the residual interference will, therefore, be

$$\begin{aligned} \text{var}[V_{j\zeta, \text{weighted}}^{(f)}] &= \left(1 - 2\lambda_f E[\hat{b}_{0,k}^{(f-1)}] + \lambda_f^2 E\left[\left(\hat{b}_{0,k}^{(f-1)}\right)^2\right]\right) \text{var}[V_{j\zeta}] \\ &= \left(1 + \lambda_f^2 - 2\lambda_f E\left[\left(\hat{b}_{0,k}^{(f-1)}\right)^2\right]\right) \text{var}[V_{j\zeta}] \\ &= \left(1 + \lambda_f^2 - 2\lambda_f \left(1 - 2Q[\sqrt{\gamma q(\delta, M)}]\right)\right) \text{var}[V_{j\zeta}] \\ &= \left((1 - \lambda_f)^2 + 4\lambda_f Q[\sqrt{\gamma q(\delta, M)}]\right) \text{var}[V_{j\zeta}] \end{aligned} \quad (\text{B.10})$$

$E[\hat{b}_{0,k}^{(f-1)}]$ has previously been taken as $1-2\rho^{(j)}[f-1]$ in the literature [Yoo93][Hui98]. $\rho^{(j)}[f-1]$ is the average BER of the receiver at the end of the $(f-1)^{\text{th}}$ stage and is extensively discussed in Chapter 2. This leads to variance of the residual MAI being given as

$$\text{var}\left[V_{j\zeta}^{(f),total}\right] = 4\rho^{(j)}[f-1]\text{var}\left[V_{j\zeta}\right] \quad (\text{B.11})$$

$$\text{var}\left[V_{j\zeta}^{(f),weighted}\right] = \left((1-\lambda_f)^2 + 4\lambda_f\rho^{(j)}[f-1]\right)\text{var}\left[V_{j\zeta}\right] \quad (\text{B.12}).$$

Figures B.1 and B.2 compares the error rate results that are obtained by using models of equations (B.11) and (B.12) with the models that are developed in this dissertation. It will be observed that our models have closer agreement with results that are obtained from simulations.

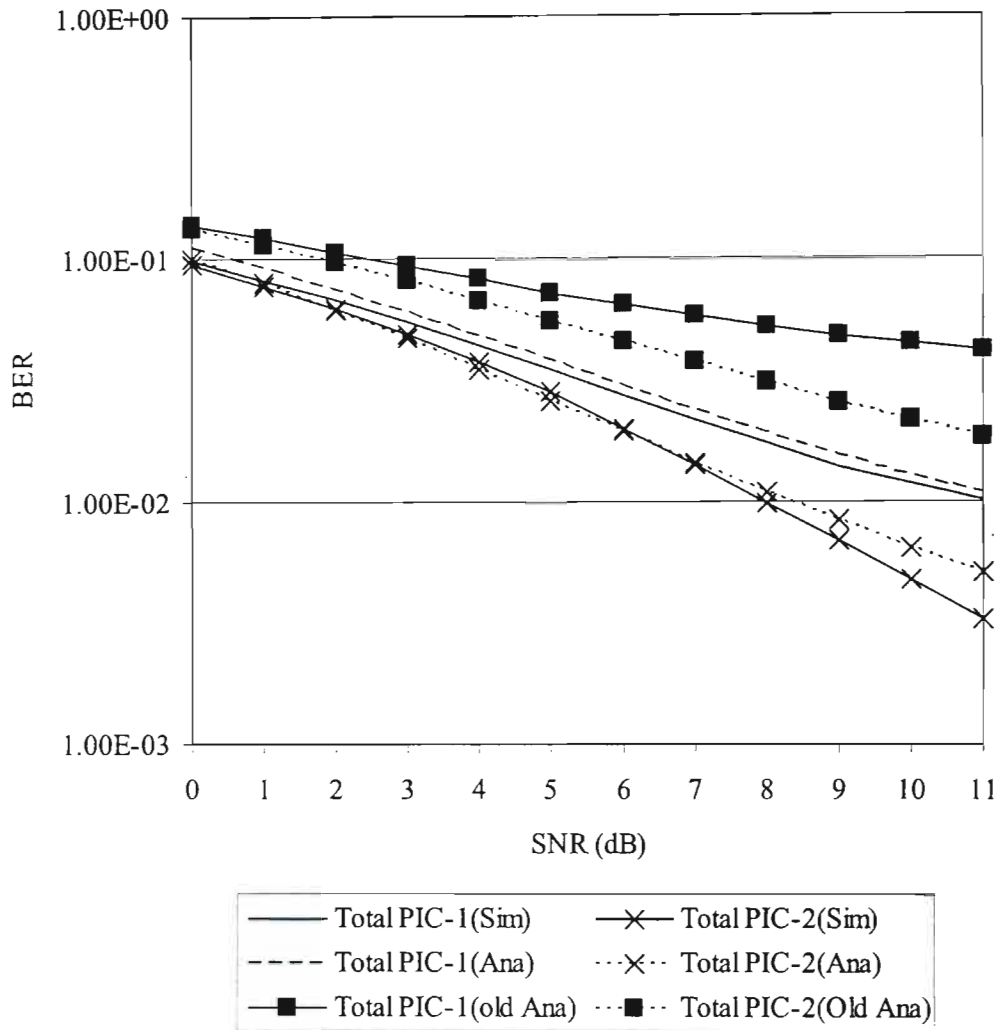


Figure B.1: BER vs SNR the first stage of Total PIC receiver. $L=3$, $M=3$, $m=1$, $\delta=0.2$, $k=10$, $N=15$.

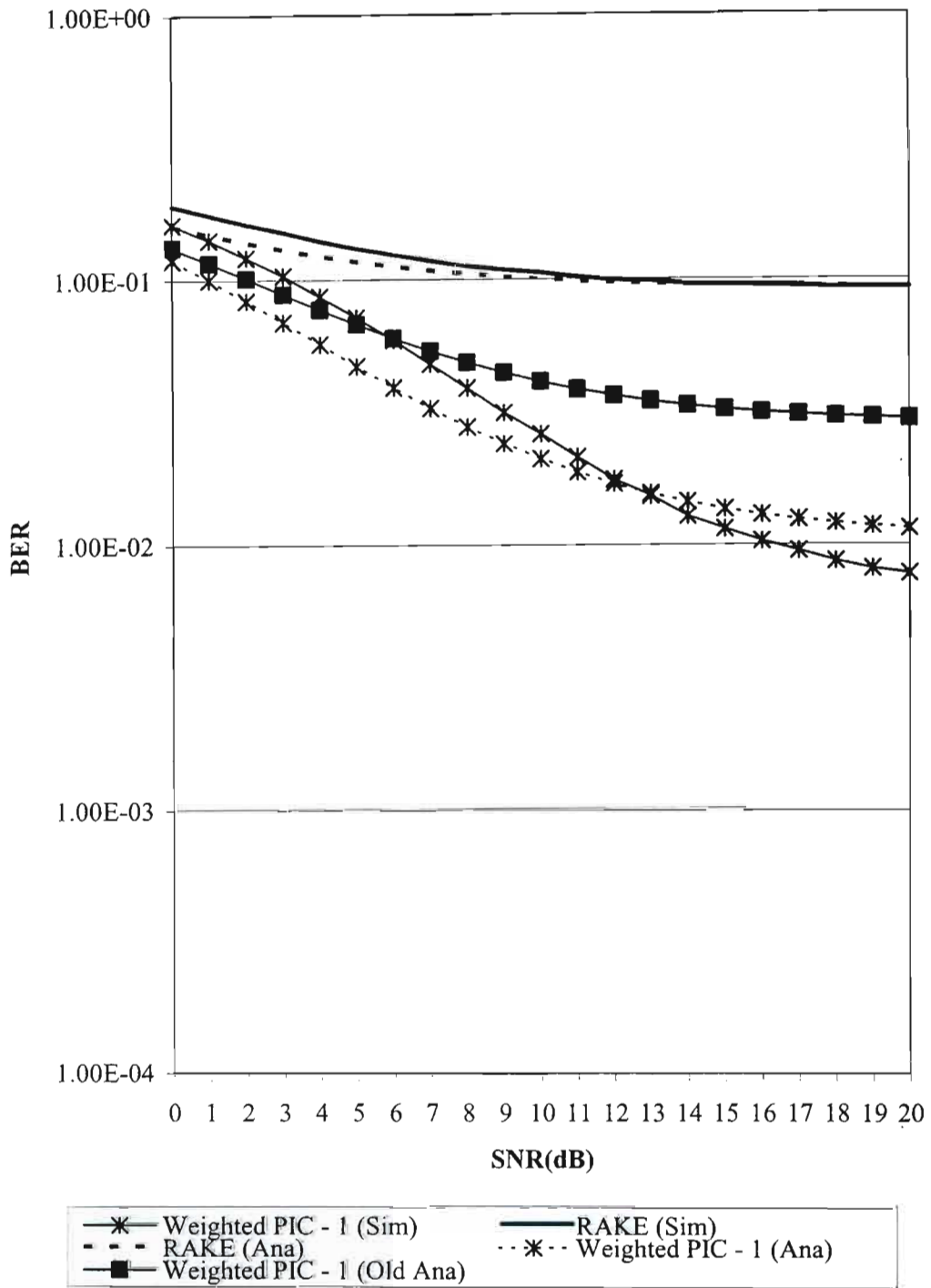


Figure B.2: BER vs SNR the first stage of weighted PIC receiver. $L=3$, $M=3$, $m=1$, $\delta=0.2$, $k=10$, $N=15$. Cancellation weight = 0.7.